Computational Investigations of the Turbulent Heat Flux (THX) Experiments

Mike Borghi, Seth Spiegel, Dennis Yoder, Justin Pesich, Mark Wernet, and Nick Georgiadis

NASA Glenn Research Center

Transformational Tools and Technologies (TTT) Project
Transformative Aeronautical Concepts Program (TACP)

October 15, 2020



Motivation



- In the computational modeling world, turbulent temperature variations and turbulent heat flux have not received much attention, yet are very important to many flows
- Example include: high Mach number applications, propulsion systems, systems requiring active cooling - to name a few
- The turbulent heat flux (THX) experiments were designed to make detailed turbulent measurements of velocities and temperatures – with goal of obtaining data to:
  1) improve understanding
  2) develop better computational models for simulation of flows involving turbulent heat flux
- In conjunction with these experiments, a detailed computational effort was undertaken to provide a baseline of RANS and scale-resolving (LES and hybrids) techniques for these flows

Outline of Talks Today

1) Introduction – Georgiadis
2) Experimental overview – Wernet
3) RANS of single-hole case – Yoder
4) LES of single-hole case using FDL3DI – Borghi
5) LES of single-hole case using GFR – Spiegel
6) RANS, hybrid RANS-LES (DDES), and CHT of multi-hole case – Pesich
7) Questions

Overview of the THX 3&4 Experiments

Mark Wernet, Nick Georgiadis, Phil Poinsatte
NASA Glenn Research Center

Doug Thurman
U.S. Army Research Laboratory

Randy Locke
HX5, LLP

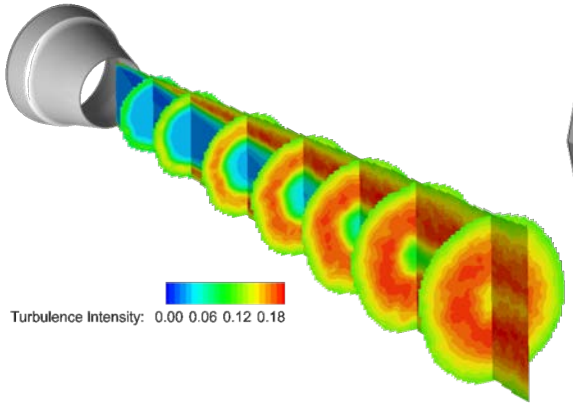
Turbulent Heat Flux (THX) Experiments

- THX is a 5-phase experimental effort, with some concurrent computational work
  - Phase I Low speed / temperature cooling hole experiments in GRC SW6
  - Phase II Subsonic jet temperature measurements: using Raman in GRC AAPL
  - Phase III Subsonic Square nozzle flow over plate with single cooling hole, PIV and Raman temperature measurements in AAPL
  - Phase IV Subsonic Square nozzle flow over perforated plate film cooling, PIV & Raman temperature measurements in AAPL
  - Phase V Series of supersonic round nozzles replicating the experiments of Seiner et al., 1992, where BOS, Raman and PIV measurements were obtained in AAPL

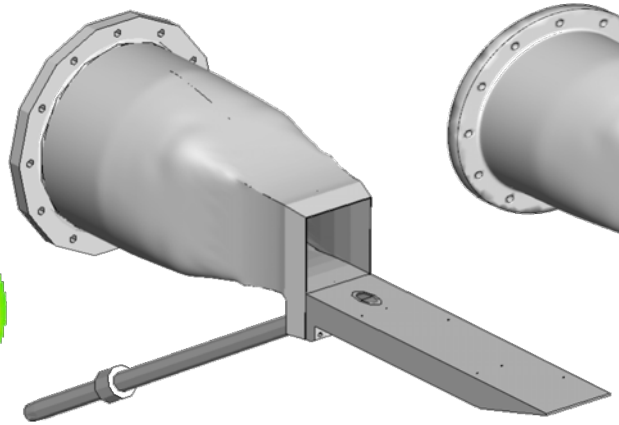
THX Phases II – V

Conducted in AAPL

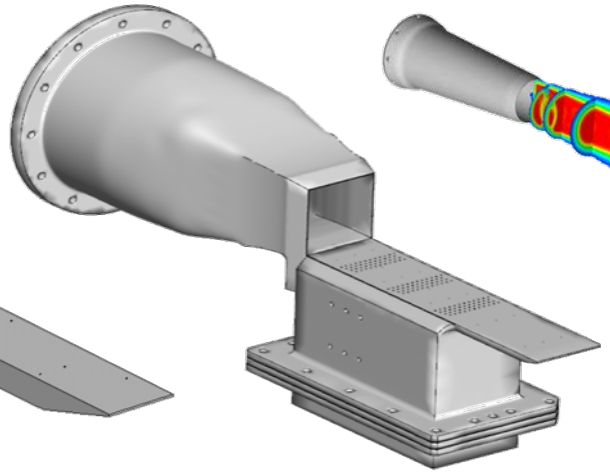
THX II
SMC000



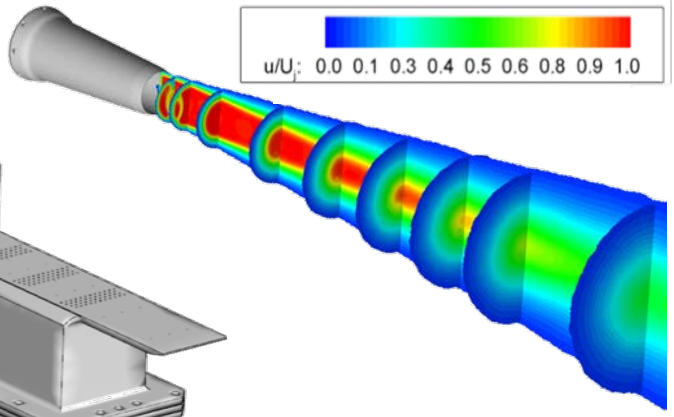
THX III
Single Hole Plate



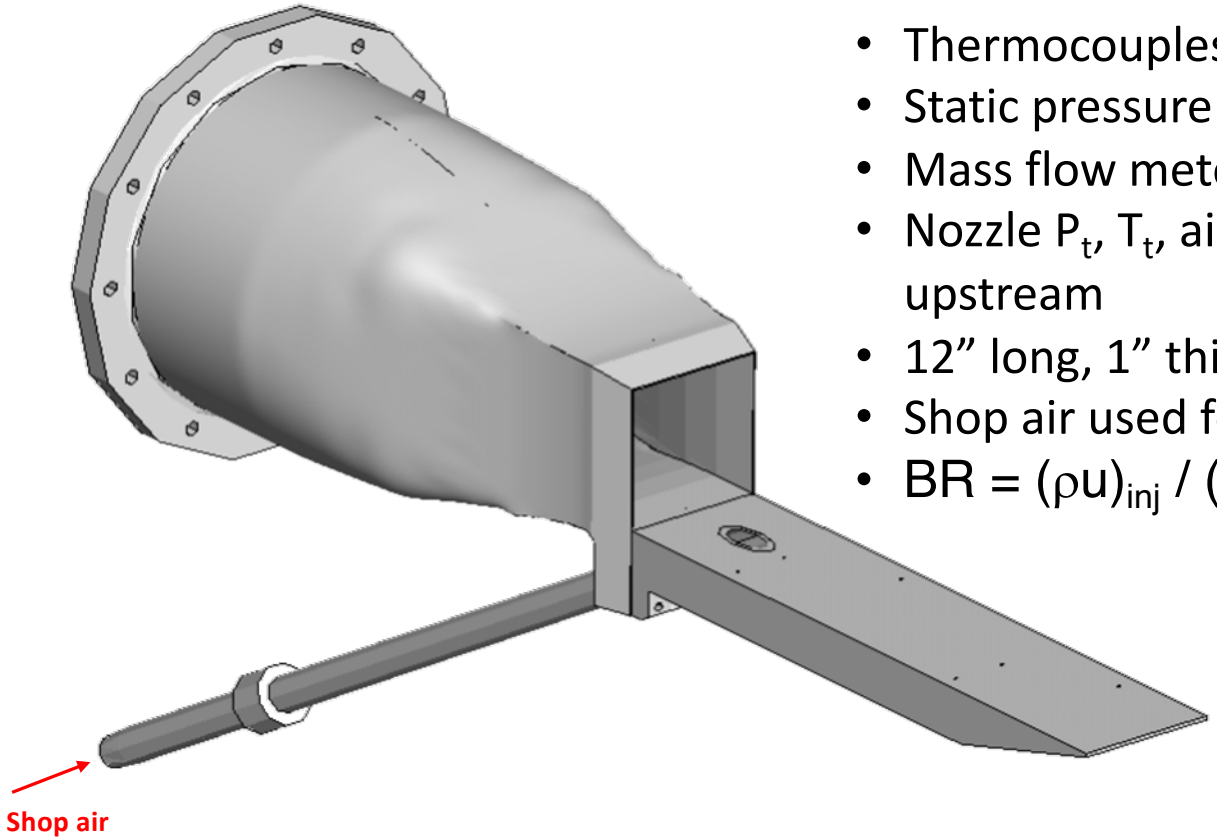
THX IV
Multi-Hole Plate



THX V
Supersonic Jets



THX Phase III

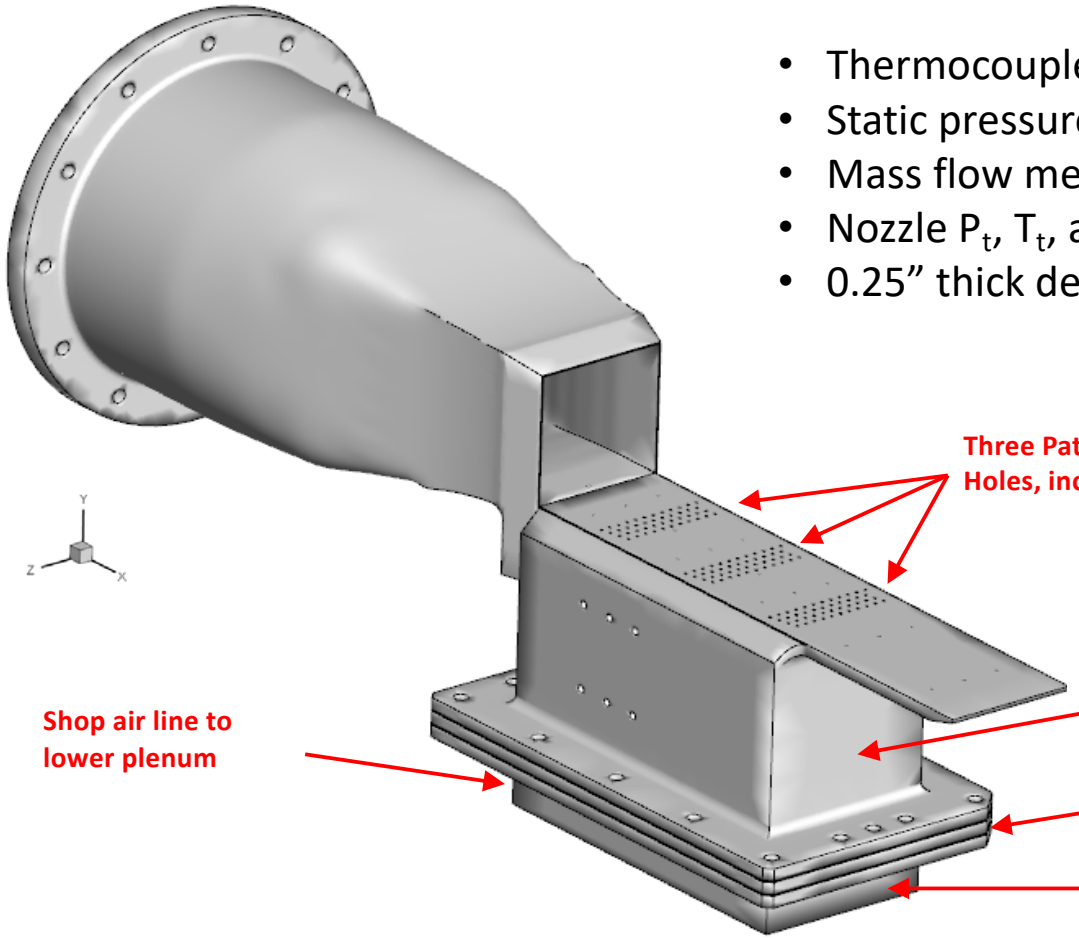


- Thermocouples embedded in plate surface
- Static pressure measured in cooling flow tube
- Mass flow meter measured injector flow
- Nozzle P_t, T_t, air & fuel flow rates measured upstream
- 12” long, 1” thick SS deck
- Shop air used for cooling flow
- BR = $(\rho u)_{inj} / (\rho u)_{jet}$

THX Phase III Test Matrix

Test Point	Tanna Matrix Set Point	Ma	TR	NPR	Mj	BR	Mass (nozzle) lbm/s	Mass (Injector) lbm/s
1	23	0.5	1.765	1.103	0.376	0.5	1.16	0.0159
2	**23**	**0.5**	**1.765**	**1.103**	**0.376**	**1.0**	**1.16**	**0.0317**
3	**23**	**0.5**	**1.765**	**1.103**	**0.376**	**2.0**	**1.16**	**0.0635**
4	27	0.9	1.765	1.36	0.677	0.5	2.09	0.0286
5	27	0.9	1.765	1.36	0.677	1.0	2.09	0.0571
6	42	0.5	2.7	1.066	0.304	0.5	0.76	0.0103
7	42	0.5	2.7	1.066	0.304	1.0	0.76	0.0208
8	46	0.9	2.7	1.227	0.548	0.5	1.37	0.0187
9	46	0.9	2.7	1.227	0.548	1.0	1.37	0.0374
10	49	1.48	2.7	1.692	0.900	0.5	2.25	0.0307
11	49	1.48	2.7	1.692	0.900	1.0	2.25	0.0614

THX Phase IV – Porous Plate Geometry



- Thermocouples embedded in plate surface
- Static pressure measured in top and bottom plenums
- Mass flow meter measured injector flow
- Nozzle P_t, T_t, air & fuel flow rates measured upstream
- 0.25" thick deck

THX Phase IV Test Matrix

Test Point	Tanna Matrix Set Point	M_a	TR	NPR	M_j	BR	Mass (nozzle) lbm/s	Mass (Injector) lbm/s	Plenum Supply Pressure psig
1	**23**	**0.5**	**1.765**	**1.103**	**0.376**	**0.0**	**1.16**	**0**	
2	23	0.5	1.765	1.103	0.376	0.5	1.16	0.0137	14.4
3	**23**	**0.5**	**1.765**	**1.103**	**0.376**	**1.0**	**1.16**	**0.0274**	**43**
4	**23**	**0.5**	**1.765**	**1.103**	**0.376**	**2.0**	**1.16**	**0.0548**	**100.4**
5	49	1.48	2.7	1.692	0.9	0.0	2.25	0	
6	49	1.48	2.7	1.692	0.9	0.5	2.25	0.0266	41.4
7	49	1.48	2.7	1.692	0.9	1.0	2.25	0.0531	96.8
8	42	0.5	2.7	1.066	0.304	0.0	0.76	0	
9	42	0.5	2.7	1.066	0.304	1.0	0.76	0.0179	*23.53*
10	42	0.5	2.7	1.066	0.304	2.0	0.76	0.0358	57.98
11	42	0.5	2.7	1.066	0.304	3.0	0.76	0.0537	92.34



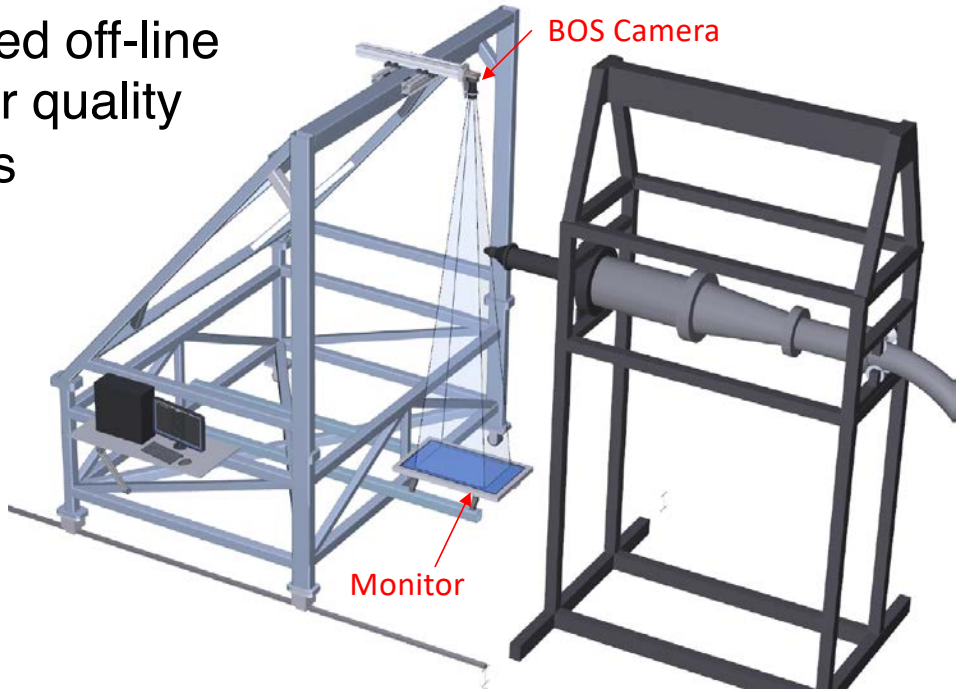
Off-Body Measurements



- Background Oriented Schlieren (BOS)
  - BOS measurements used to optimize the Raman measurement grid depending on cooling film thickness
- Raman Scattering
  - Molecular scattering technique for measuring the gas temperature
  - Composition of the gas is known, only interested in temperature
  - Measure both the mean and rms temperature
  - Measurements at a single point
- Particle Image Velocimetry (PIV)
  - Streamwise plane of 2-component measurements
  - Cross-stream planes of 3-component measurements
  - Planar measurements

Real-Time Background Oriented Schlieren

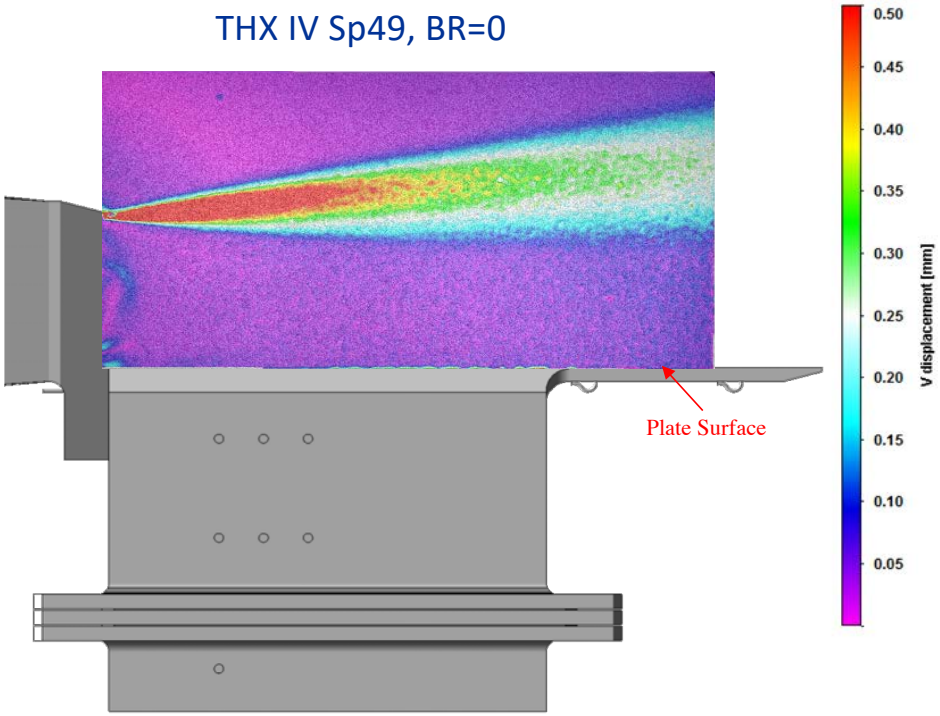
- RT-BOS enables on-line visualization of density variations in the flow
- Single program for BOS image acquisition and real-time display
- Single camera images a speckle pattern displayed on a 4K monitor
- RT-BOS images are then processed off-line to provide higher resolution, higher quality density gradient maps using DaVis

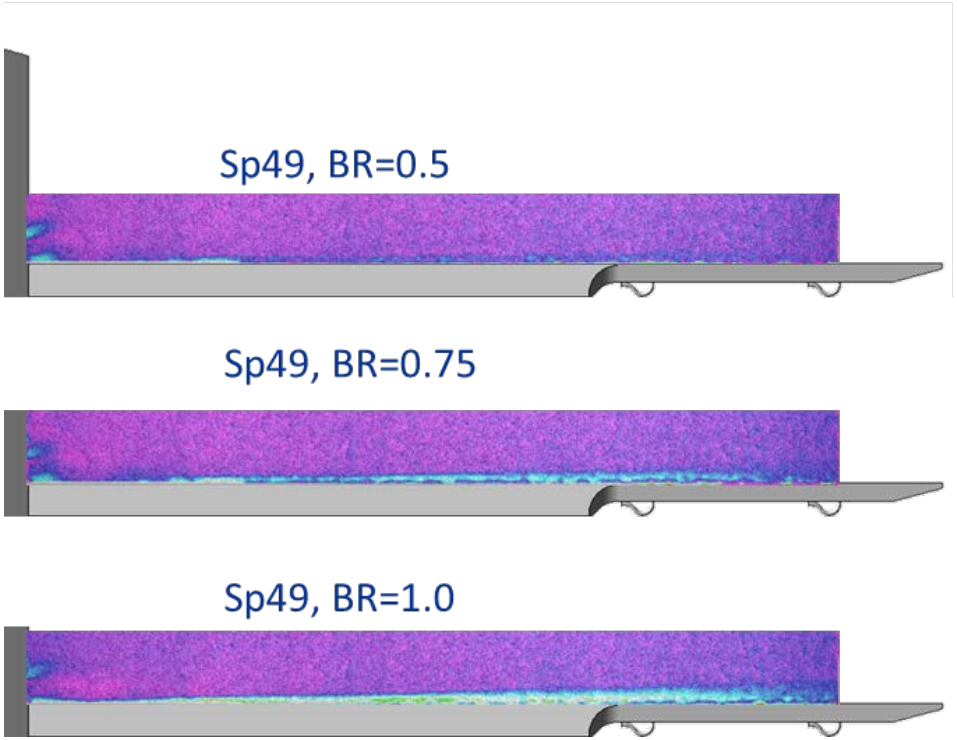


Background Oriented Schlieren on THX IV

- BOS displays the thickness of the film cooling layer
- From BR = 0 (no blowing) up to BR=2, the thickness and extent of the cooling film is observed

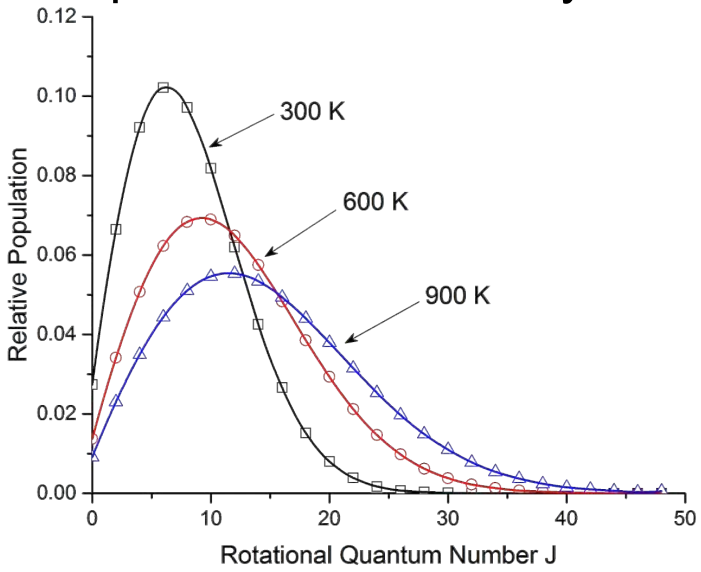
THX IV Sp49, BR=0

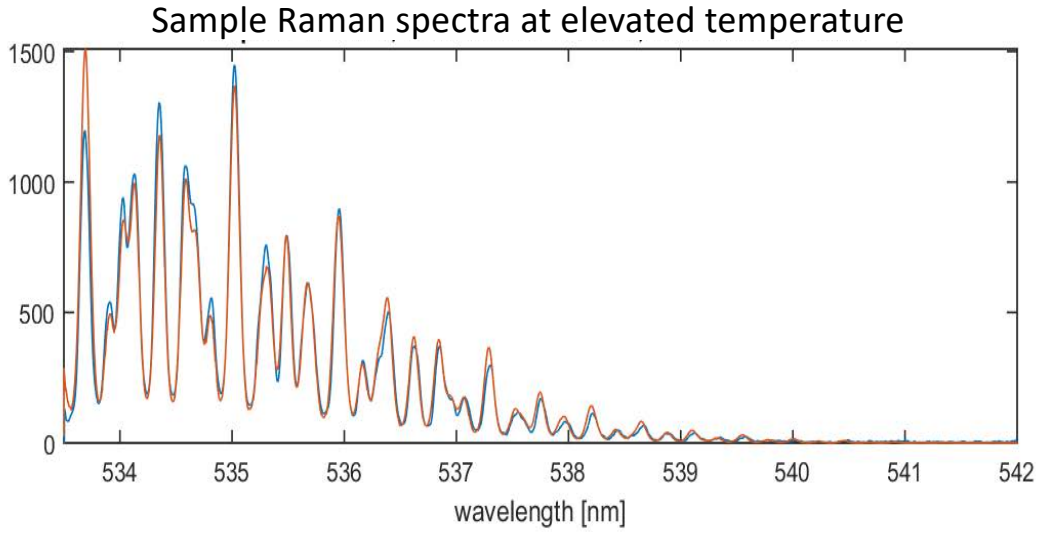




Temperature Dependence of Raman Spectra

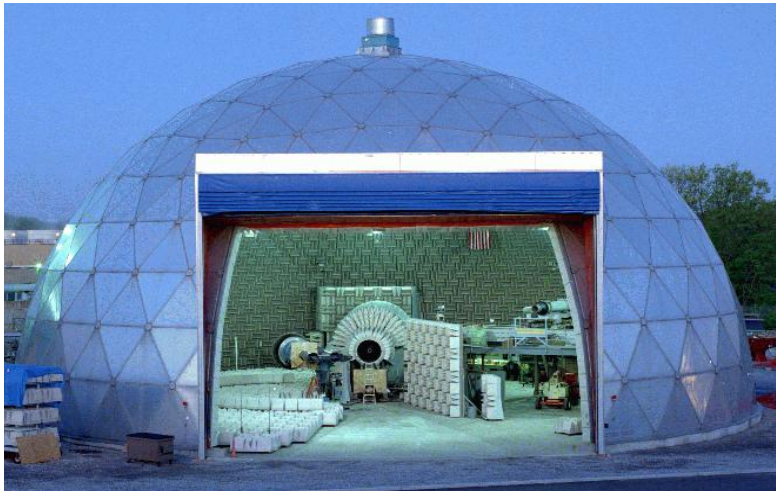
- In Raman scattering, the Boltzmann distribution defines the number of occupied states as a f(T)
- The “envelope” of the rotational Raman signal increases to longer wavelengths (higher rotational quantum number) with increasing temperature
- Acquire 1000 shots to yield mean and rms temperature estimates
- Raman probe volume is a cylinder 70 μm in diameter by 1.2 mm in length





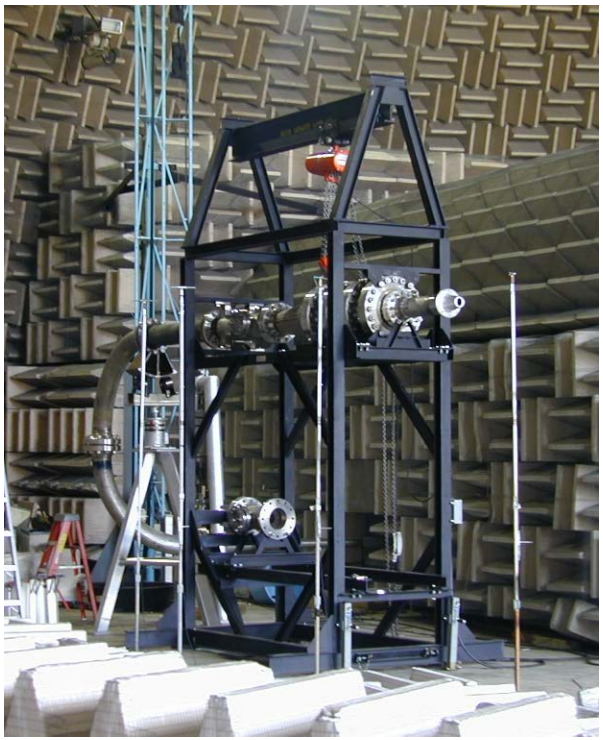
THX in the AAPL

AeroAcoustic Propulsion Laboratory (AAPL)



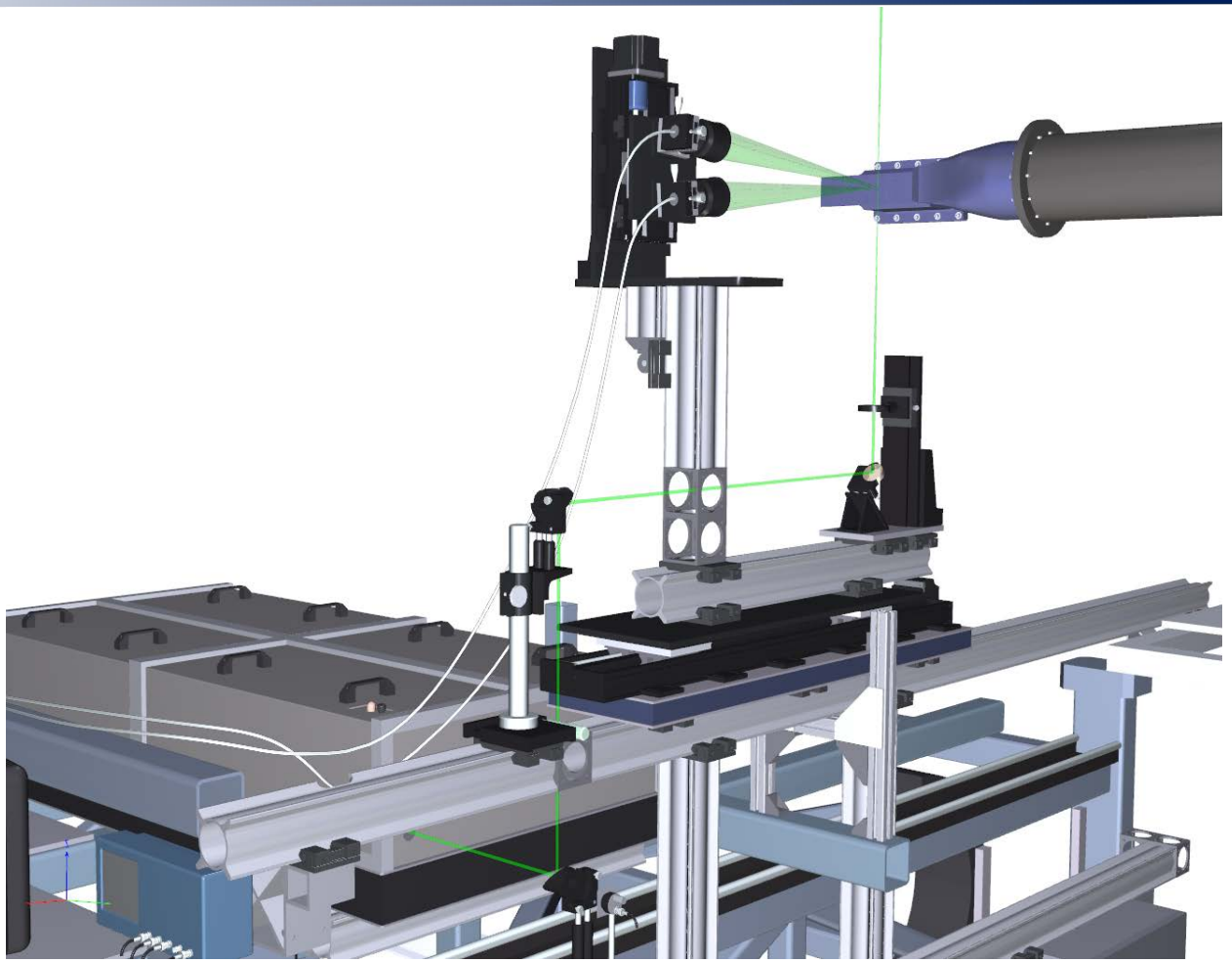
- AAPL: 65ft. radius geodesic dome Anechoic environment
- Small Hot Jet Acoustic Rig:
  - Flows up to Mach 2
  - Temperature ratios up to 2.8
  - 50.8 mm diameter nozzle

THX Phases II, III and IV have been conducted in the Small Hot Jet Acoustic Rig (SHJAR)

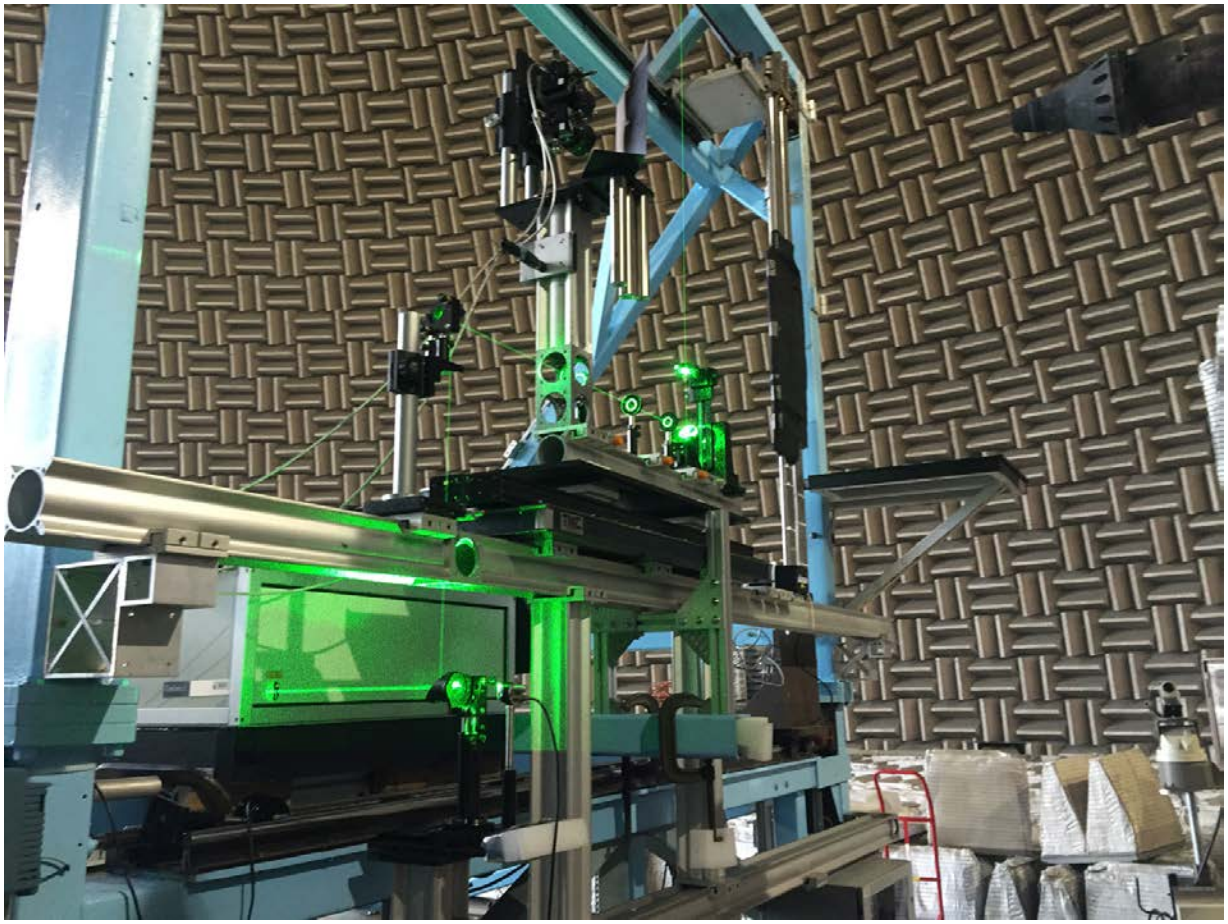


15

Raman Scattering System Installation in SHJAR

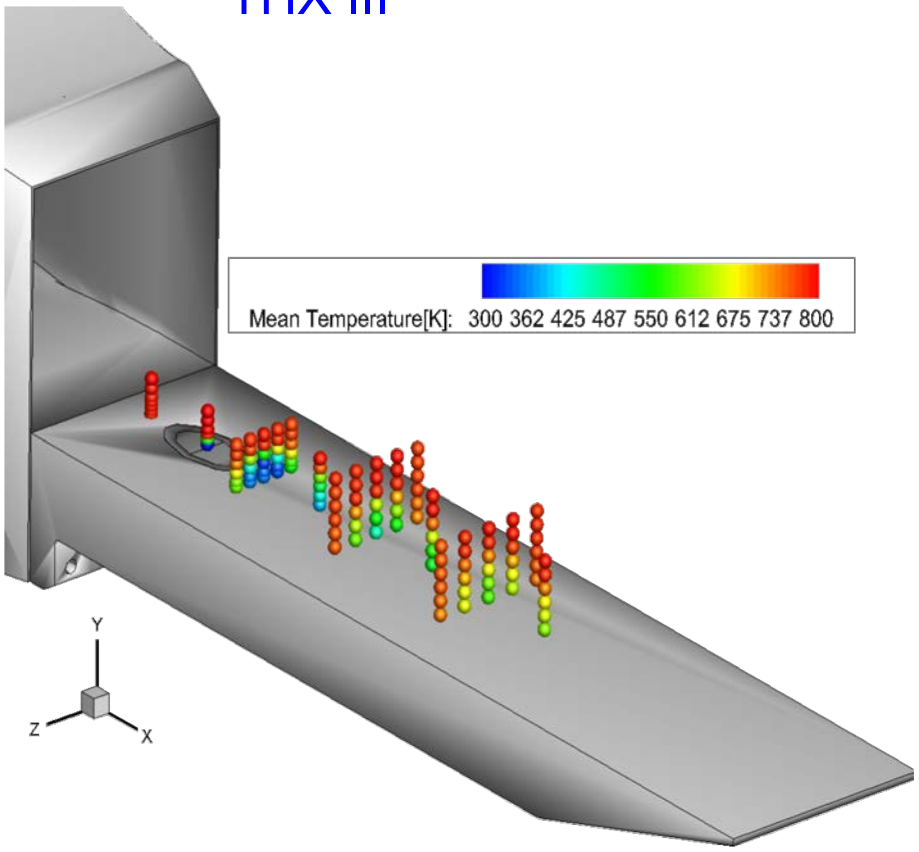


Actual Raman Hardware Installed in SHJAR

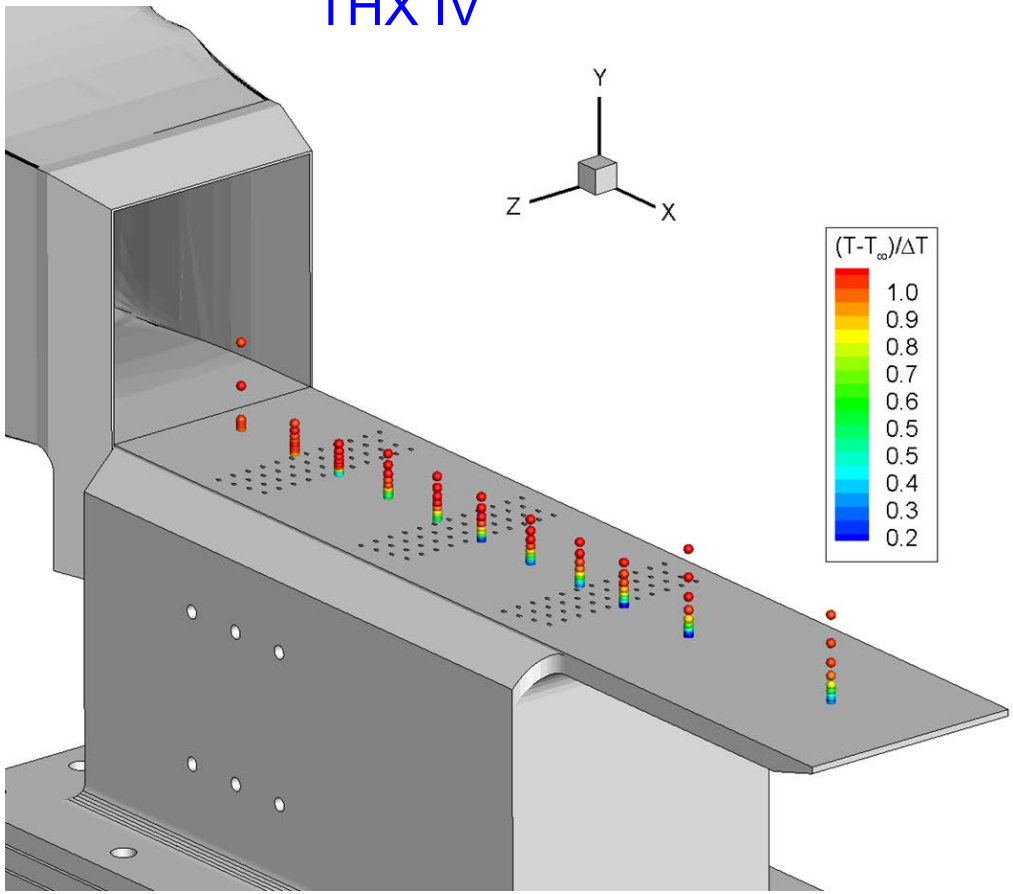


Raman Temperature Measurements

THX III

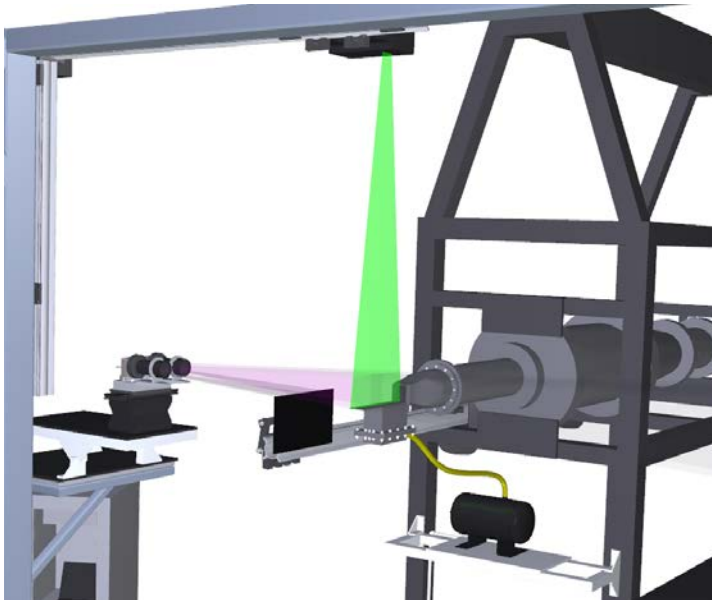


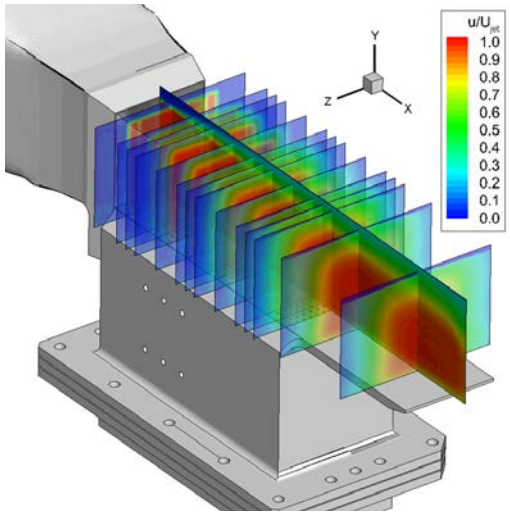
THX IV



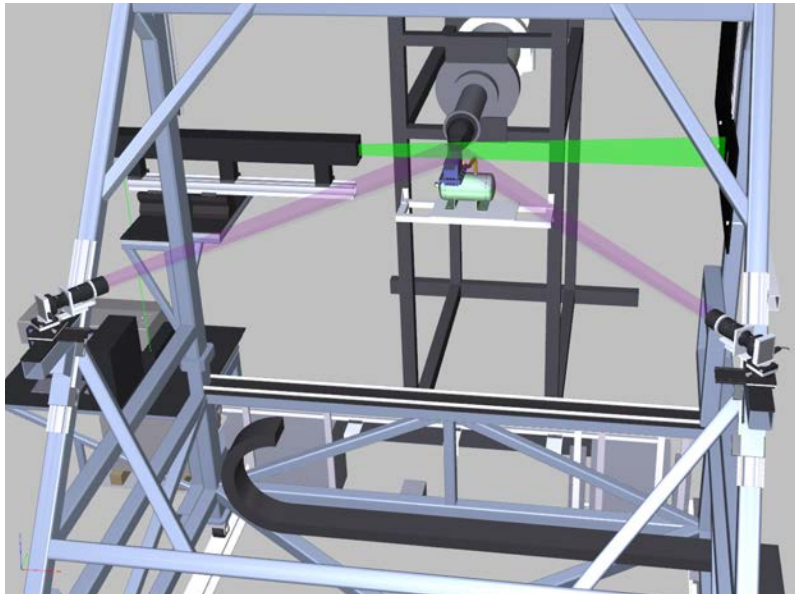
PIV Configurations

Streamwise PIV



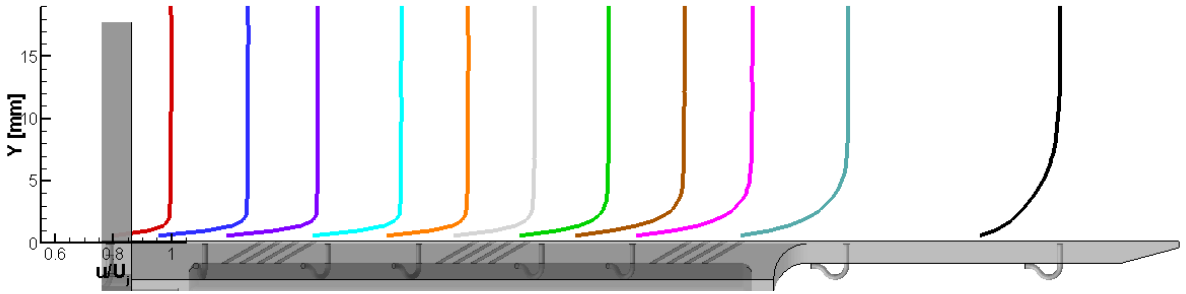


Cross-Stream PIV

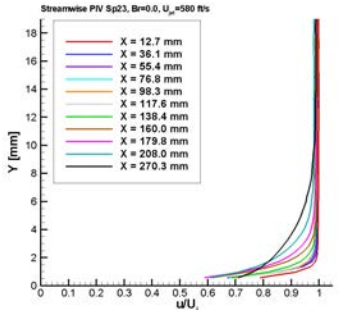


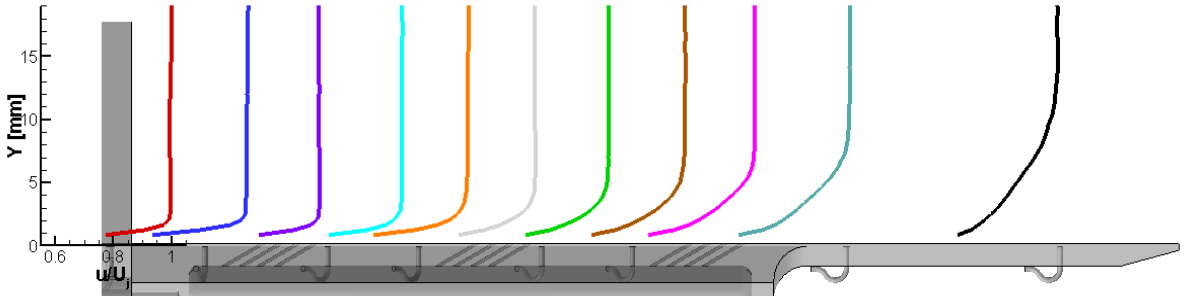
PIV Measurements Set Point 49, BR =1.0

PIV Measurements – THX IV: Set Point 23
(mean axial velocity)

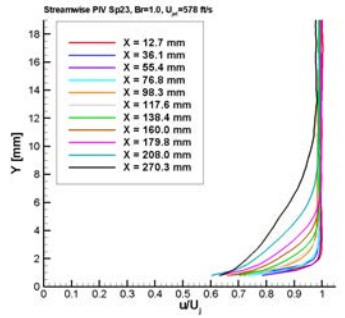


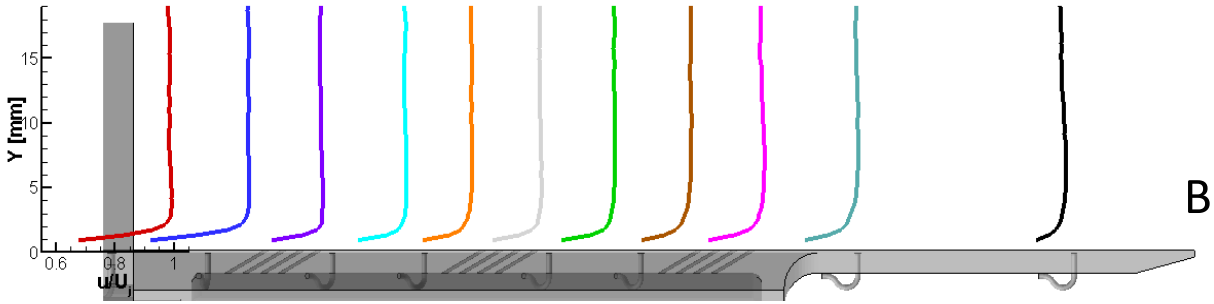
BR = 0



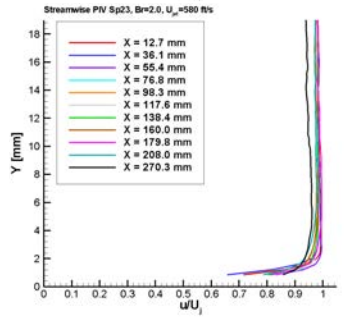


BR = 1.0

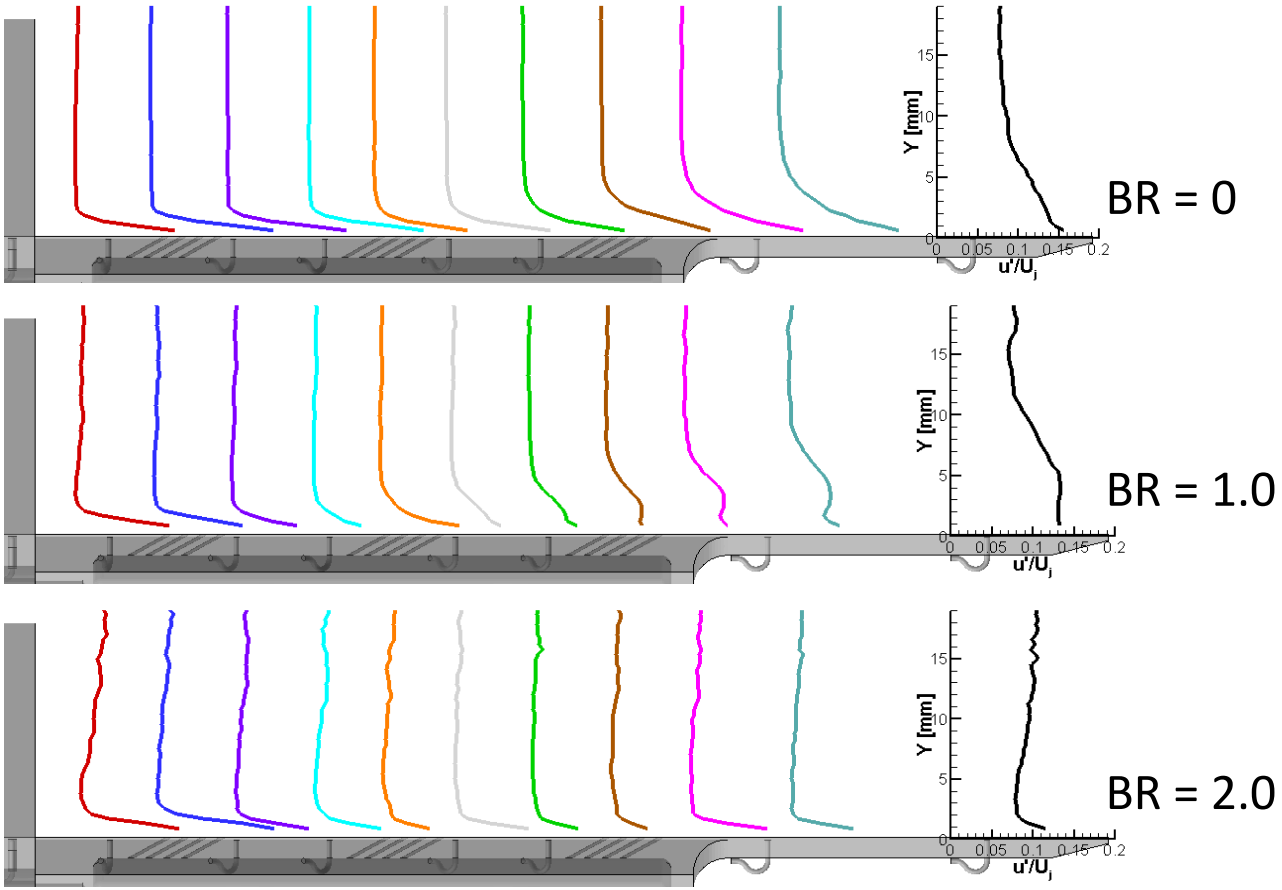




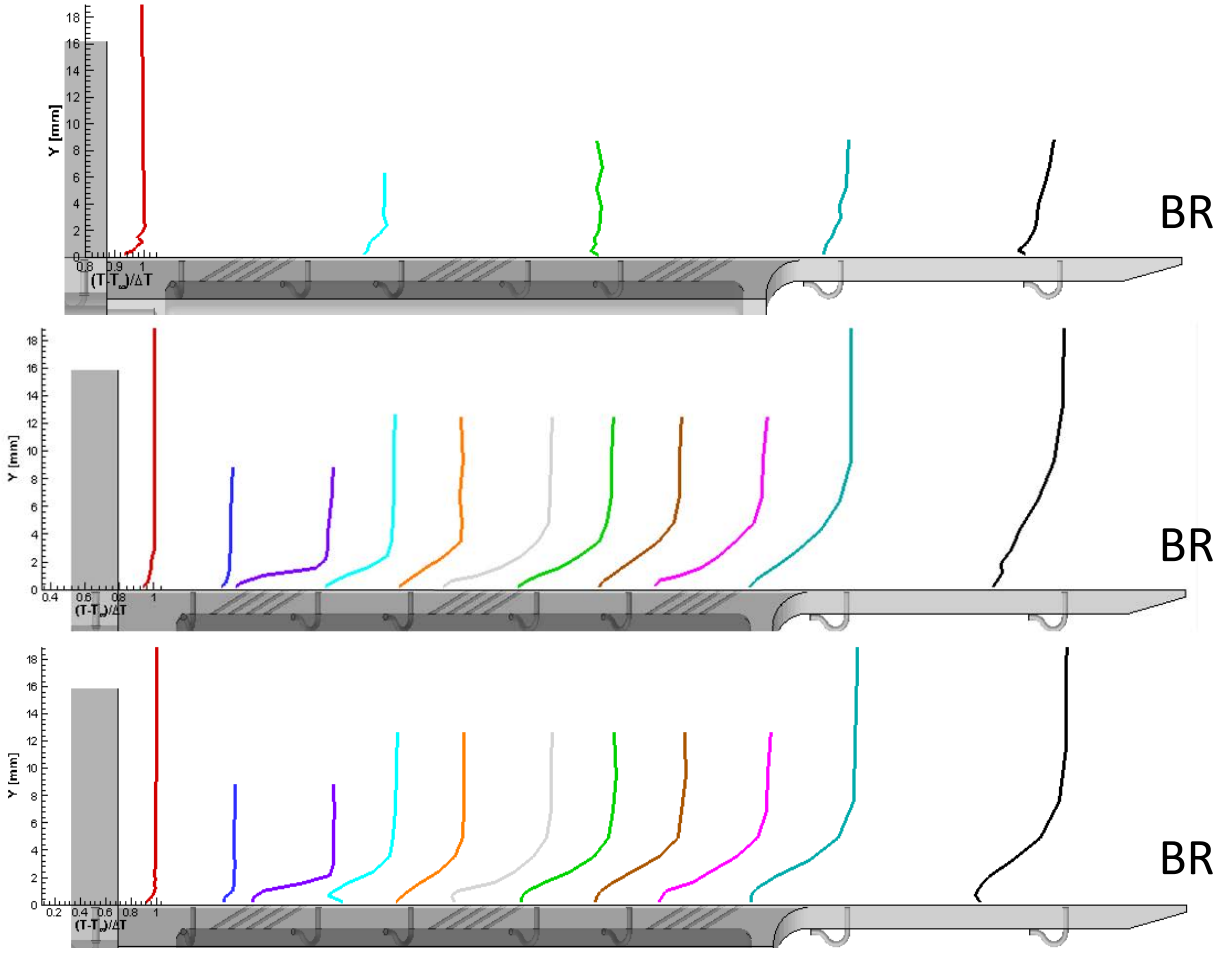
BR = 2.0



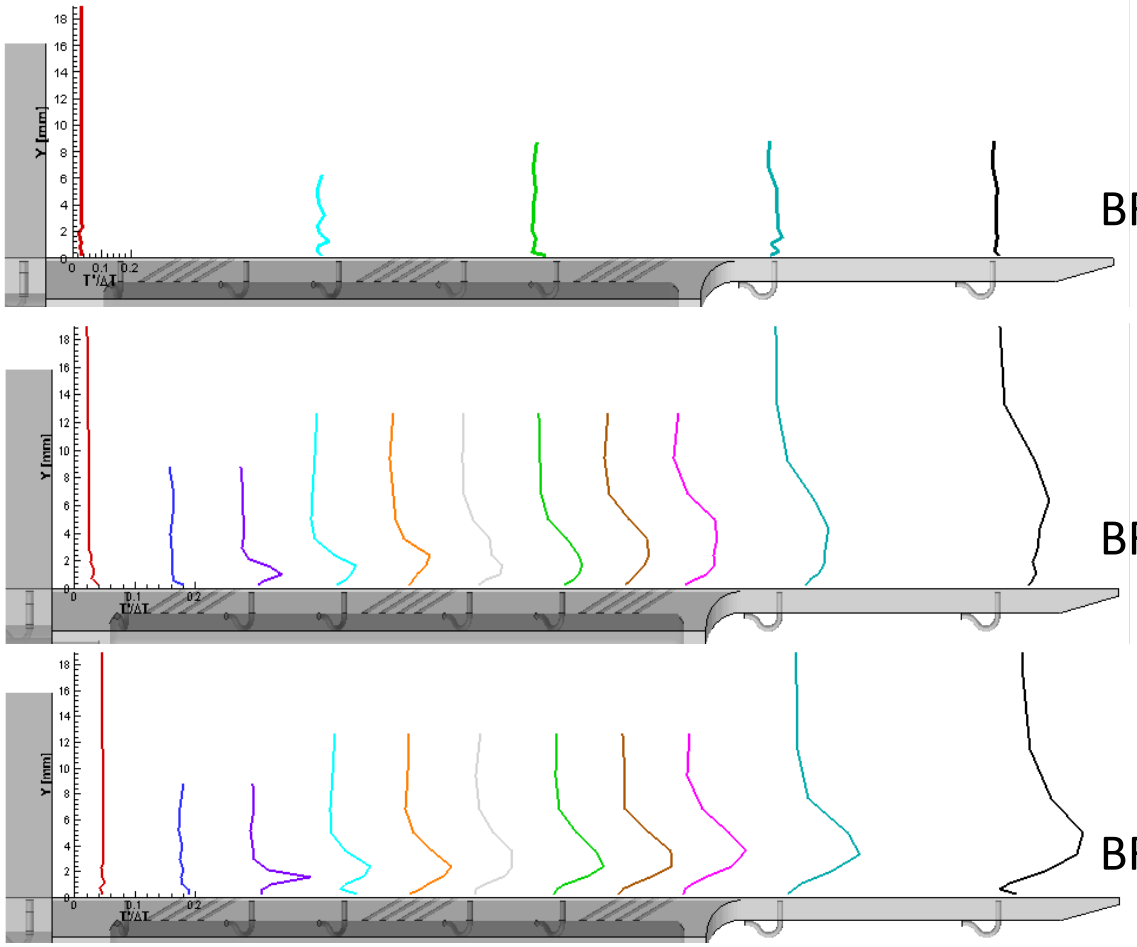
PIV Measurements – THX IV: Set Point 23
(rms of axial velocity)



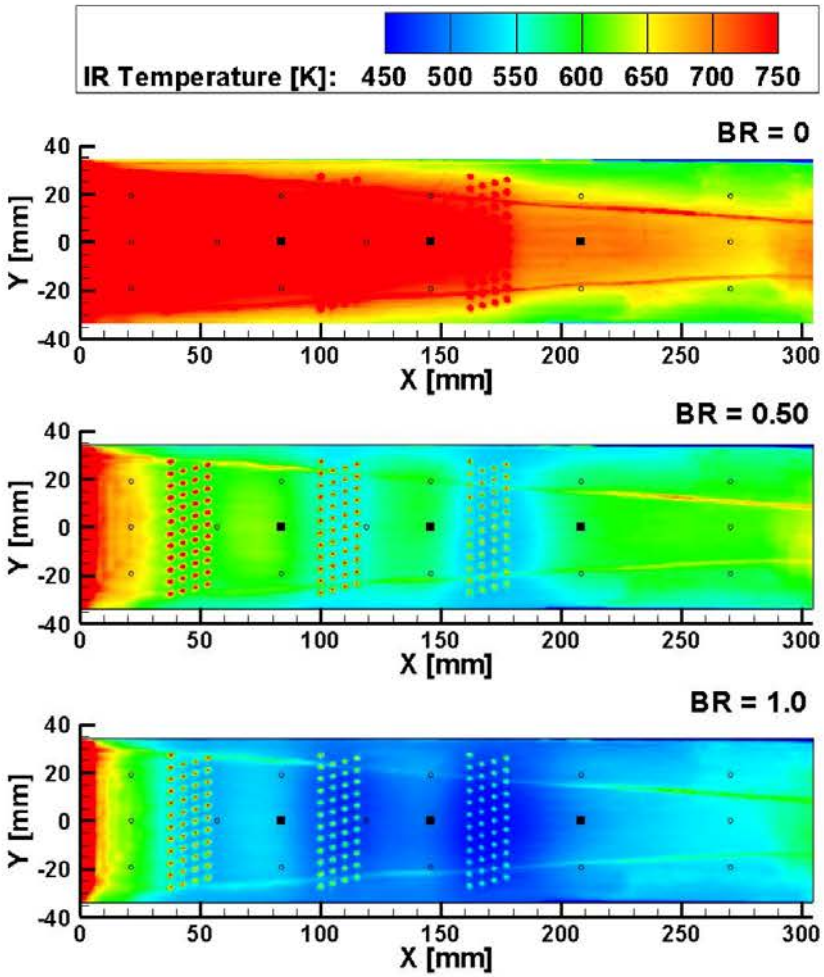
Raman Measurements – THX IV: Set Point 23
(mean Temperature)



Raman Measurements – THX IV: Set Point 23
(rms of Temperature)



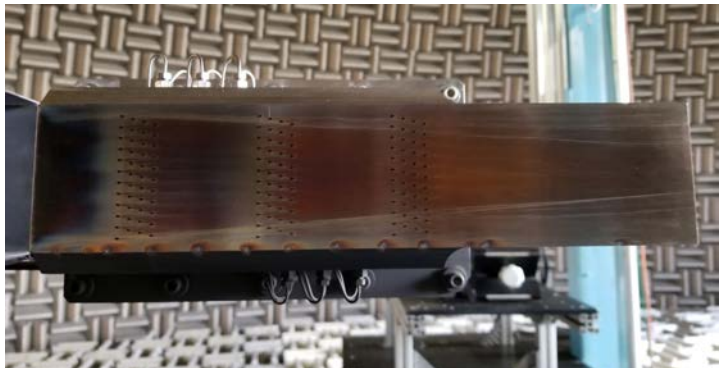
Raw IR Temperature Contour Plots, THX IV: SP49



FLIR SC655 infrared camera

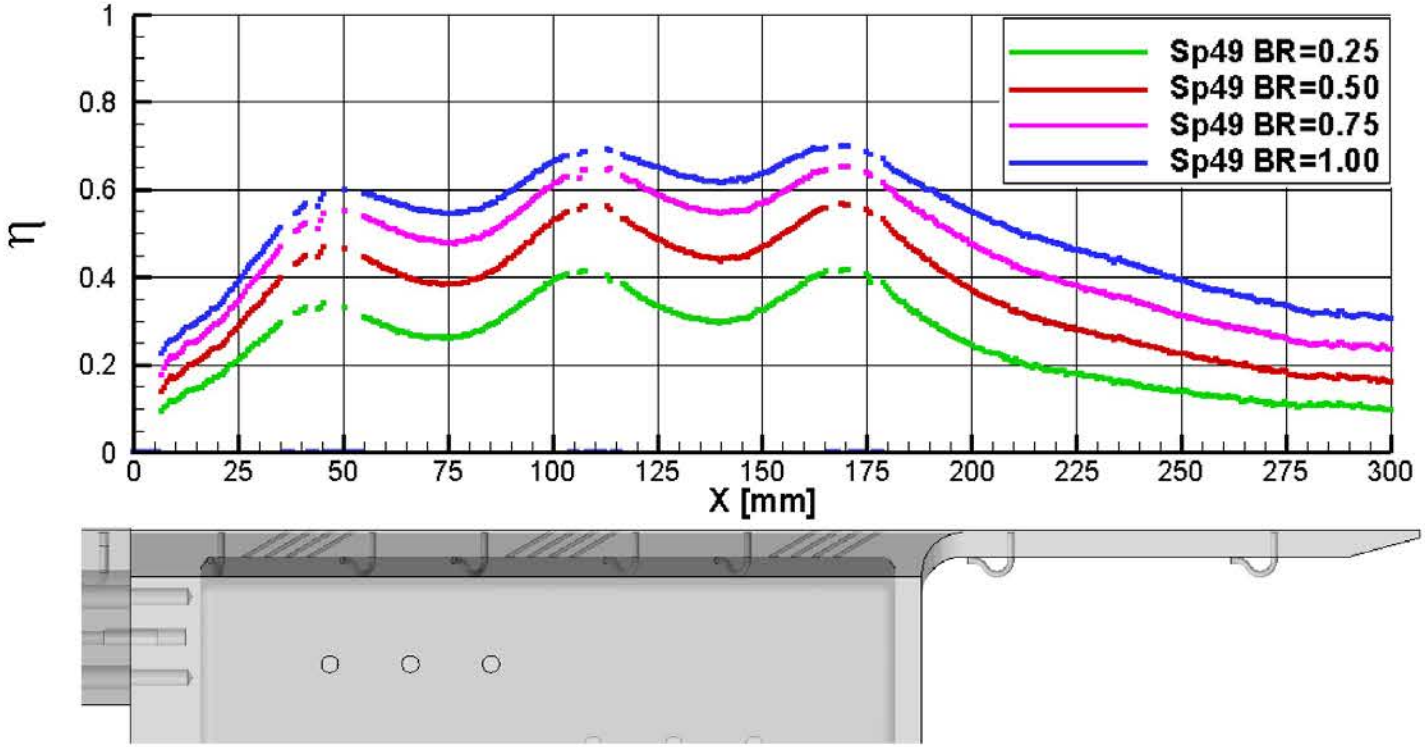
- 640 x 480 pixels (roughly 0.024”/pixel)
- Stainless steel plate not painted black
- Emissivity of surface was nominally 0.2

Plate Discoloration due to Jet Shear Layer



Centerline Film Cooling Effectiveness: THX IV

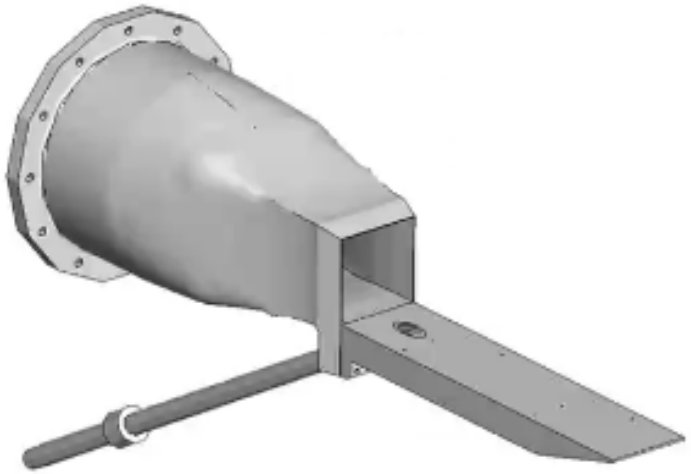
$$\eta = \frac{T_{Br=0} - T_{Br}}{T_{Br=0} - T_{Plenum}}$$



Publications from 5-Phases of THX

(THX Data sets available from NASA STI Office)

- **Phase I**: (2015-2018) PIV and hotwire measurements in a small scale tunnel (SW6) – cooling flow configuration:
  - ***NASA TM-2016-219074; AIAA Paper 2017-1004; AIAA Paper 2018-3867***
- **Phase II**: (2016-2018) Raman measurements in Small Hot Jet Acoustic Rig (SHJAR) on simple round nozzle (SMC000):
  - Mean and rms temperature data obtained to complement existing database of PIV data on SMC000
  - ***NASA TM-2017-219504; MS&T Vol. 29, 2017;*** computational work in **AIAA Paper 2017-3610; AIAA Journal, Vol. 56, 2018**
- **Phase III**: (2017) Raman and PIV measurements for square nozzle flow over 12" long flat plate with a single air injection hole; high nozzle velocity and temperature:
  - ***NASA TM-2018-219739; also as AIAA-2018-3857 paper***
- **Phase IV**: (2018-2020) Raman and PIV for same square nozzle, plate with distributed cooling holes; also surface TC's & IR measurements:
  - ***NASA TM-2019-220227 – also as AIAA-2020-1230 paper***
- **Phase V:** (2019-2020) Supersonic jet study
  - Velocity, Temperature and Density Measurements in Supersonic Jets
  - **NASA TM-2020-5007269 In publication**



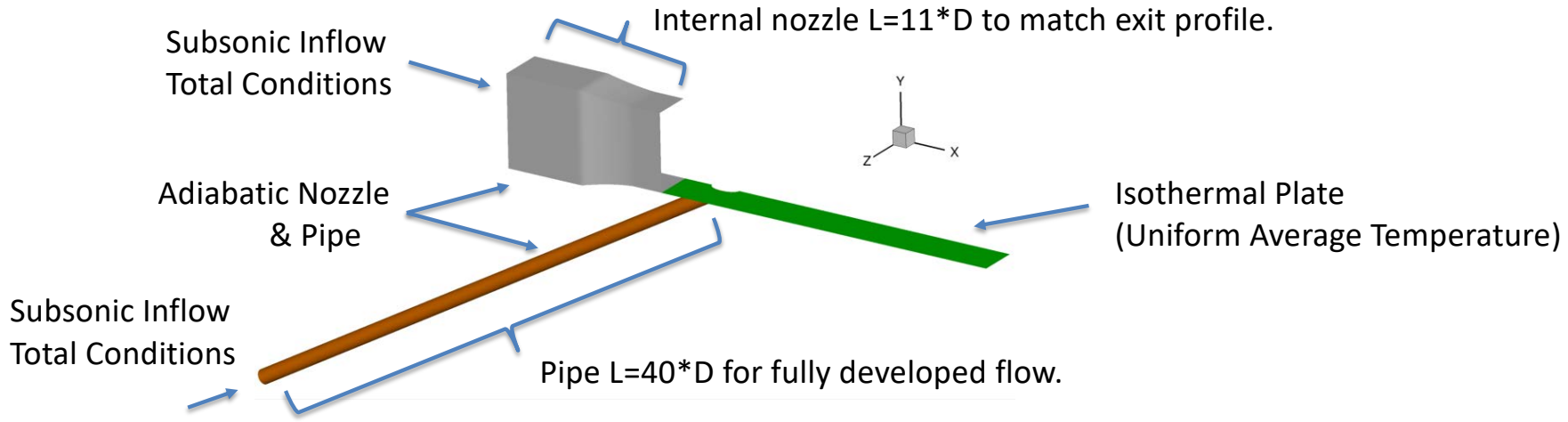
THX Phase III RANS Simulations

Dennis A. Yoder
NASA Glenn Research Center

Oct. 15, 2020

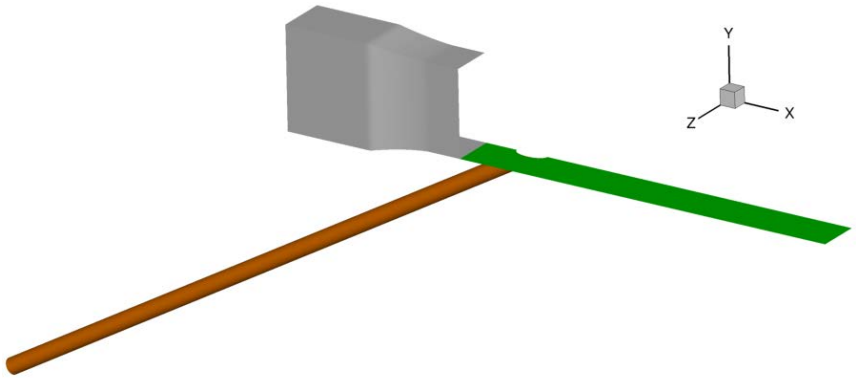
THX Phase 3: RANS Flow Solver

- FUN3D Version 13.6
  - Unstructured Finite Volume Flow Solver
- Turbulence models study (γ=1.40, Pr_t=0.90):
  - SST - Linear Shear-Stress Transport
  - QCR - Nonlinear Quadratic Constitutive Relation used with SST
  - RSM - Differential SSG/LRR Reynolds Stress Model
- Boundary Conditions (Half-Symmetry)



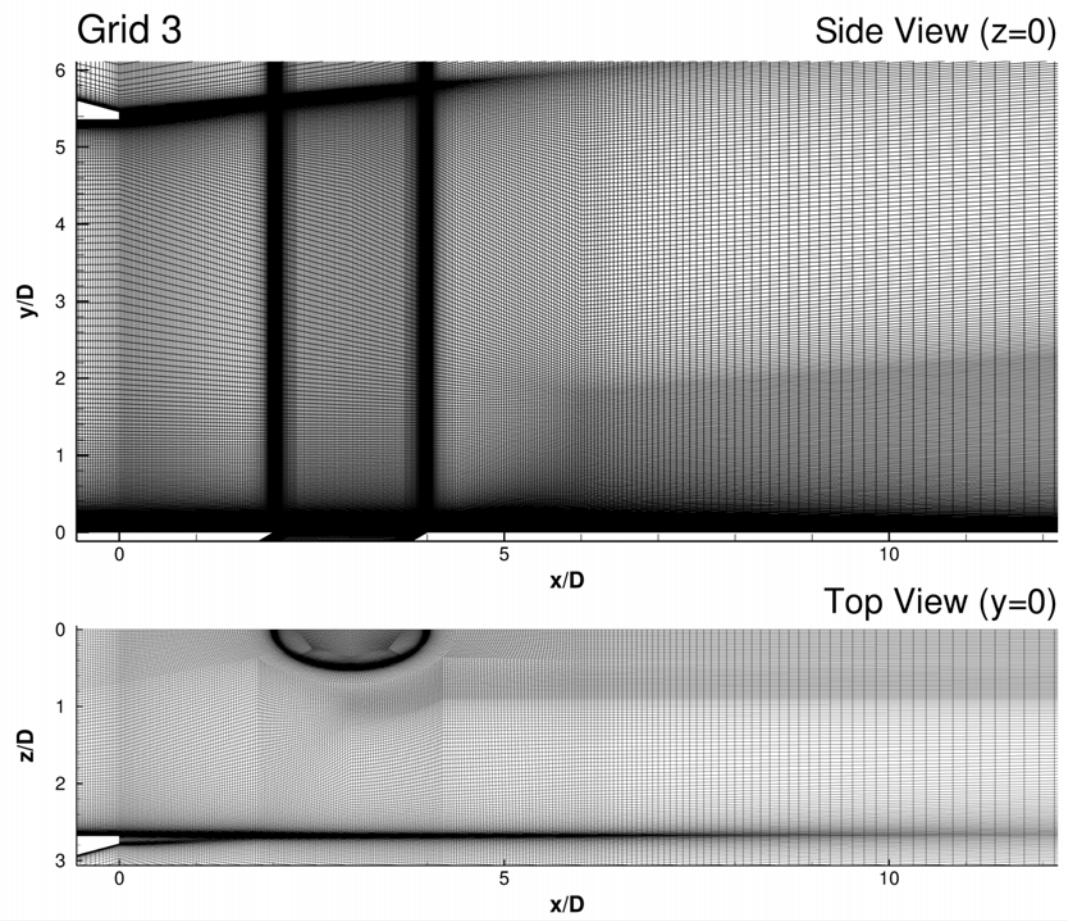
THX Phase 3: RANS Grids

- Half-symmetry structured (hex) grid topology at three resolutions.

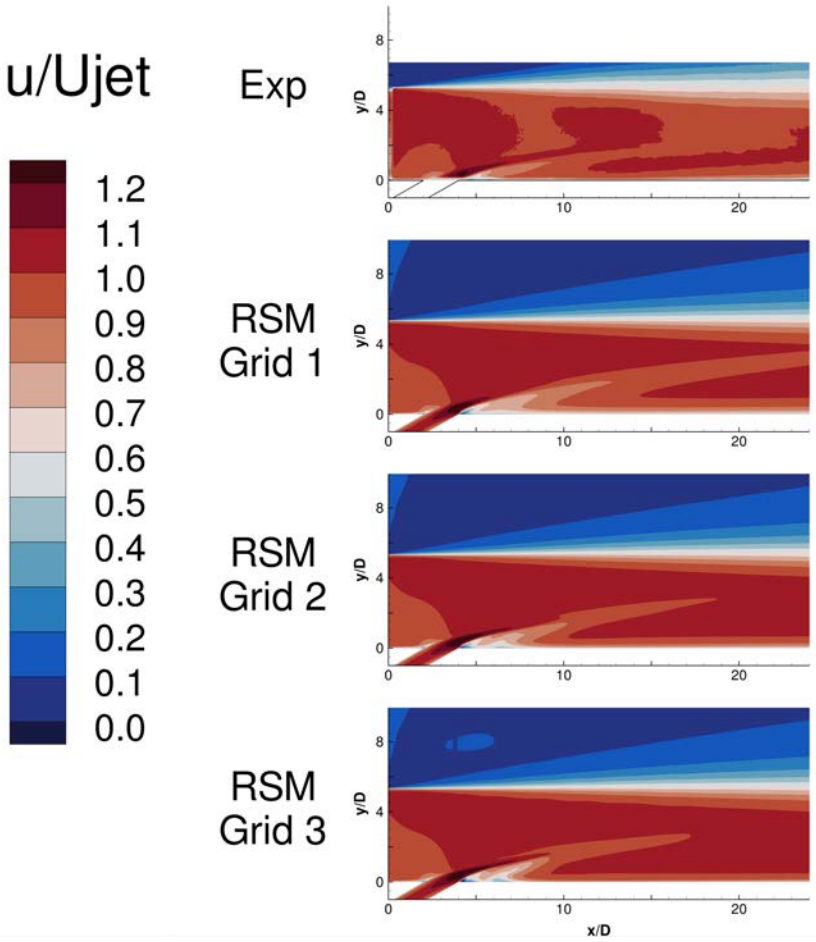


- Set point 23, Blowing ratio 1.0 & 2.0.

		Blowing Ratio		
Grid Level	Grid Nodes	SST	QCR	RSM
1 – Coarse	3,490,727	2.0	2.0	1.0, 2.0
2 – Medium	13,550,019	2.0	2.0	1.0, 2.0
3 – Fine	33,151,725	1.0, 2.0	1.0, 2.0	1.0, 2.0

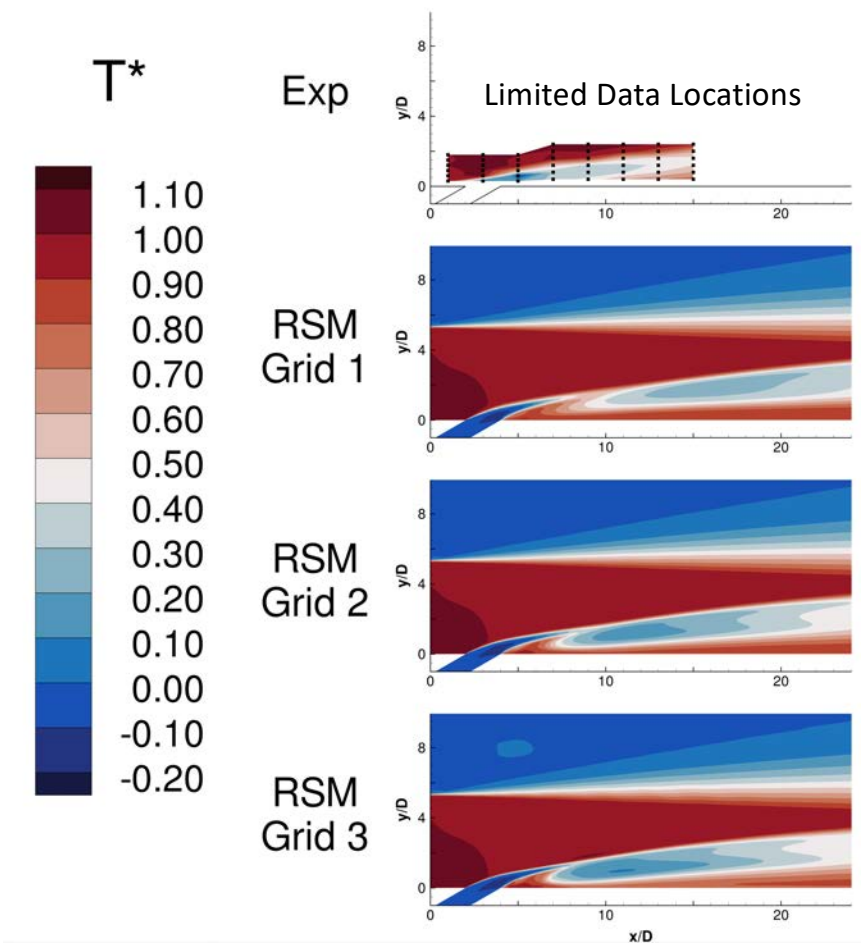


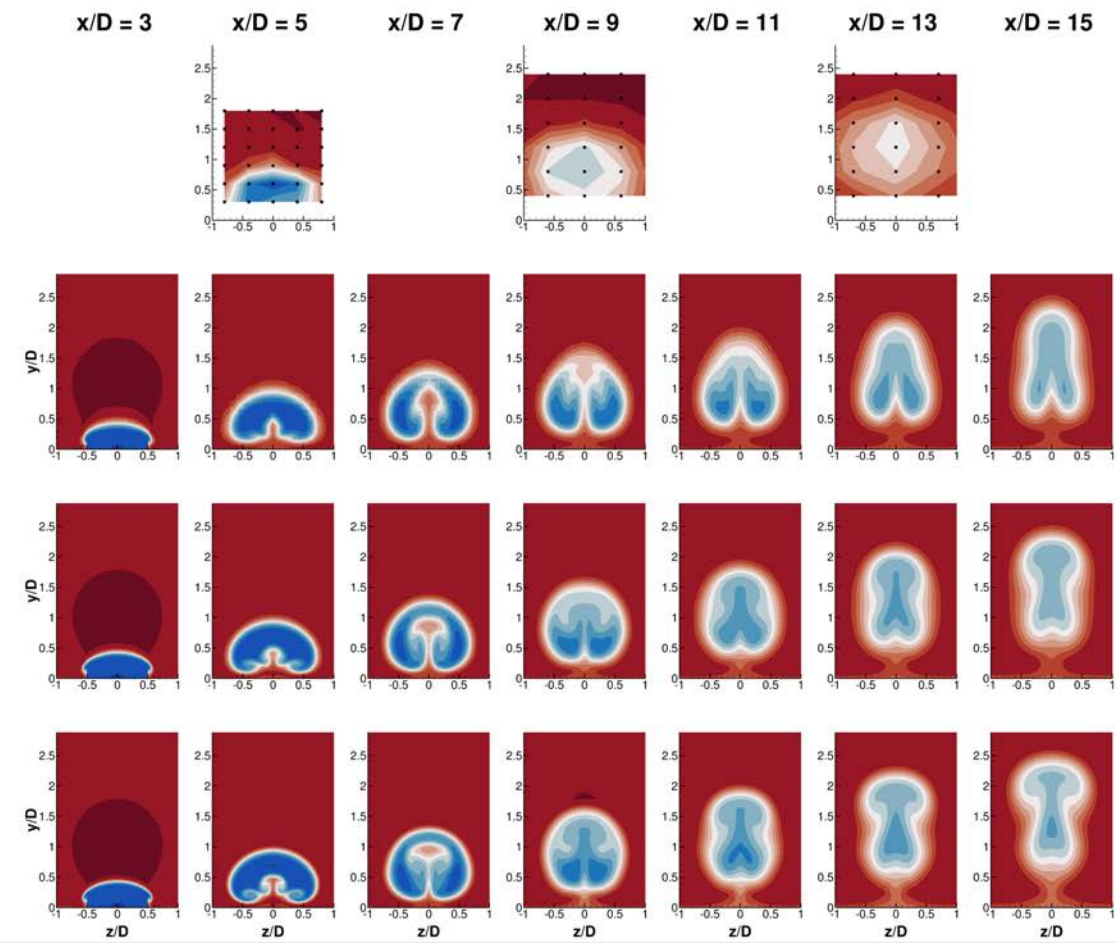
BR=2.0: RSM Grid Study – Velocity Contours



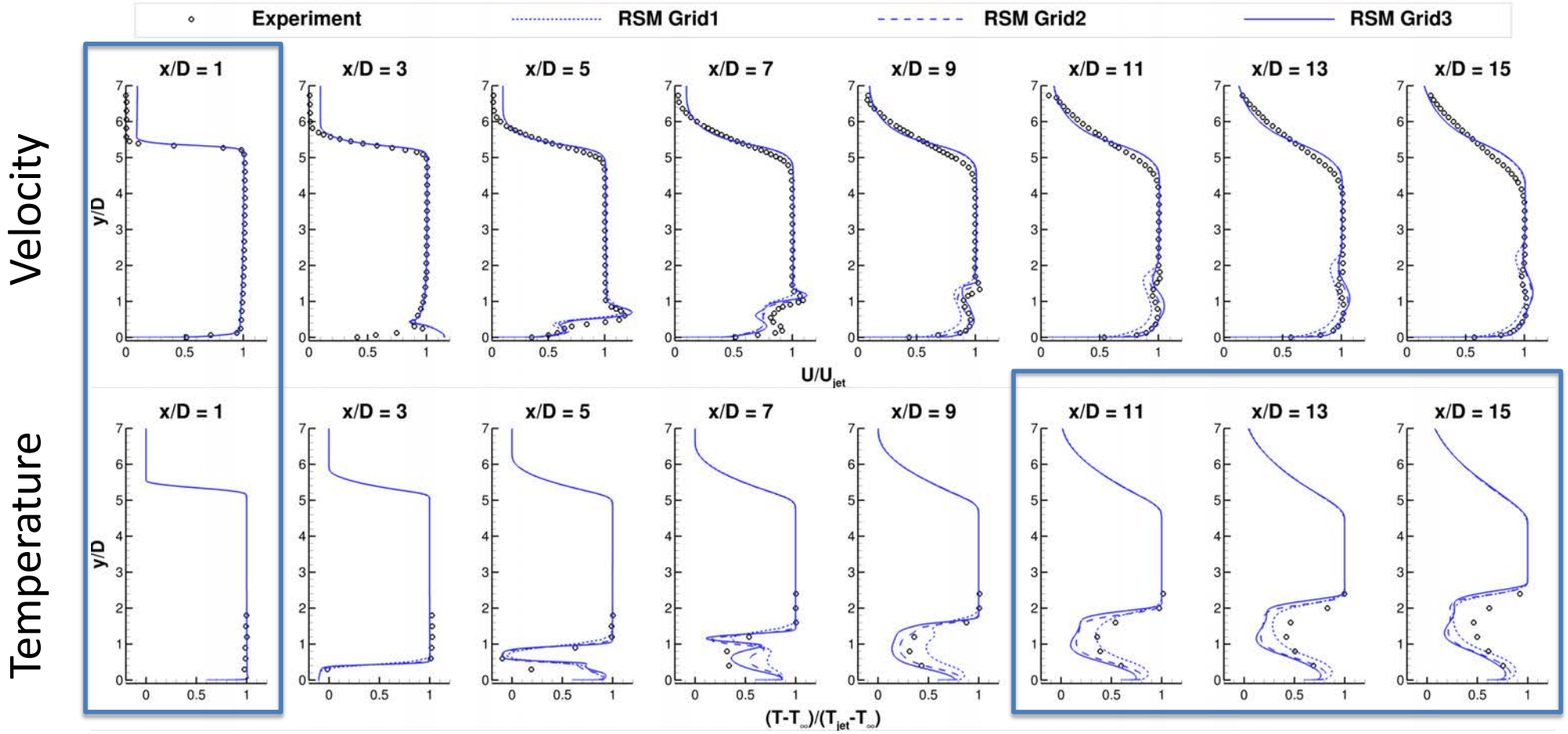


BR=2.0: RSM Grid Study – Temperature Contours

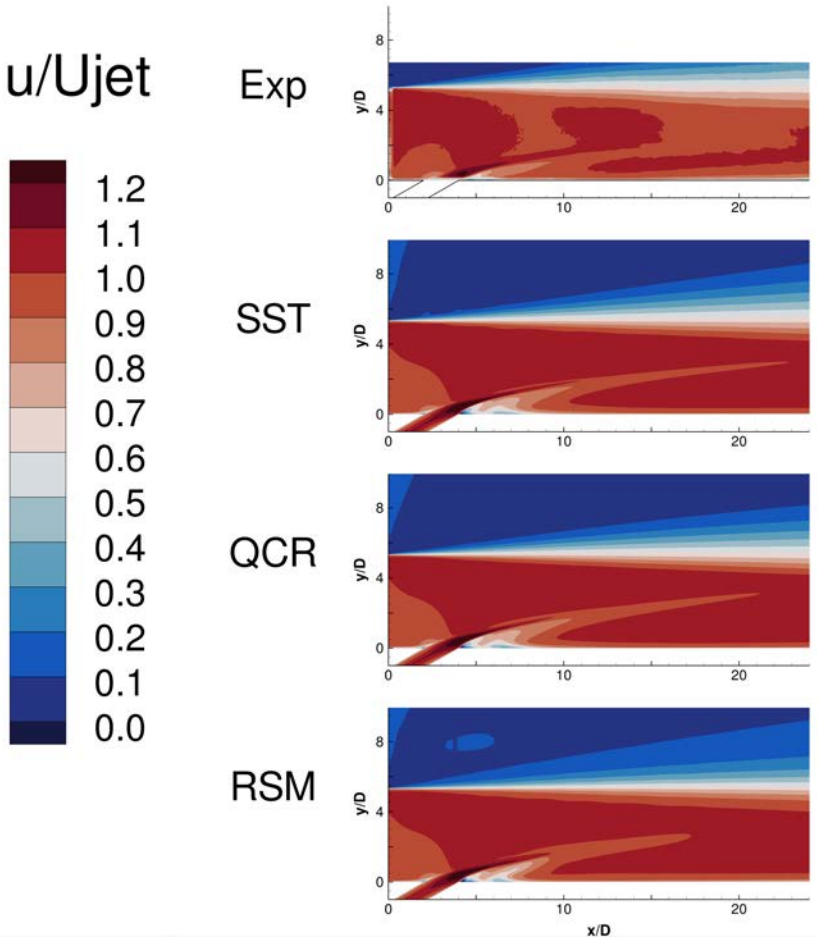


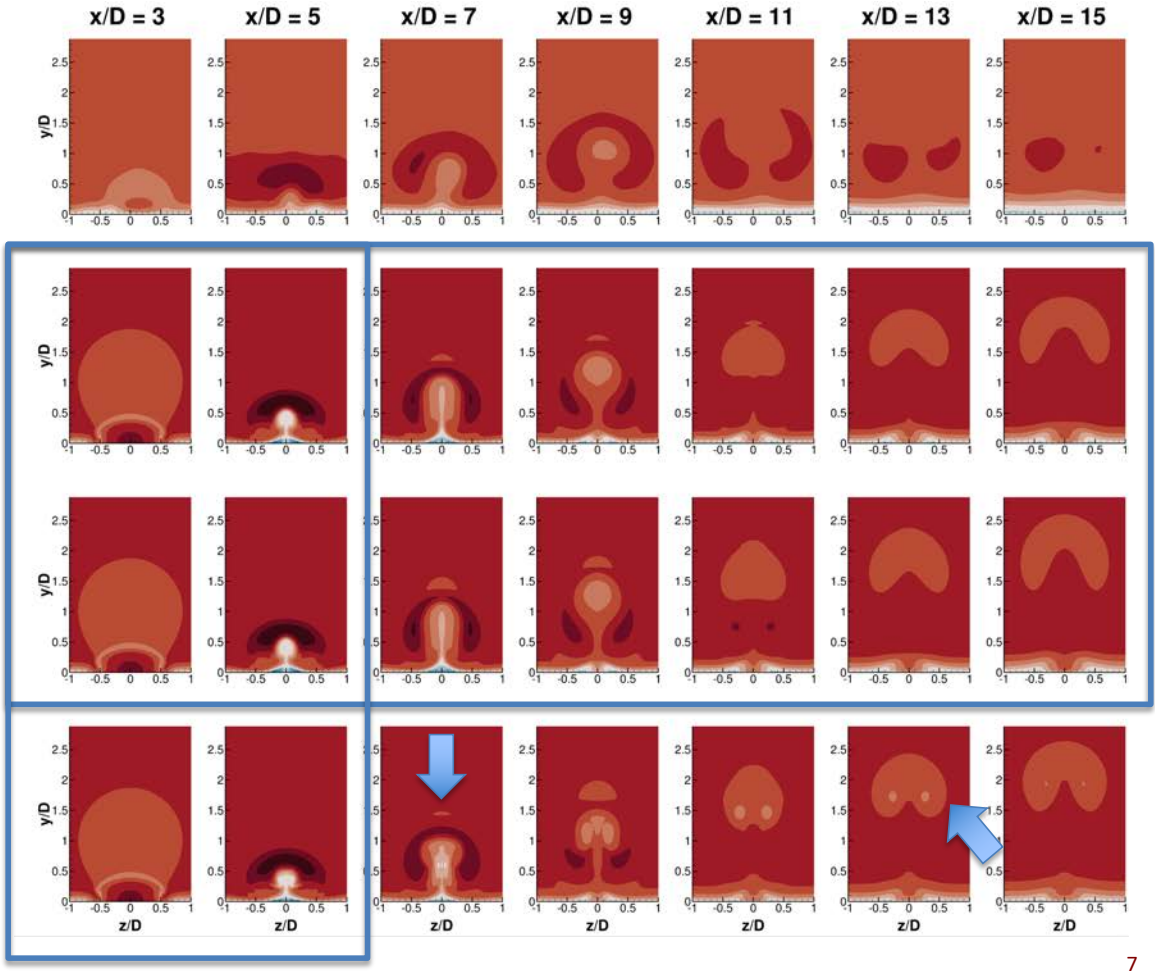


BR=2.0: RSM Grid Study – Centerline Profiles

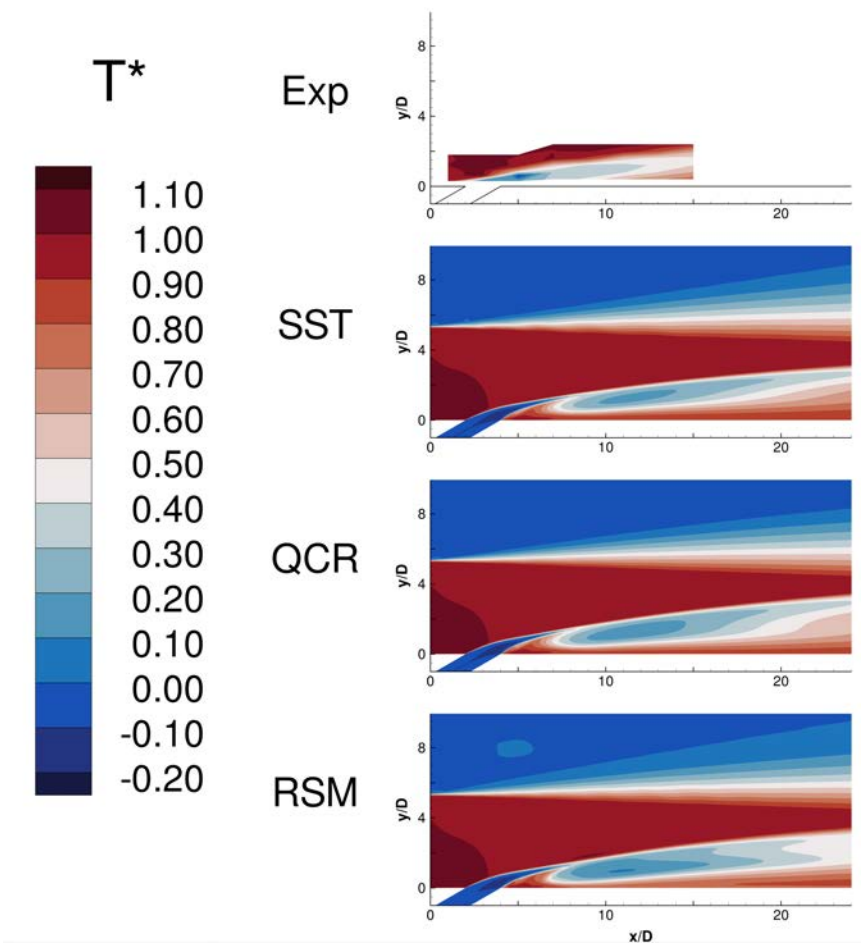


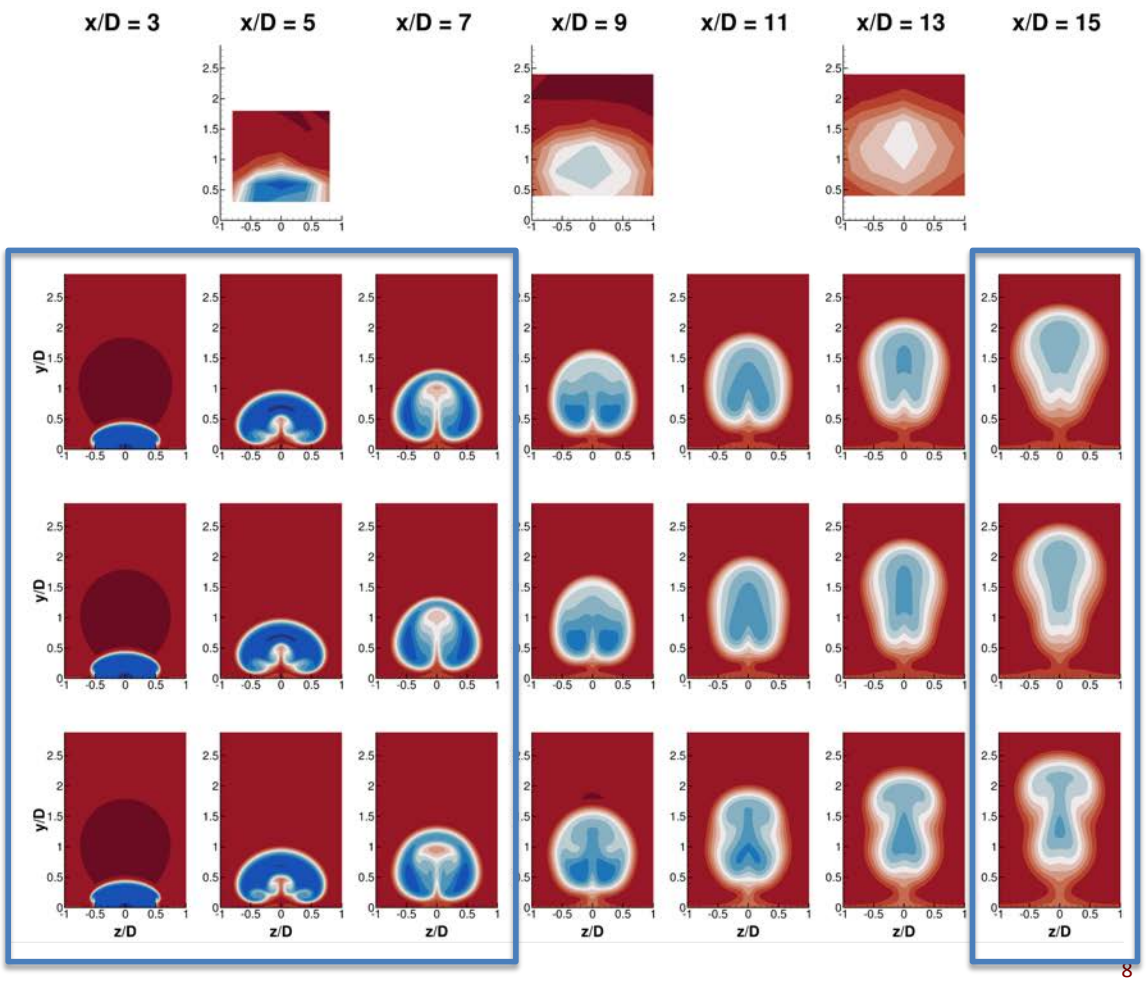
BR=2.0: RANS Study – Velocity Contours



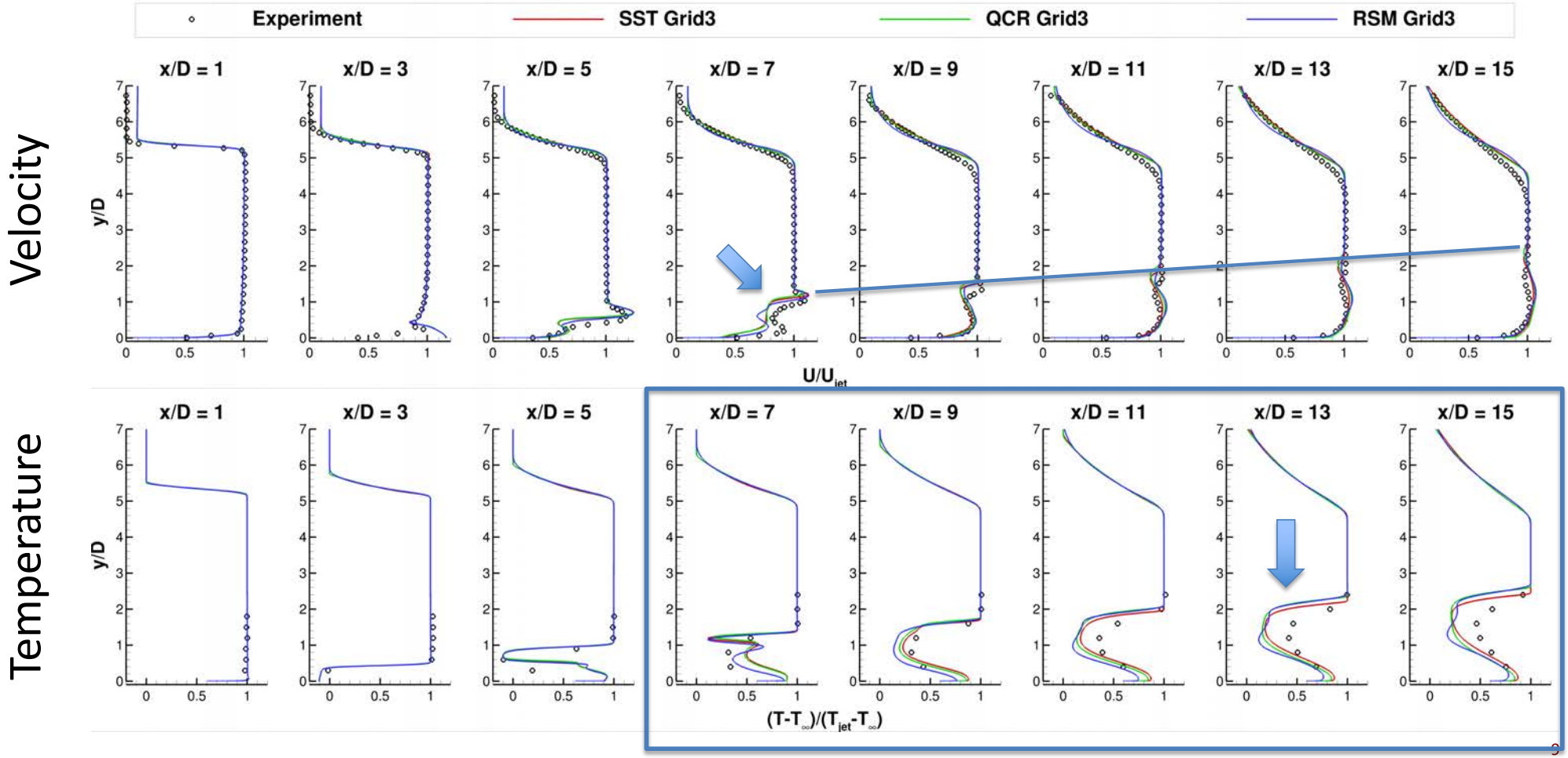


BR=2.0: RANS Study – Temperature Contours

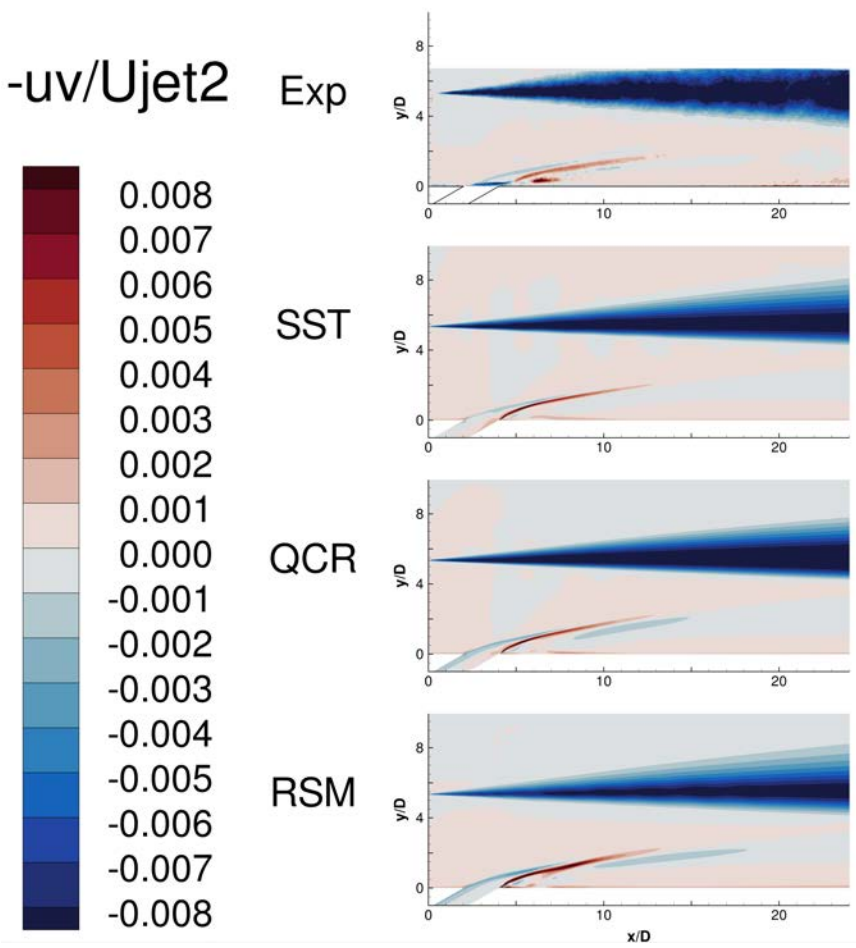


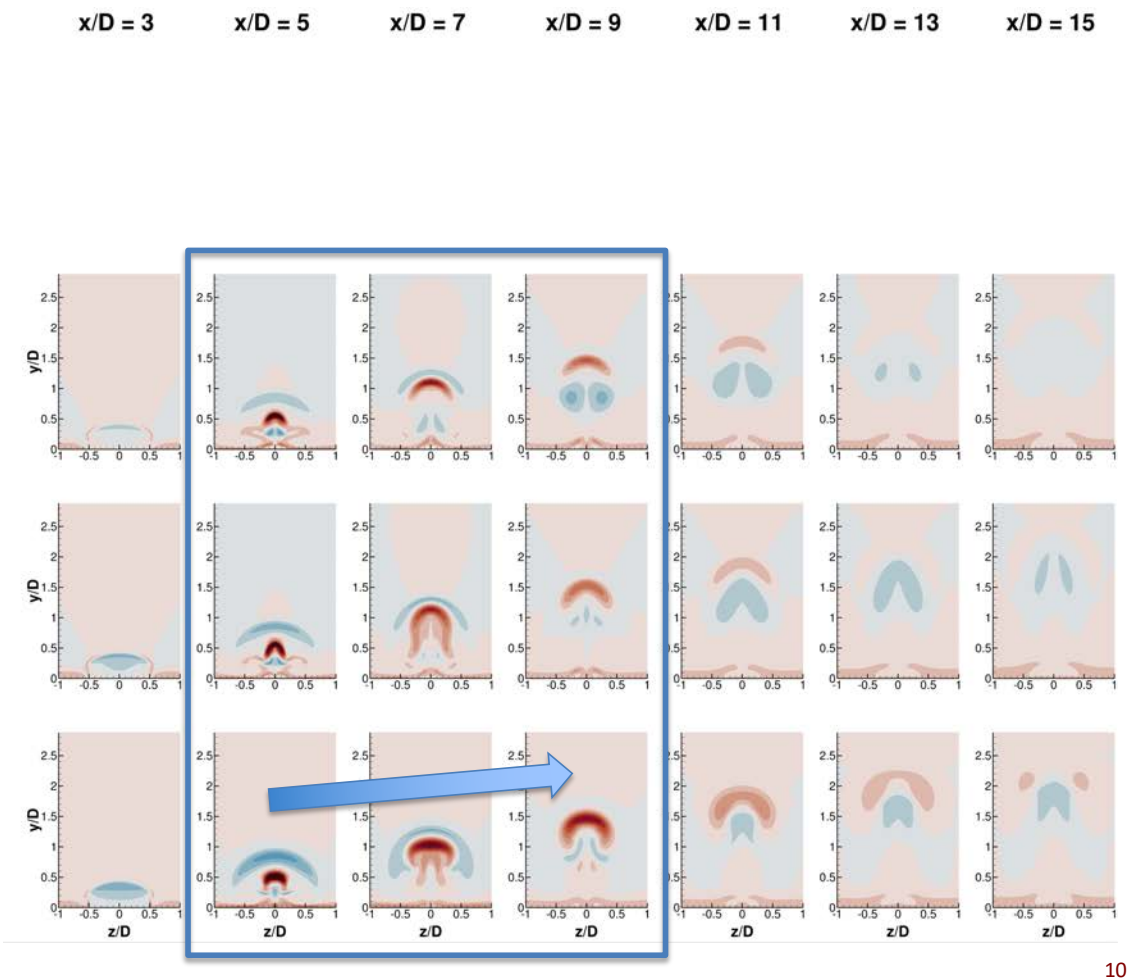


BR=2.0: RANS Study – Centerline Profiles

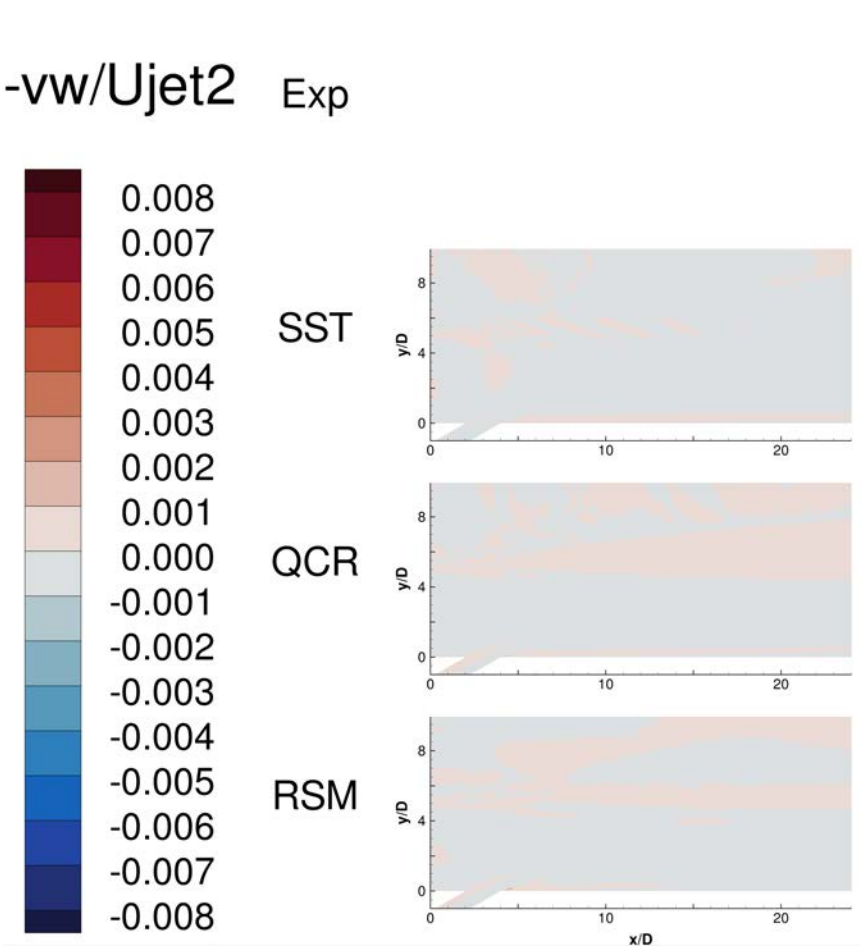


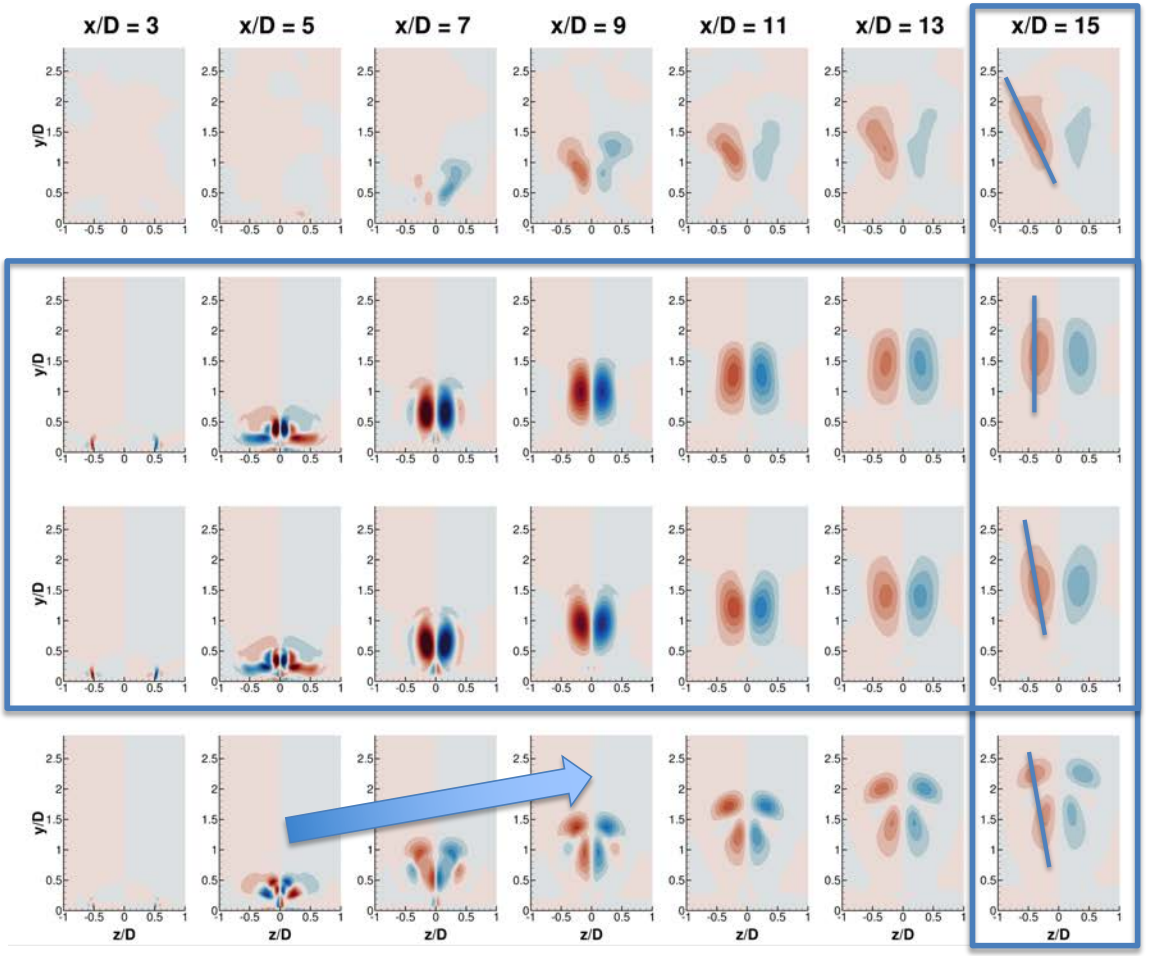
BR=2.0: RANS Study – uv Shear Stress



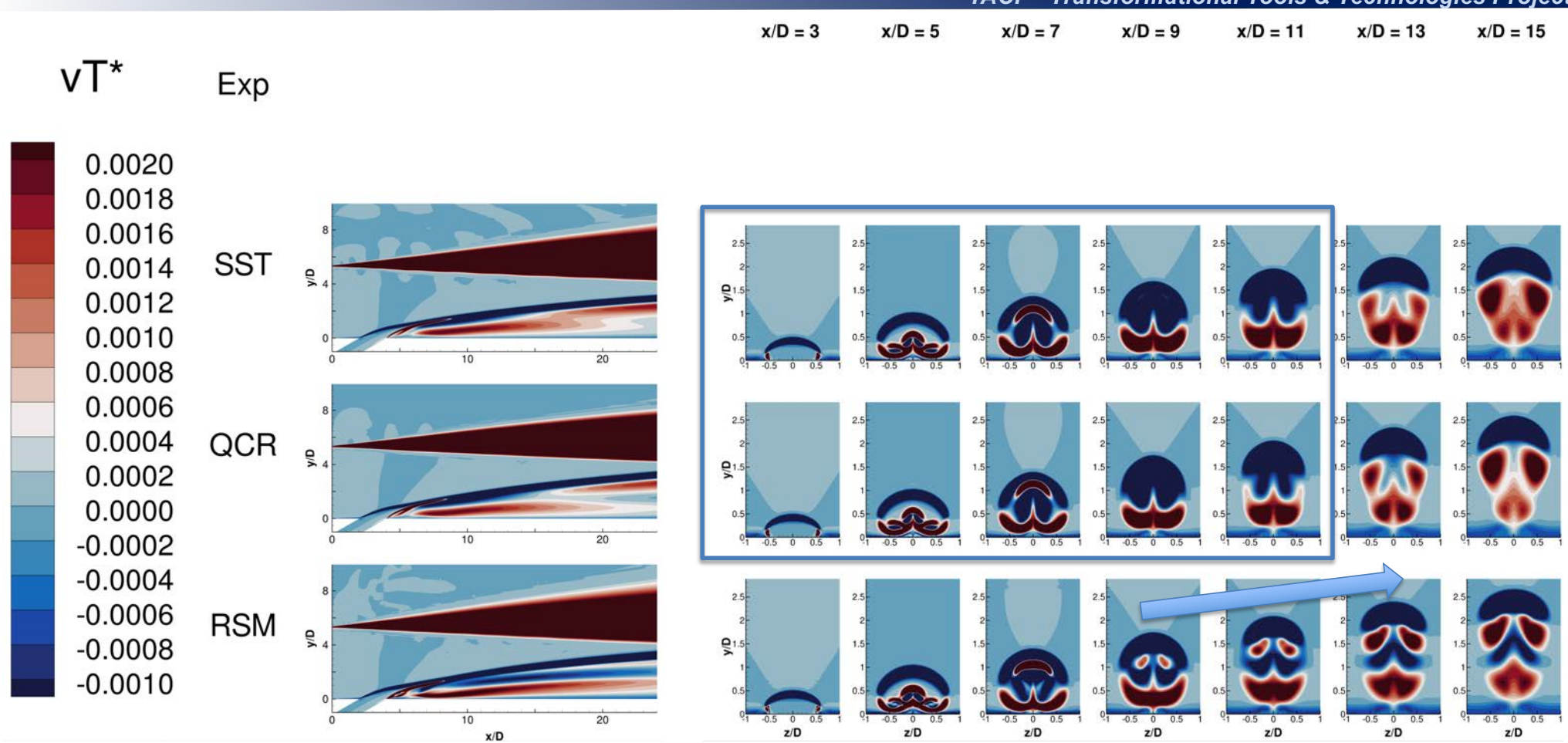


BR=2.0: RANS Study – vw Shear Stress





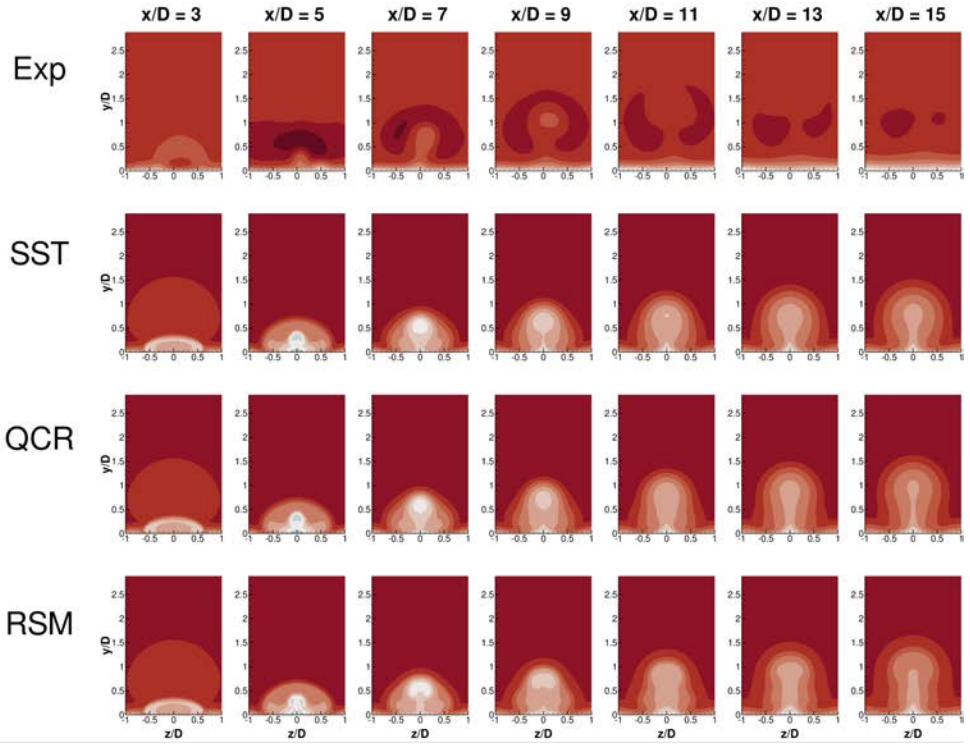
BR=2.0: RANS Study – Vertical Heat Flux



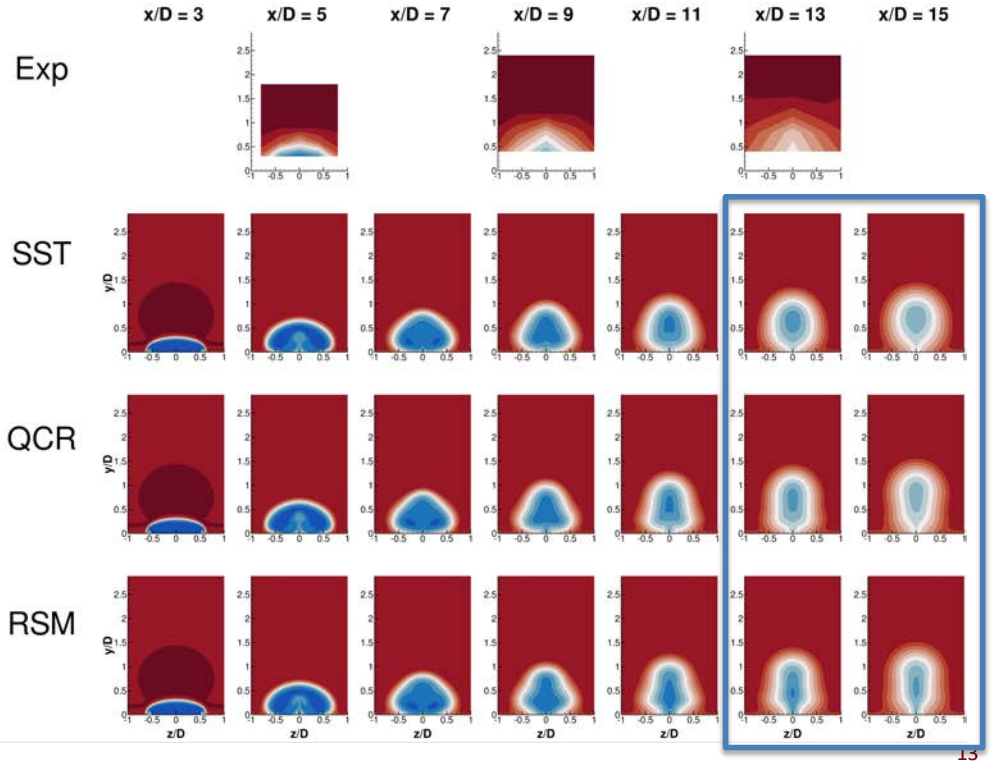
BR=1.0: RANS Study – Contours

- Model differences less evident for this more benign case.

Velocity



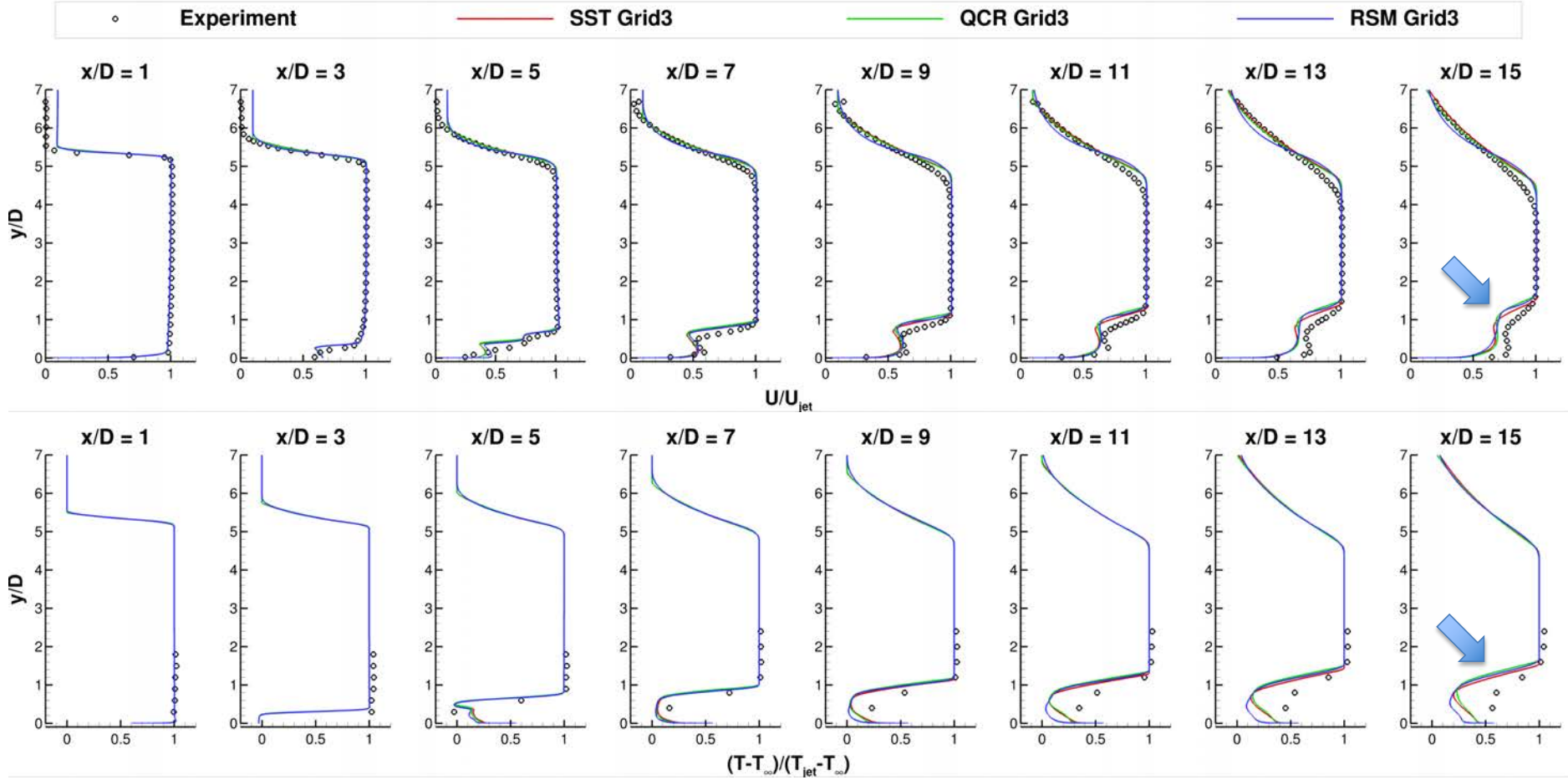
Temperature



BR=1.0: RANS Study – Centerline Profiles

Velocity

Temperature





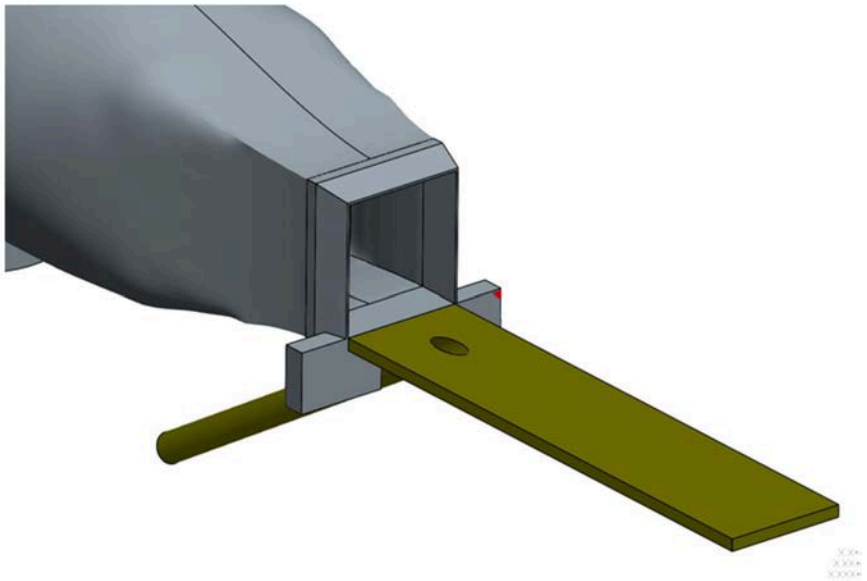
RANS Summary



- Conclusions
  - Differences between RANS models is not as large as expected, particularly for (weaker) blowing ratio 1.0.
    - RSM has stronger three-dimensionality and turbulence anisotropy.
    - QCR mimics some RSM characteristics.
  - All of the RANS models are deficient in predicting jet-in-crossflow physics.
    - Injection penetration is over-predicted.
    - Mixing and centerline wake recovery is too slow.
    - Temperature predictions are worse than velocity.
      - $\overline{\rho u_i'' h''} = -\frac{\mu_t}{Pr_t}\frac{\partial \tilde{h}}{\partial x_i}$ Turbulent Heat Flux: Gradient Diffusion Approximation
- Ongoing Work
  - Unstructured grid assessment.
  - Preparing paper for 2021 AIAA Aviation Conference.

THX 3 (Single Hole) Results

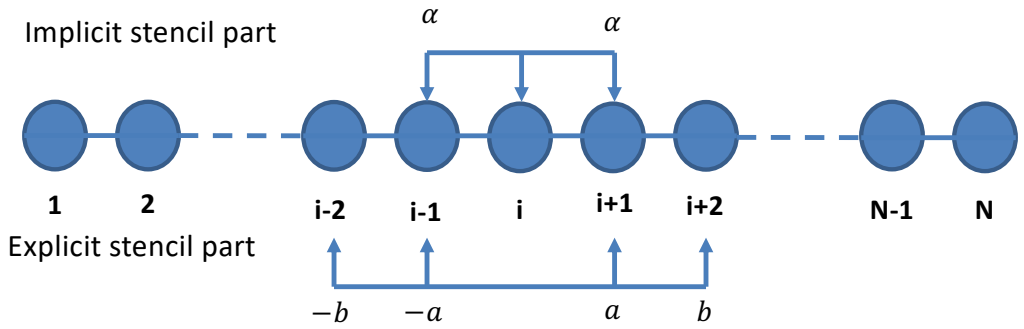
Michael Borghi
NASA GRC
Turbomachinery and Turboelectric Systems Branch



FDL3DI Code

- Developed by USAF AFRL at WPAFB
- Structured grid solver – allowed sequencing, or a subset of largest grid to be solved, enables methodical grid sensitivity studies.
- High order "Compact" numerical scheme
  - 6th order spatial accuracy stencil
  - 8th order filter
- Implicit LES – No sub-grid model
- Overset grid topology allow for most complex geometries

Compact Difference Interior Scheme



$$\alpha\phi'_{i-1} + \phi'_i + \alpha\phi'_{i+1} = \frac{b}{4}(\phi_{i+2} - \phi_{i-2}) + \frac{a}{2}(\phi_{i+1} - \phi_{i-1})$$

Non-dimensional Navier-Stokes

$$\frac{\partial \rho}{\partial t} + \frac{\partial}{\partial x_i}(\rho u_i) = 0$$

$$\frac{\partial}{\partial t}(\rho u_i) + \frac{\partial}{\partial x_i}\left(\rho u_i u_j + p\delta_{ij} - \frac{1}{Re} t_{ij}\right) = 0$$

$$\frac{\partial}{\partial t}(\rho e_0) + \frac{\partial}{\partial x_i}\left[u_i(\rho e_0 + p) - \frac{1}{Re}(u_j t_{ij}) + \frac{1}{(\gamma-1)PrM^2Re} q_i\right] = 0$$

$$e_0 = e + \frac{1}{2}u_i u_i \qquad q_i = -\mu\frac{\partial T}{\partial x_i} \qquad t_{ij} = 2\mu s_{ij} - \frac{2}{3}\frac{\partial u_k}{\partial x_k}$$

Non-dimensionalizations

$$x_i^* = \frac{X_i}{L} \qquad u_i^* = \frac{u_i}{Vref} \qquad t^* = \frac{tV_{ref}}{L} \qquad \rho^* = \frac{\rho}{\rho_{ref}}$$

$$P^* = \frac{p}{\rho_{ref}V_{ref}^2} \qquad T^* = \frac{T}{T_{ref}} \qquad \mu^* = \frac{\mu}{\mu_{ref}} \qquad e^* = \frac{e}{V_{ref}^2}$$

$$Re = \frac{\rho_{ref}V_{ref}L}{\mu_{ref}} \qquad \Pr = \frac{\mu_{ref}C_p}{\kappa_{ref}} \qquad M = \frac{V_{ref}}{\sqrt{\frac{\gamma p_{ref}}{\rho_{ref}}}}$$

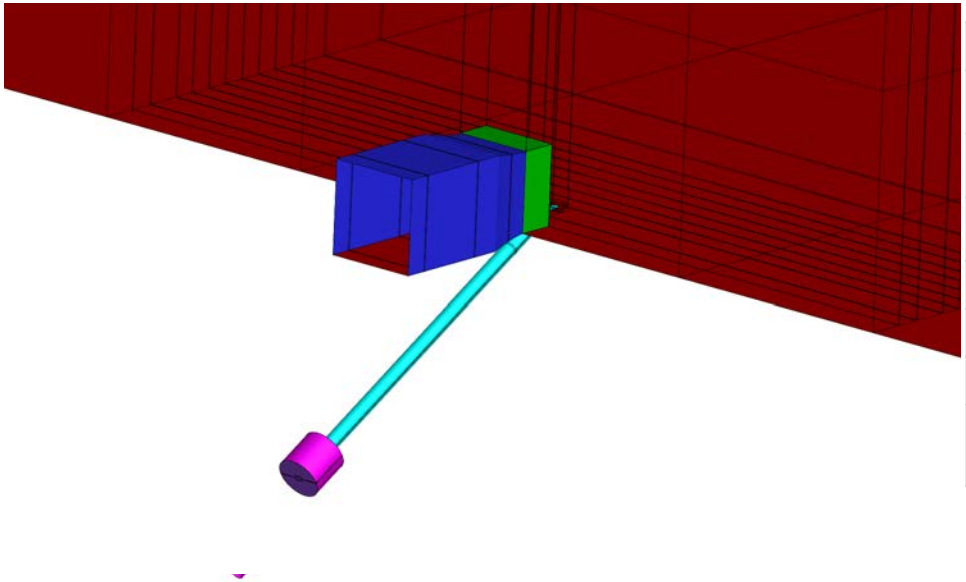
FDL3DI Grid Details

- Grids originate from the same family of sequenceable grids
- Full Mesh comprised of 36 overset blocks
  - 000 – 3.1 Billion points (Not run)
  - 010 – 1.52 Billion points
  - 111 – 356 Million points
- O-H overset grid topology for cooling hole

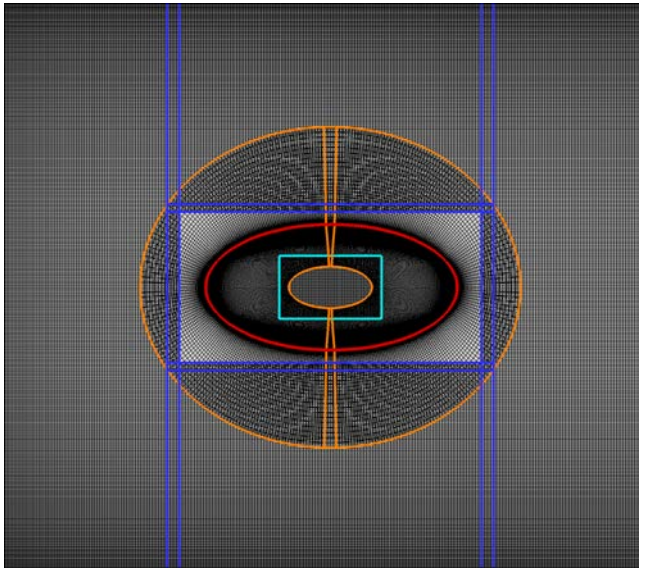
Grid Spacings and Cases run

Blowing Ratio	Grid	Points/DOF	# CPU Cores	x+	z+	Y+ wall
1.0	111	356,000,000	8,000	30	18.75	2
2.0	111	356,000,000	8,000	30	18.75	2
2.0	010	1,520,000,000	16,000	15	9.4	2

Computational Domain and Boundary Conditions



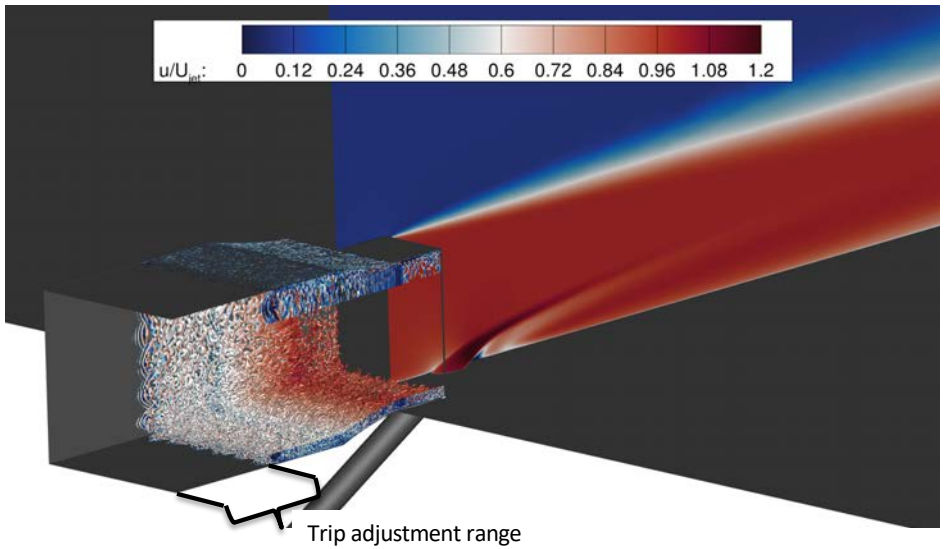
Red:	Isothermal wall - Plate
Light Blue:	Isothermal wall – Tube
Dark Blue:	Adiabatic wall – Nozzle interior
Green:	Adiabatic wall - Nozzle exterior
Pink:	Adiabatic wall - Plenum
Orange:	Pressure outflow
Yellow:	Subsonic velocity inlet
Purple:	Hold totals – Nozzle and plenum



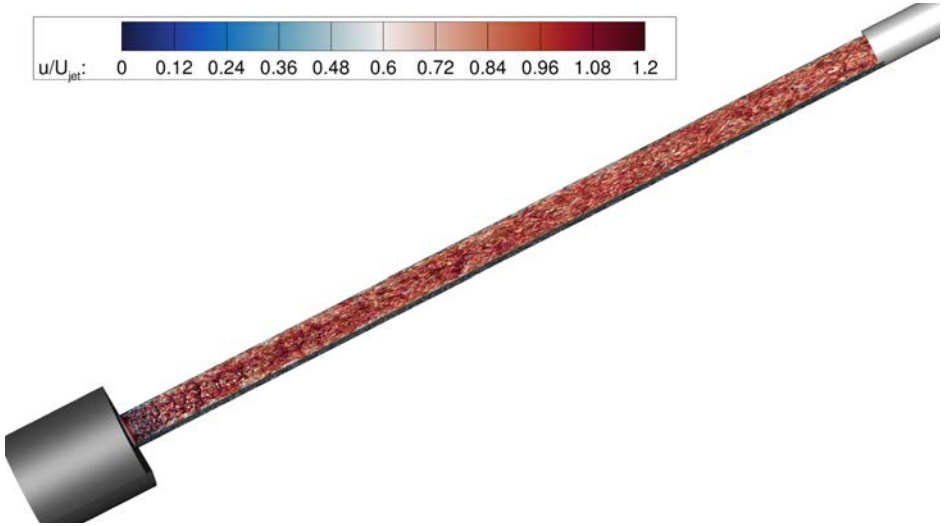
Sponge region from end of the plate (x/D = 24) to outflow
where D is the cross-section diameter of the injector tube (0.5 in.)

O-H overset topology for cooling hole mesh

FDL3DI Grid Details



Iso-surfaces of Q-criterion highlighting the BL trip



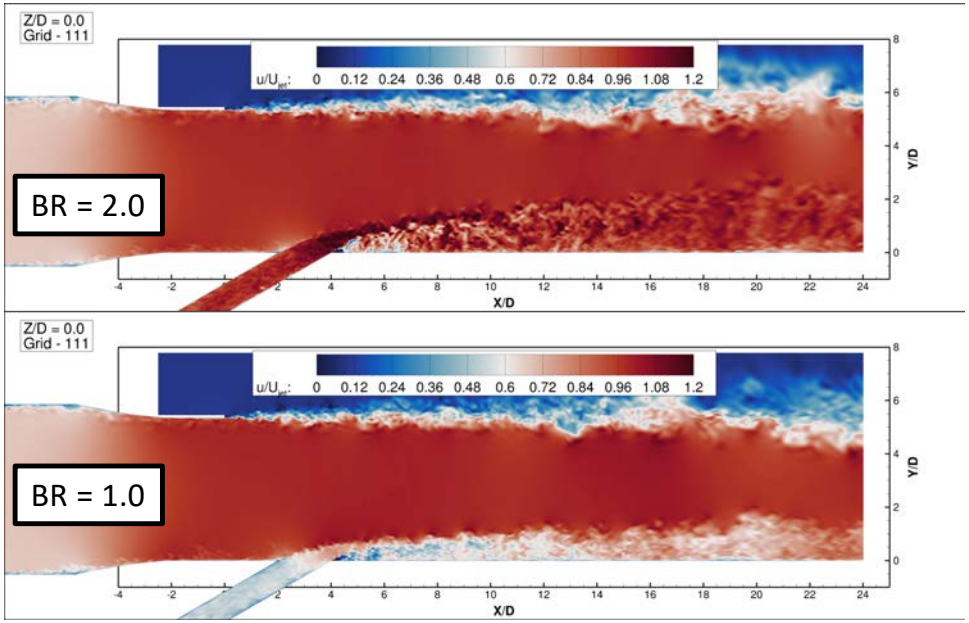
Iso-surfaces of Q-criterion highlighting the natural transition of the tube

- Momentum source term used to trip Nozzle boundary layer
  - Source term adapted from Poggie et al. 2015
- Trip location and strength varied to better match experimental data
- Sharp transition from Plenum to tube naturally trips flow

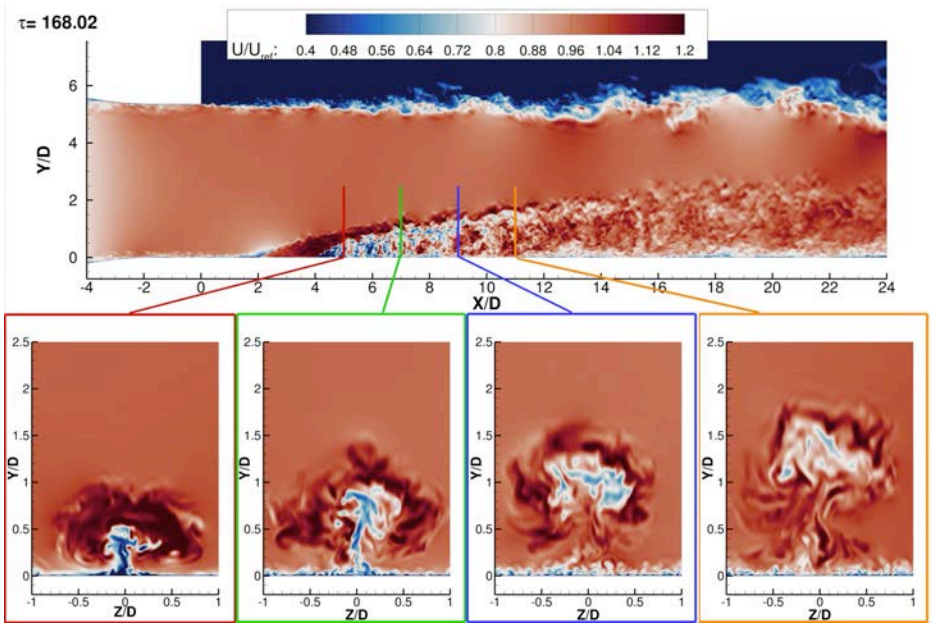
$$f = \frac{2D_c}{\pi l_1 l_2 l_3} \sin^2\left(\pi \frac{x_3 - X_3}{l_3}\right) \exp\left[-\left(\frac{x_1 - X_1}{l_1}\right)^2 - \left(\frac{x_2 - X_2}{l_2}\right)^2\right]$$

$$f_1 = f\cos(\theta)$$
$$f_2 = f\sin(\theta)$$
$$f_3 = 0$$

THX Phase 3 LES using the FDL3DI Code



Instantaneous U-velocity contours for BR=2.0 and BR=1.0

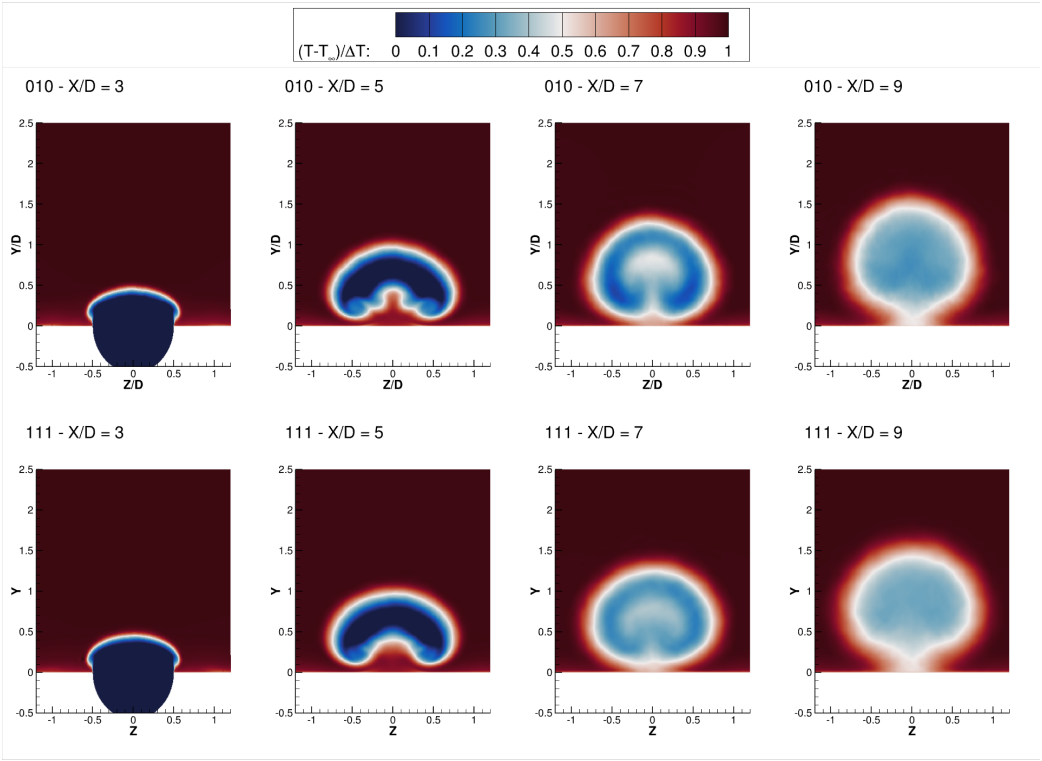


Animation of U-velocity for BR=2.0 at Z/D = 0, and X/D = [3,5,7,9]

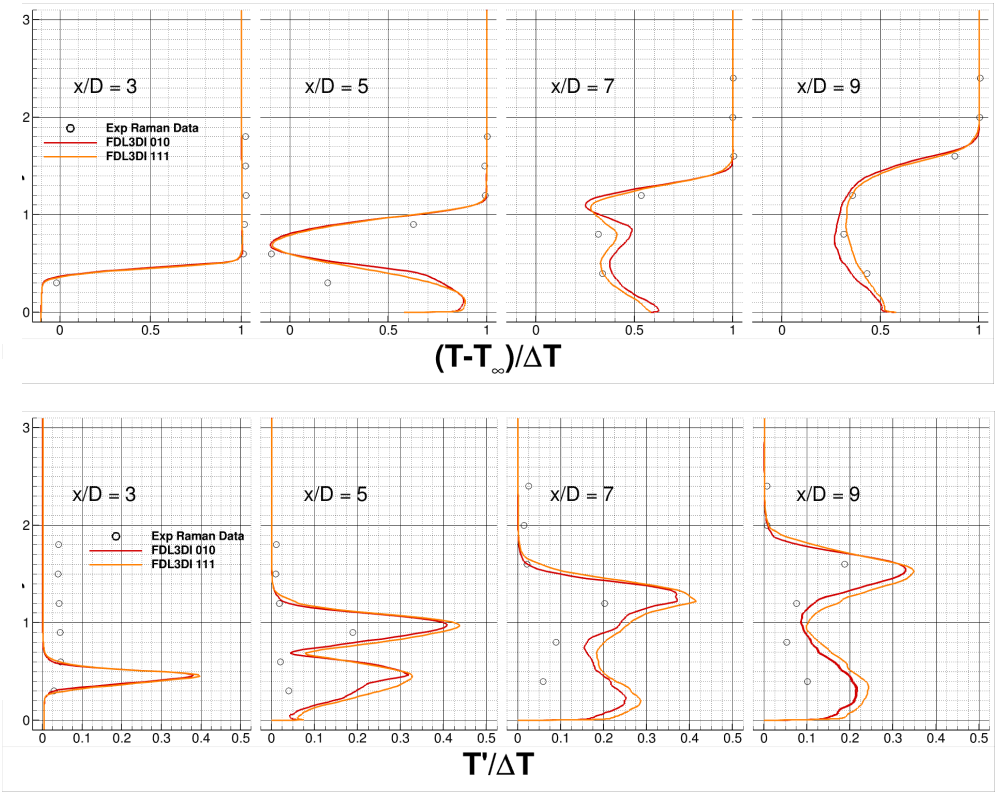
THX3 LES cases run with FDL3DI v2

Blowing Ratio	Grid	Points/DOF	# Cores	dt (tau)	Time Scheme	Tau averaged	x+	z+
2.0	111	356,000,000	8,000	2.0e-4	Beam-Warming	232	30	18.75
2.0	010	1,520,000,000	16,000	2.0e-4	Beam-Warming	142	15	9.4
1.0	111	356,000,000	8,000	2.0e-4	Beam-Warming	253	30	18.75

THX Phase 3 LES Effect of Grid 010 vs 111



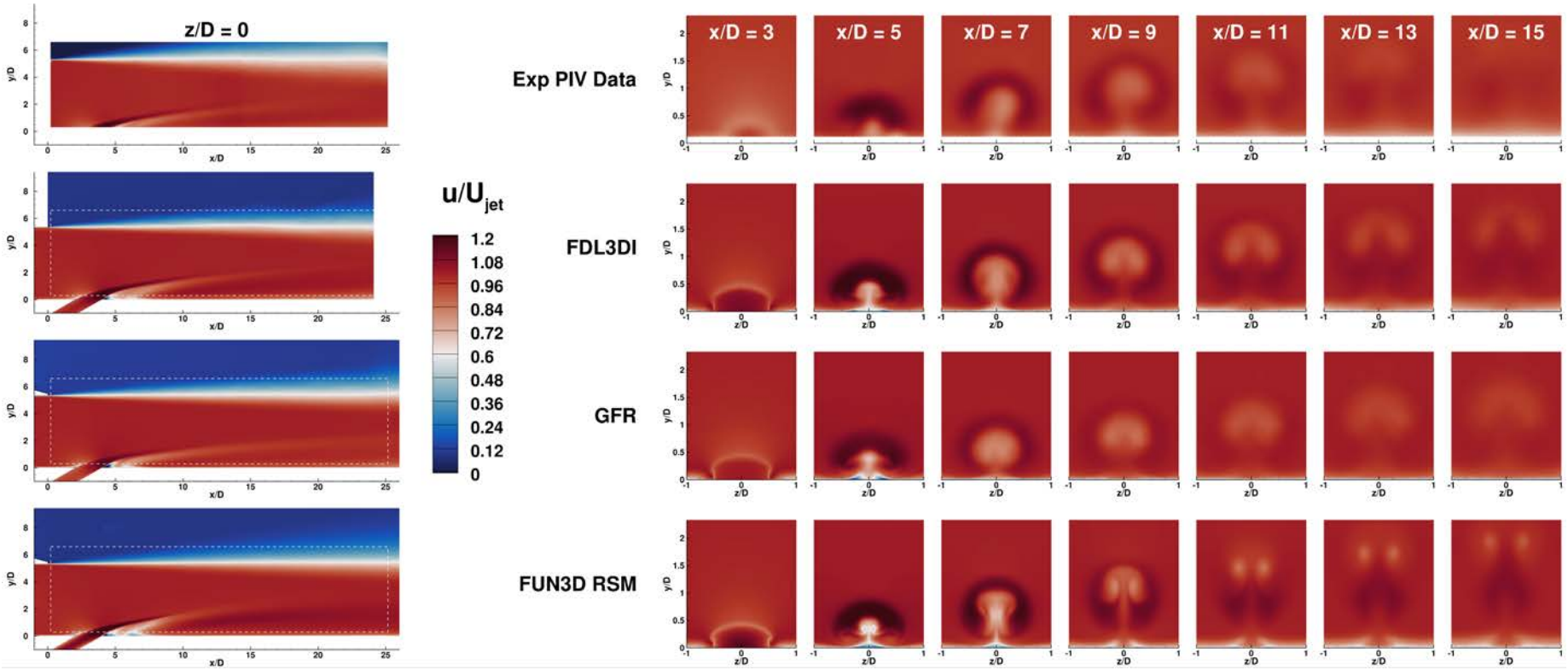
Instantaneous Temperature contours for BR=2.0 on the 010 (top) and 111 (bottom) Grid Levels



Mean and RMS Temperature profiles for BR=2.0 on the 010 and 111 Grid Levels

Numerical Results

Streamwise Mean Velocity Contours



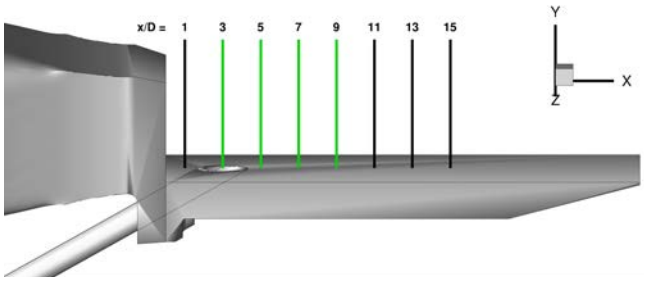
- FDL3DI and GFR have strong agreement throughout the flow domain.
- RANS predicts the cooling jet lifting off from the plate more, while maintaining the CRVP longer

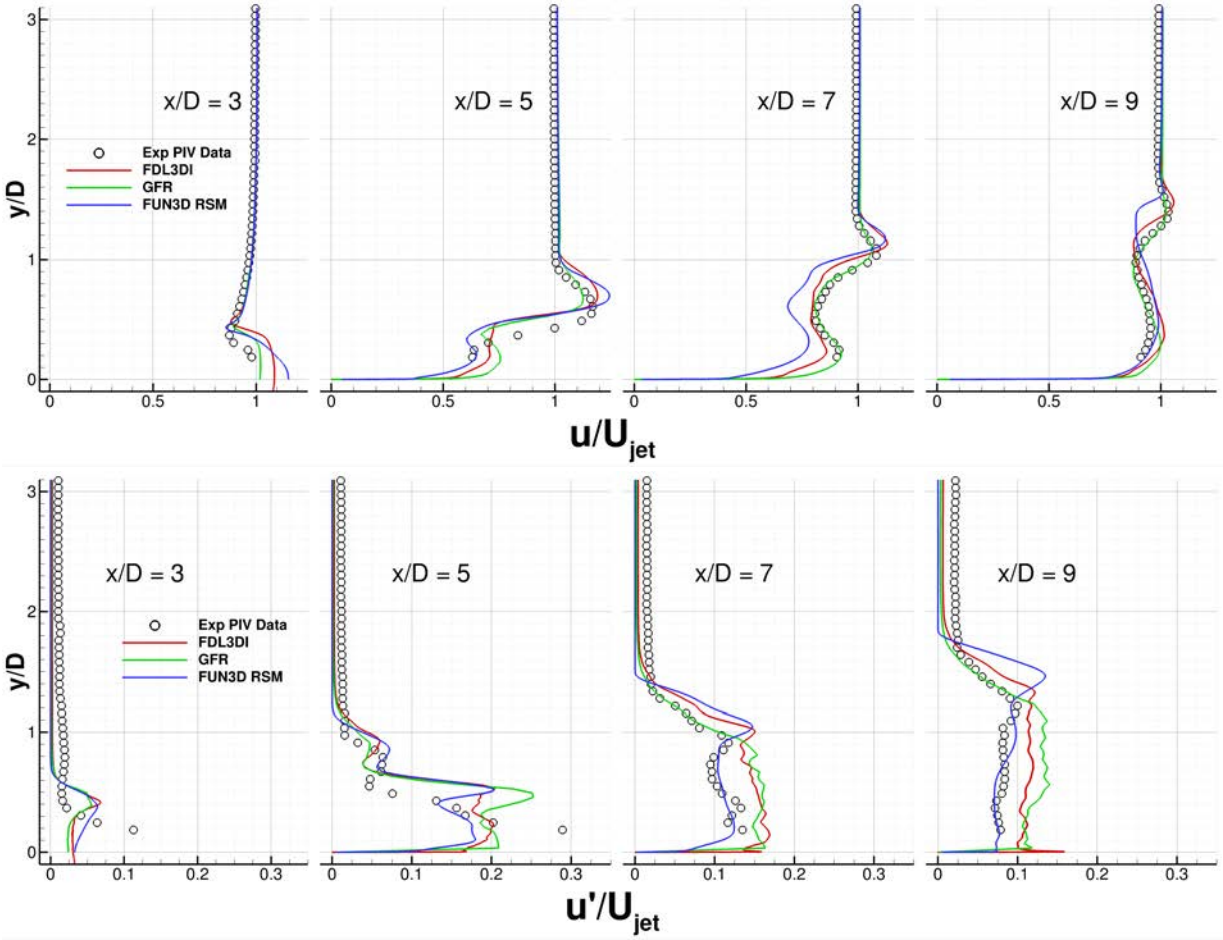
Numerical Results

Set Point 23, Blowing Ratio = 2.0

Streamwise Mean and RMS (turbulent) Velocities

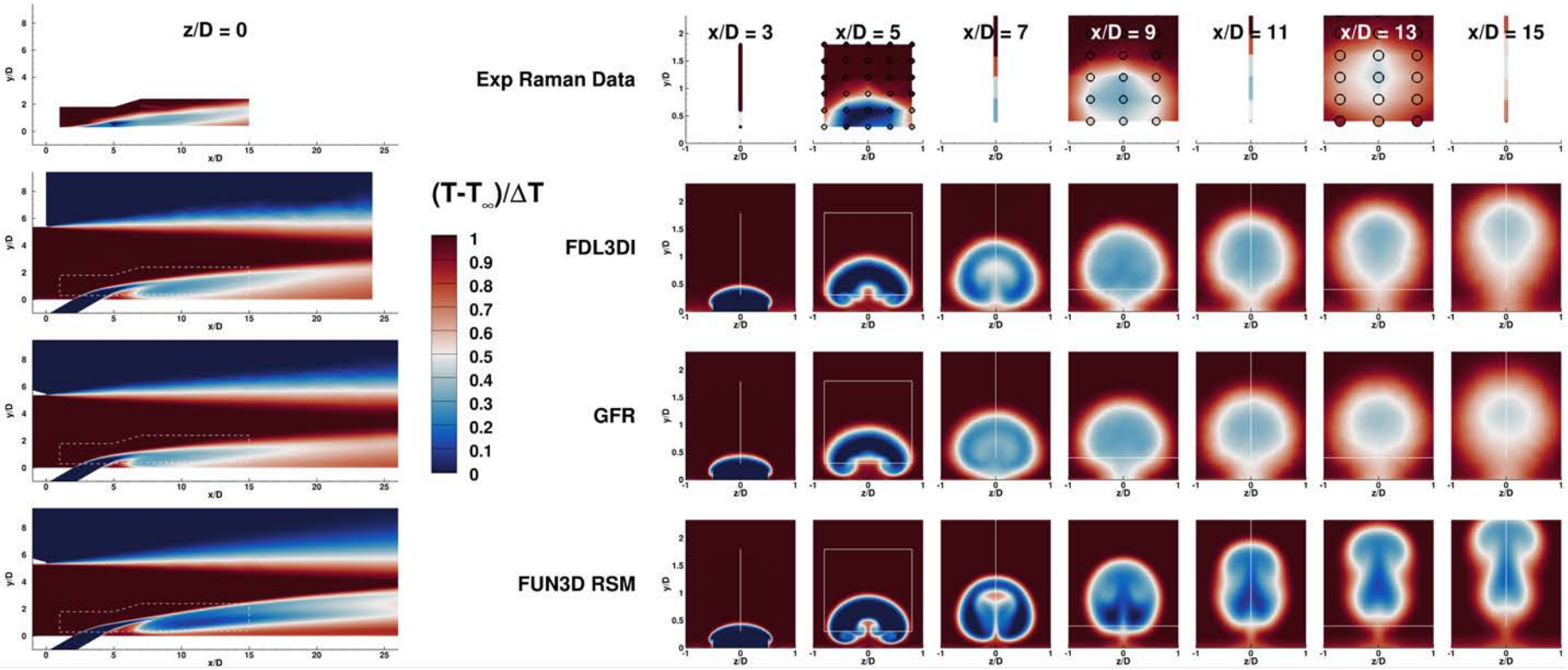
- Both LES approaches agree very well with each other and experiment for u.
- RSM enables good prediction of u' near the wall (better than eddy viscosity RANS).
- RSM over penetrates downstream.





Numerical Results

Mean Temperature Contours



- The Raman data is very coarse (compared to PIV)
  - The streamwise data has 8x6 data points at z/D = 0
  - The cross-stream data has 5x6 data points at x/D = 5,9,13
  - The cross-stream data has 6 vertical data points at x/D = 3,7,11,15

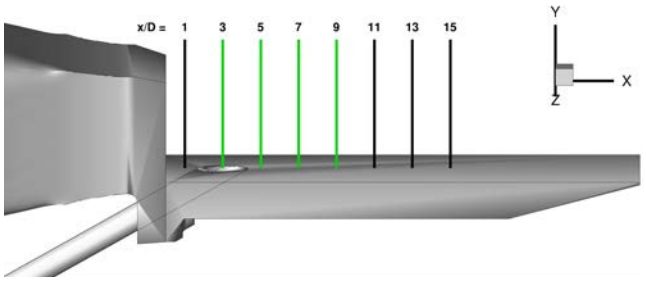
- FDL3DI and GFR show good agreement.
- GFR has a slightly thicker base compared to FDL3DI
- RANS predicts more elongated jet downstream.

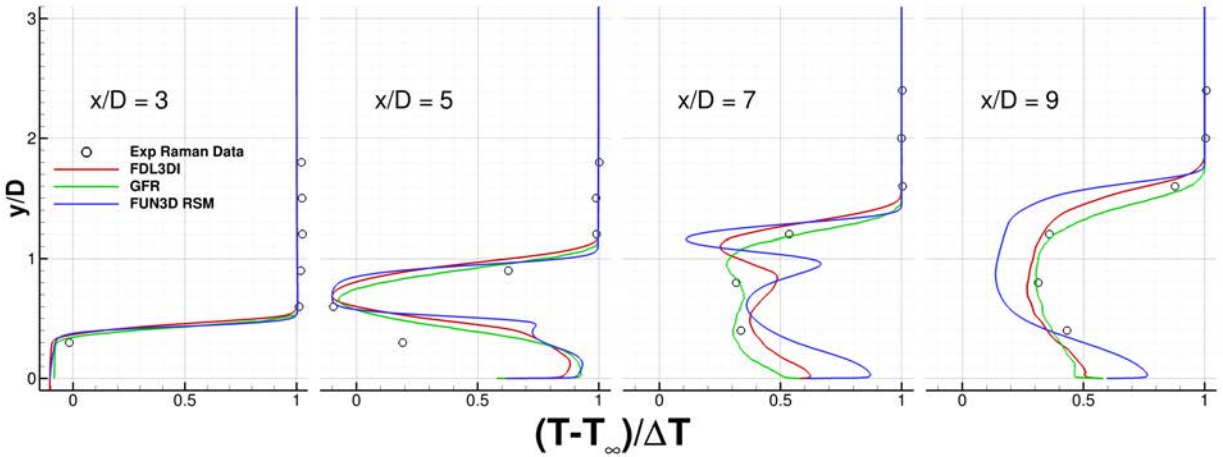
Numerical Results

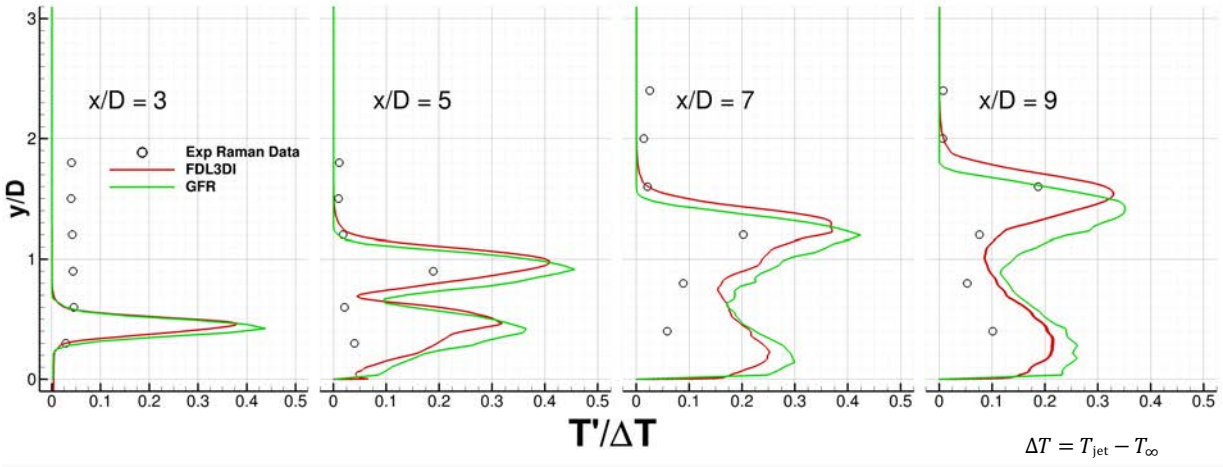
Set Point 23, Blowing Ratio = 2.0

Mean and RMS (turbulent) Temperatures

- Standard RANS methods do not provide T'
- LES approaches follow similar trends
- LES predicts higher T', but similar trends
  - This has also been seen in previous results comparing LES of heated jets to Raman T' (THX II)



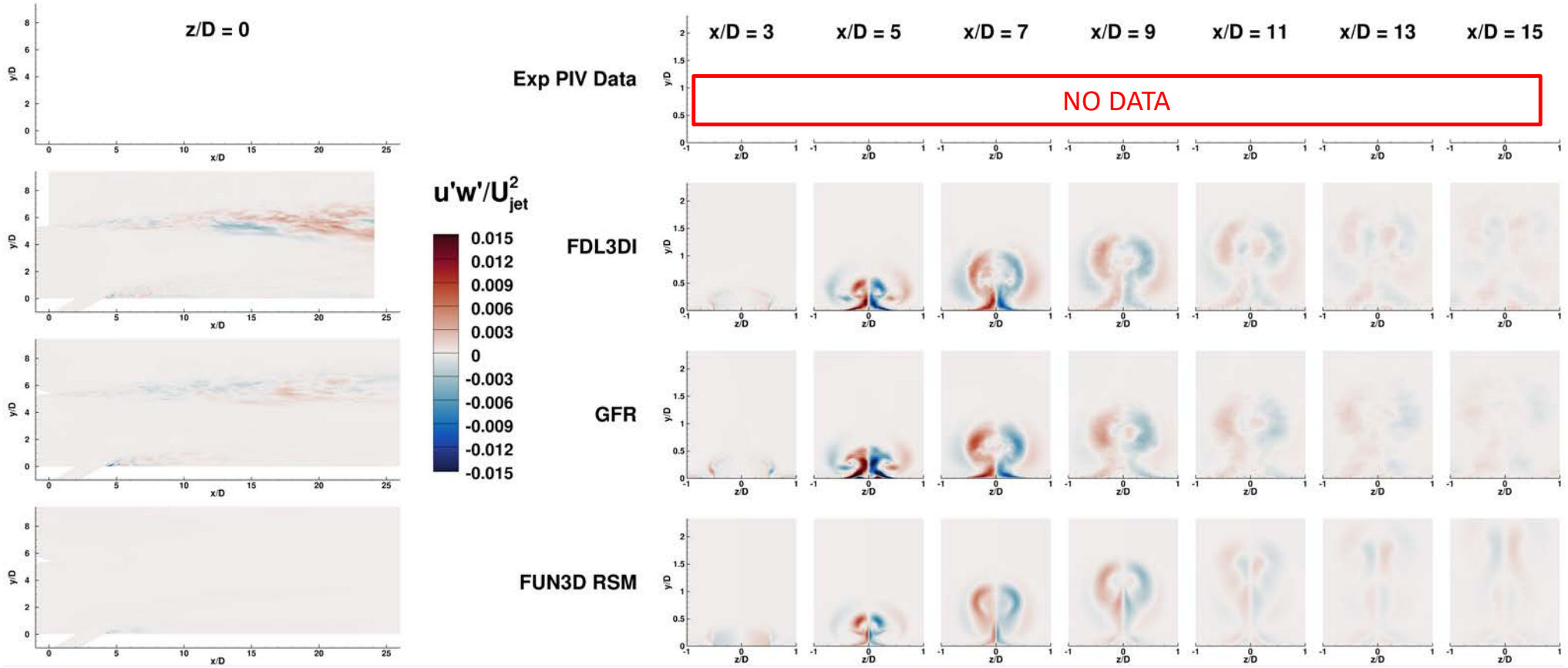




$\Delta T = T_{jet} - T_{\infty}$

Numerical Results

Shear Stress Contours

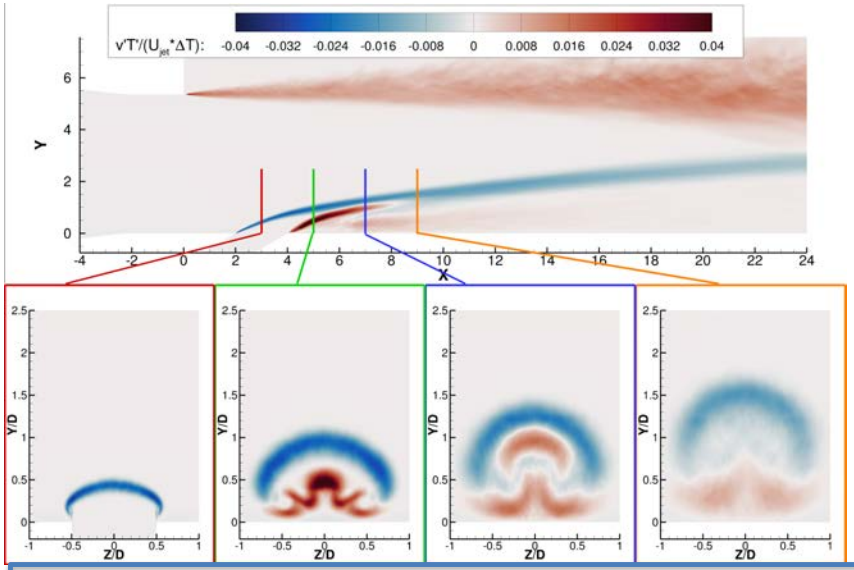


THX Phase 3: Turbulent Heat Flux

- Averaging of energy equation requires turbulent heat flux closure
- Conventional RANS method is gradient diffusion hypothesis (GDH)

$$-\overline{u_j{}'T'} = -\frac{\nu_t}{Pr_t}\frac{d\overline{T}}{dx_j}$$

- The GDH has been shown to be insufficient for many real problems
- Difficult to directly measure experimentally
  - Requires simultaneous measurement of temperature and velocity
- LES and SRS can directly obtain the turbulent heat flux terms



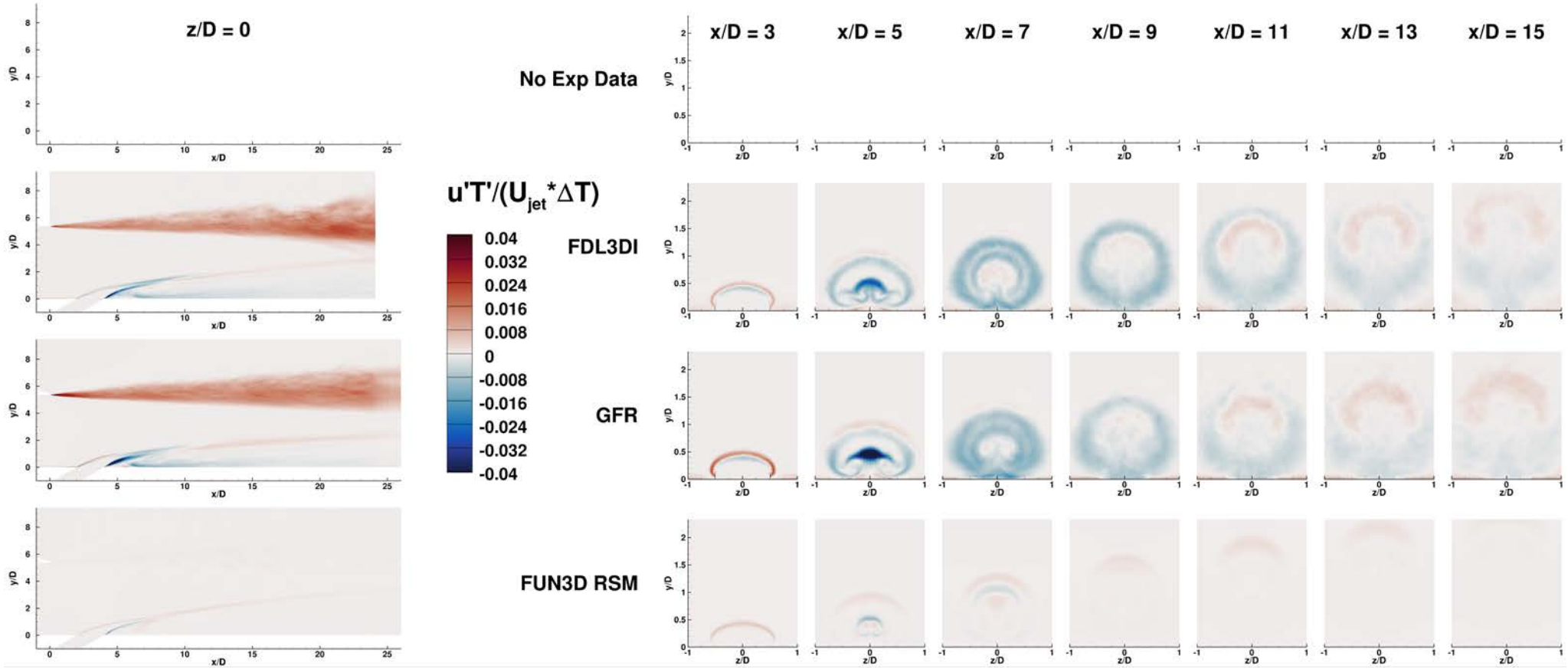
Favre-Averaged Energy Equation

$$\frac{\partial(\bar{\rho}\hat{E})}{\partial t} + \frac{\partial}{\partial x_j}(\hat{u}_j\bar{\rho}\hat{H}) = \frac{\partial}{\partial x_j}(\overline{\sigma_{ij}}\hat{u}_i + \overline{\sigma_{ij}u_i'}) - \frac{\partial}{\partial x_j}(\bar{q}_j + c_p\overline{\rho u_j'T'} - \hat{u}_i\tau_{ij} + \frac{1}{2}\overline{\rho u_i'u_i'u_j'})$$

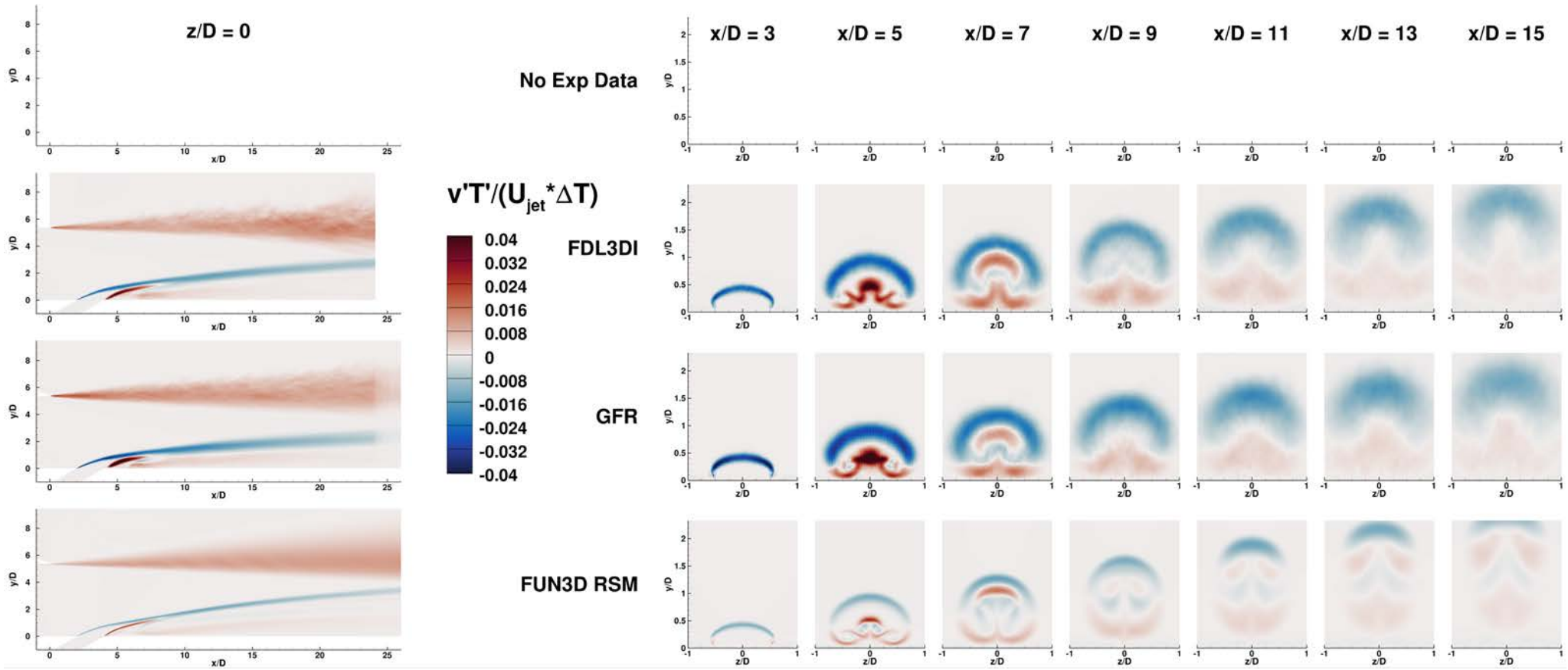
Turbulent Heat Flux

$$q_t = c_p\overline{\rho u_j'T'}$$

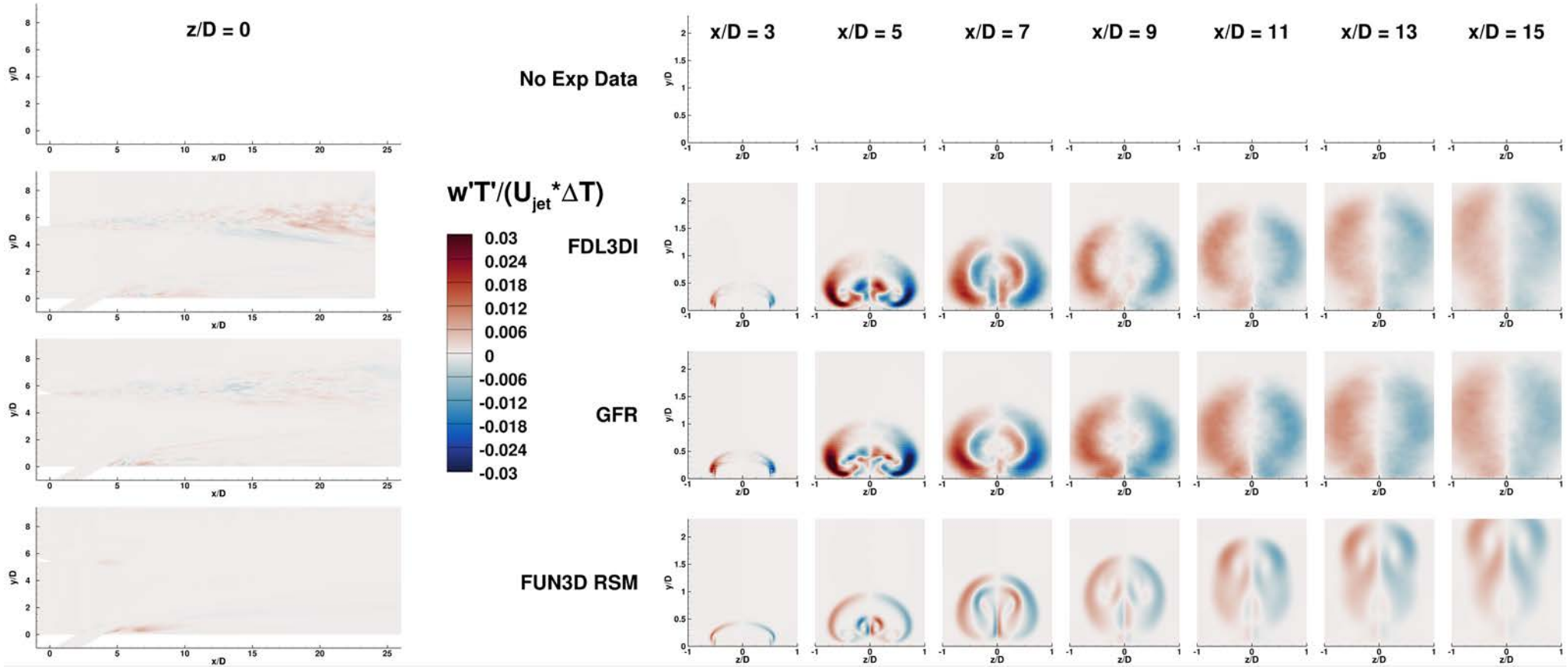
Numerical Results – Axial Turbulent Heat Flux



Numerical Results – Vertical Turbulent Heat Flux



Numerical Results – Spanwise Turbulent Heat Flux

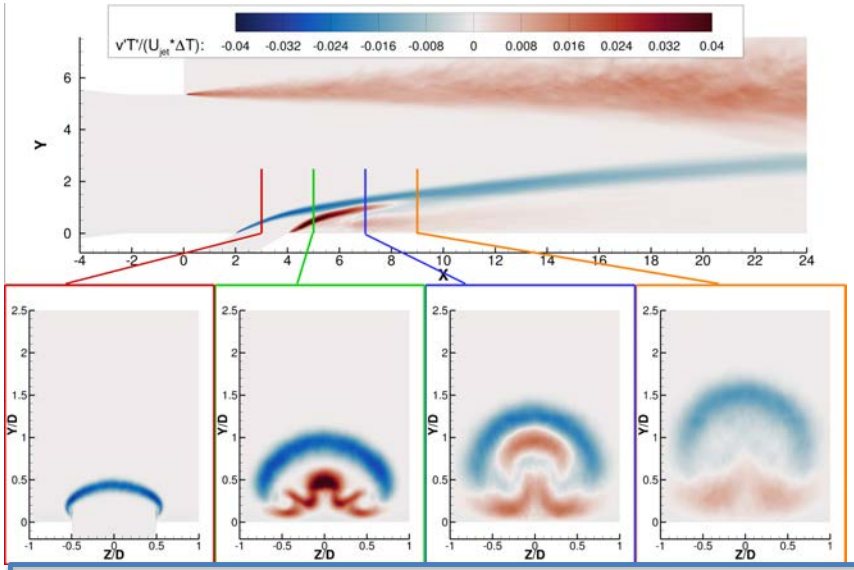


THX Phase 3: Turbulent Heat Flux Gradient

- Averaging of energy equation requires turbulent heat flux closure
- Conventional RANS method is gradient diffusion hypothesis (GDH)

$$-\overline{u_j{}'T'} = -\frac{\nu_t}{Pr_t}\frac{d\overline{T}}{dx_j}$$

- The GDH has been shown to be insufficient for many real problems
- Difficult to directly measure experimentally
  - Requires simultaneous measurement of temperature and velocity
- LES and SRS can directly obtain the turbulent heat flux terms



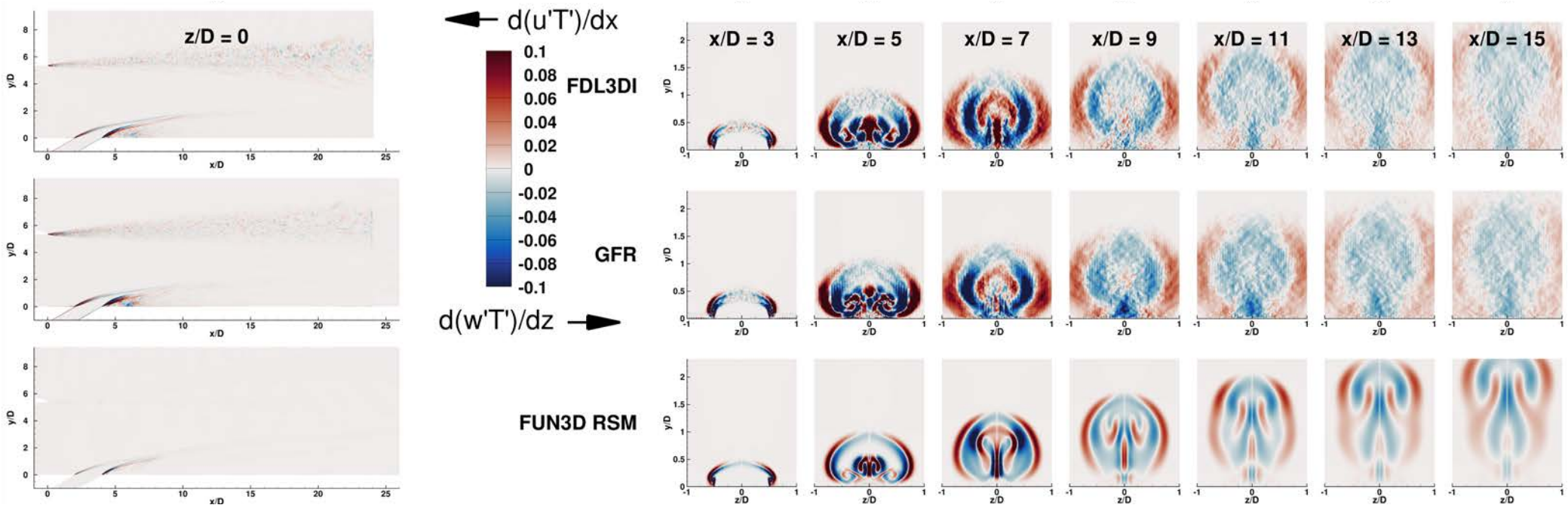
Favre-Averaged Energy Equation

$$\frac{\partial(\bar{\rho}\hat{E})}{\partial t} + \frac{\partial}{\partial x_j}(\hat{u}_j\bar{\rho}\hat{H}) = \frac{\partial}{\partial x_j}(\overline{\sigma_{ij}}\hat{u}_i + \overline{\sigma_{ij}u_i'}) - \frac{\partial}{\partial x_j}(\bar{q}_j + c_p\overline{\rho u_j'T'} - \hat{u}_i\tau_{ij} + \frac{1}{2}\overline{\rho u_i'u_i'u_j'})$$

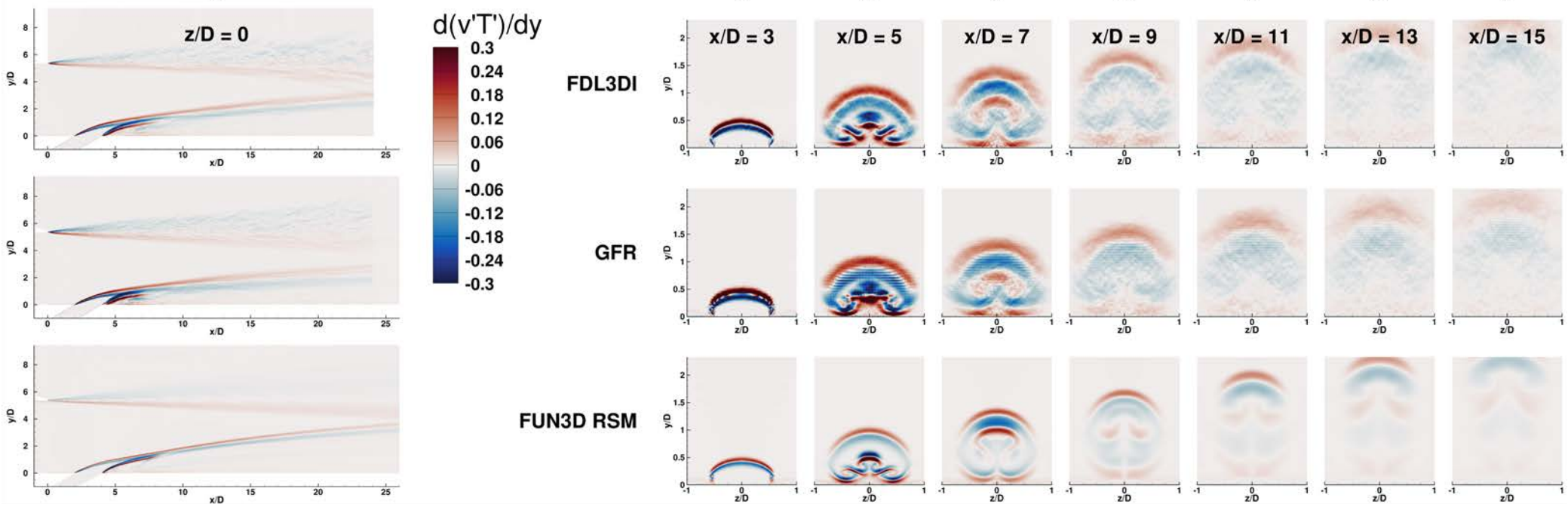
Turbulent Heat Flux

$$q_t = c_p\overline{\rho u_j'T'}$$

Turbulent Heat Flux Gradient



Turbulent Heat Flux Gradient





Conclusions and Future Work



- Large scale, Implicit Large Eddy Simulations were done on the THX III configuration @ SP23, BR=1 and BR=2
- The two LES approaches (GFR and FDL3DI) show exceptional agreement with each other, as well as the experimental data
- The FUN3D RSM does a reasonable job of matching velocities and stresses near the plate
  - Typical RANS over penetration of the jet occurs further downstream
- RANS particularly struggles with the axial turbulent heat flux ($\overline{u'T'}$)
- Regions of turbulent heat flux in RANS appear thinner in comparison to the LES results

- Further investigation into the treasure trove of data provided by the LES cases
  - Look into transport budgets for both Reynolds stresses and turbulent heat fluxes
  - Consider other unsteady data analysis techniques
- Run the 010 SP23, BR=1.0 test point
- Paper for 2021 AIAA Aviation conference



Acknowledgments



- NASA's Transformative Aeronautics Concepts Program (TACP) and Transformational Tools and Technology Project (TTT)
- Resources supporting this work were provided by the NASA High-End Computing (HEC) Program through the NASA Advanced Supercomputing (NAS) Division at Ames Research Center
- Air Force Research Lab (AFRL) at WPAFB for the use of FDL3DI
- Dr. Dan Garmann and Dr. Nick Bisek for their generous FDL3DI support

GFR (Glenn Flux Reconstruction) Code

and

THX3 Set Point 23, Blowing Ratio 1.0

Seth Spiegel

NASA Glenn Research Center
Inlets and Nozzles Branch

Oct. 15, 2020



Outline



- GFR Overview
- Numerical Results for THX 3: Set Point 23, BR=1.0
- Conclusions
- Future Work



GFR Capabilities

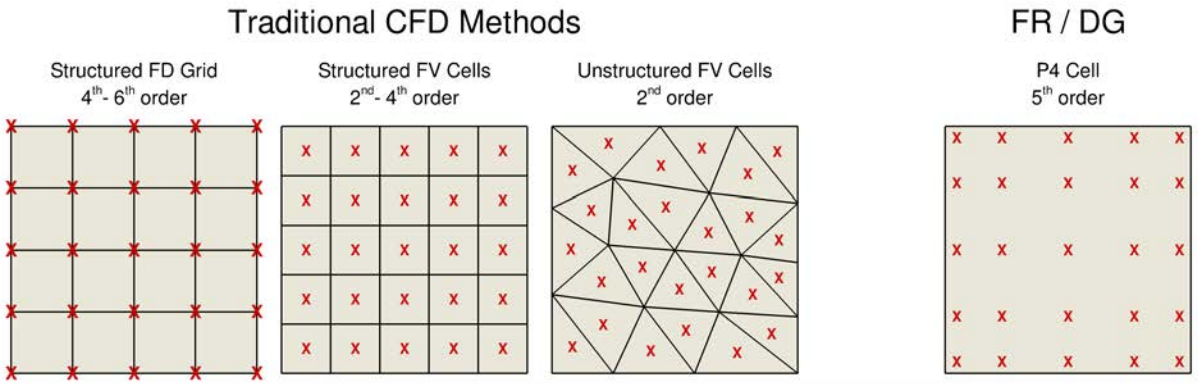


- **Arbitrary order of accuracy using flux reconstruction method**
  - Input parameter for degree of solution polynomial, P
  - Simulation order of accuracy is typically P+1
- **Explicit time marching**
- **Time-accurate turbulent flows using Implicit LES**
- **Written in latest Modern Fortran Standard**
  - Easily reuse or interface with existing legacy code at Glenn
- **Parallel using MPI**
  - Largest case to date using 40,000 CPU cores of the Electra supercomputer at NAS
- **Various de-aliasing/stabilization techniques**
  - Limiting, filtering, and over-integration
  - Maintains accuracy while preventing a simulation from diverging
- **3D brick and 2D mixed elements**
- **High-order representation of curved surface geometries**
  - Utilizing new high-order grid generation tool in Pointwise
- **Experimental GPU implementation using OpenACC**
  - Work resulting from NASA Langley GPU Hackathon (August 2017)
  - Approximately 25x speedup versus single CPU core
  - New version 2.5x faster than old version on CPU's

Flux Reconstruction Concepts

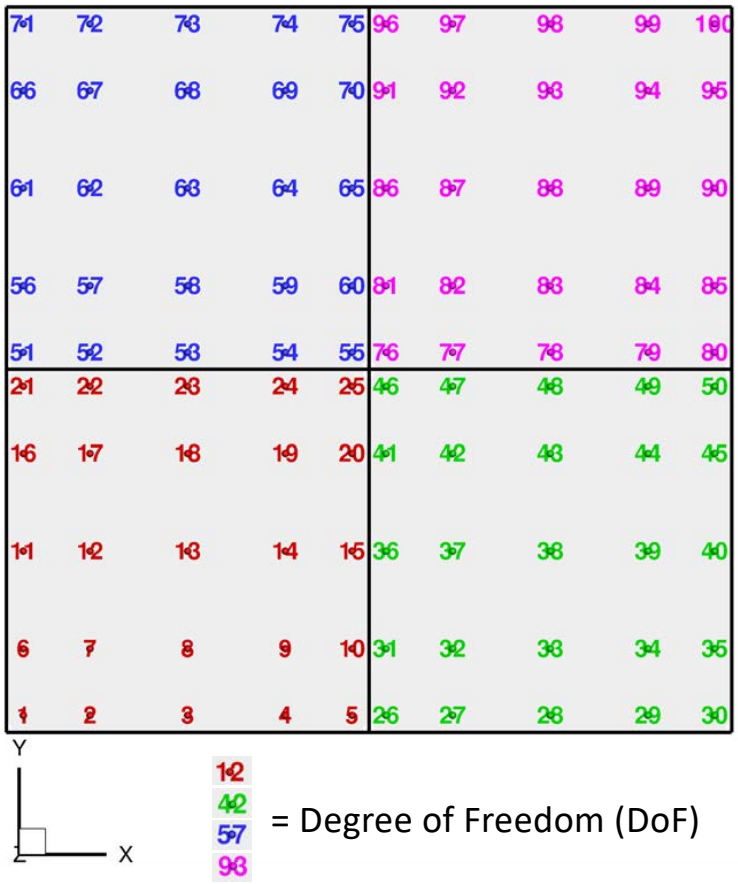
Degree of Freedom (DoF)

point in space where we are solving the governing equations



Four P4 (5th order) Quadrilateral Cells

100 DoF (25 per cell)

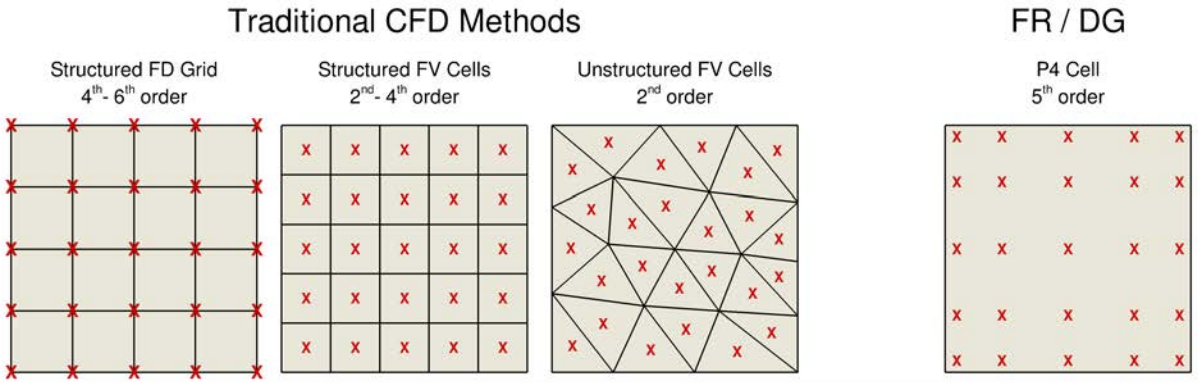


= Degree of Freedom (DoF)

Flux Reconstruction Concepts

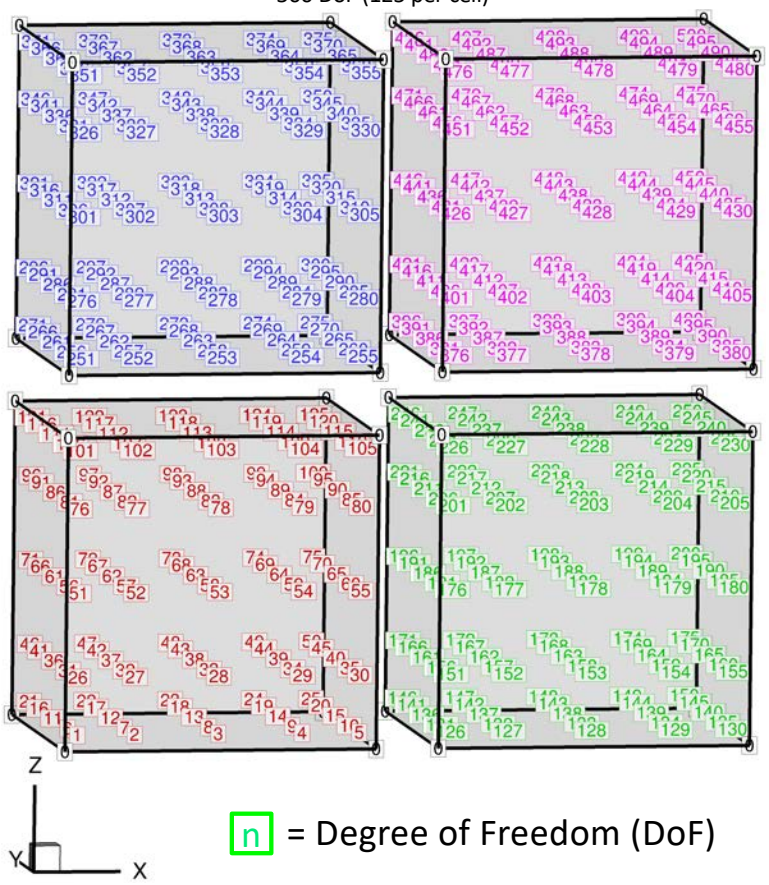
Degree of Freedom (DoF)

point in space where we are solving the governing equations



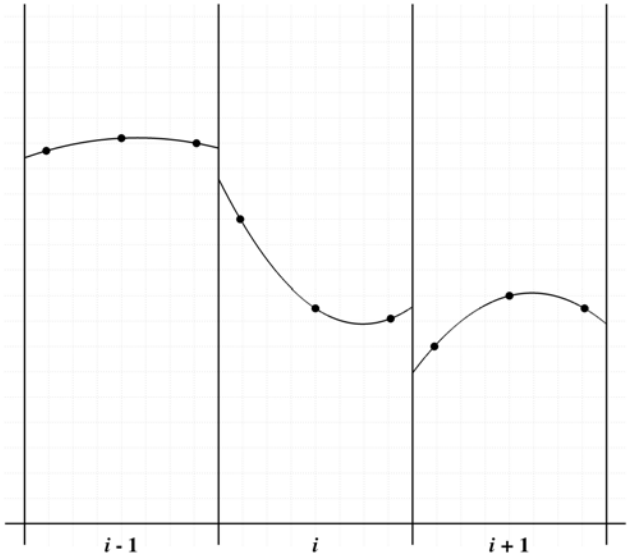
Four P4 (5th order) Hexahedra Cells

500 DoF (125 per cell)



n = Degree of Freedom (DoF)

Flux Reconstruction Concepts



Flux Reconstruction / Nodal Discontinuous Galerkin Methods

- The solution within each grid cell is defined by a polynomial of degree P.
- Solution is generally discontinuous at cell interfaces.
- Value of the solution polynomial is stored at $(P+1)^d$ solution points within each cell, where *d* is the spatial dimension.

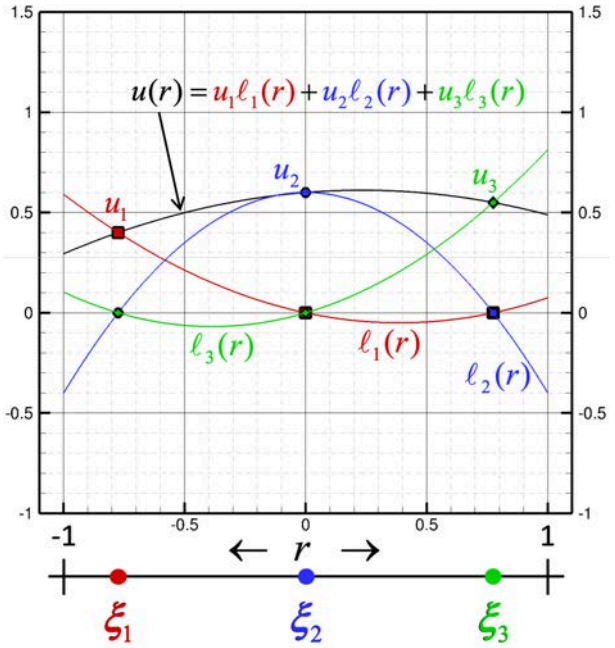
Solution polynomial within a grid cell

$$u(r) = \sum_{n=1}^{N_P} u_n \ell_n(r) \qquad u_n = u(\xi_n)$$

Store u_n at each degree of freedom (DoF)
(1 solution point = 1 DoF)

Lagrange Interpolating Polynomial

$$\ell_n(r) = \prod_{\substack{i=1 \\ i \neq n}}^{N_P} \frac{r - \xi_i}{\xi_n - \xi_i} \qquad \ell_i(\xi_j) = \delta_{ij}$$



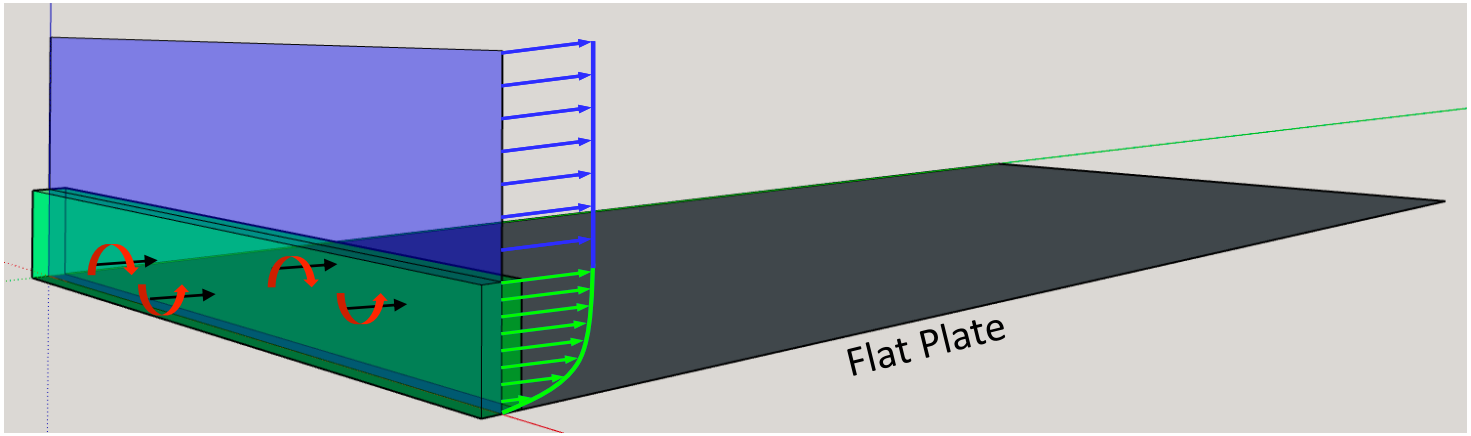
Further details can be found in:

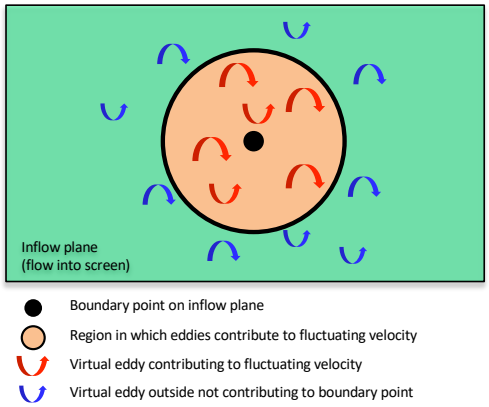
Huynh, H., "A Flux Reconstruction Approach to High-Order Schemes Including Discontinuous Galerkin Methods," AIAA Paper 2007-4079, June 2007.
Karniadakis, G. and Sherwin, S., *Spectral/hp Element Methods for Computational Fluid Dynamics*, Oxford University Press, 2nd ed., 2013.
Hesthaven, J. S. and Warburton, T., *Nodal Discontinuous Galerkin Methods: Algorithms, Analysis, and Applications*, Vol. 54 of Texts in Applied Mathematics, Springer New York, 2008.
Kopriva, D. A., *Implementing Spectral Methods for Partial Differential Equations: Algorithms for Scientists and Engineers*, Springer Science & Business Media, 2009.

Synthetic Eddy Method

Traditional Inflow BC

Unsteady Inflow (SEM)

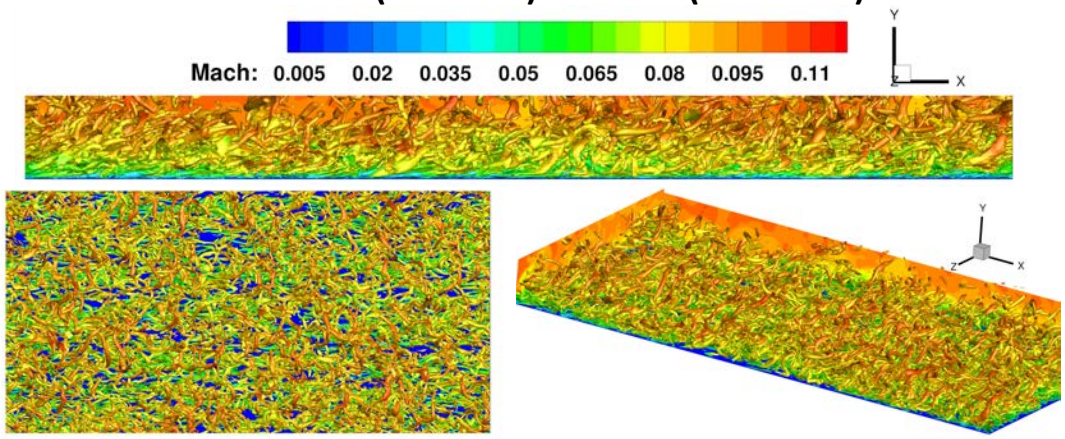




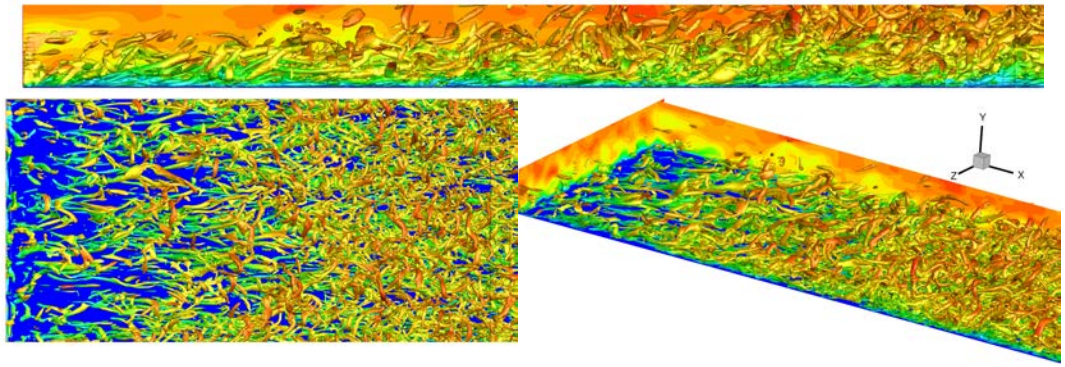
- Randomly placed virtual eddies are convected through a box (green) located on the inflow plane (blue).
- A fluctuating velocity at each inflow point is computed by summing all eddies within a certain distance.
- Finally, the unsteady boundary condition for each inflow point is found by correlating the fluctuating velocity with a 1D input profile containing averaged velocities and stresses.

Synthetic Eddy Method

Periodic P7 (8th order) solution (70 M DoF)

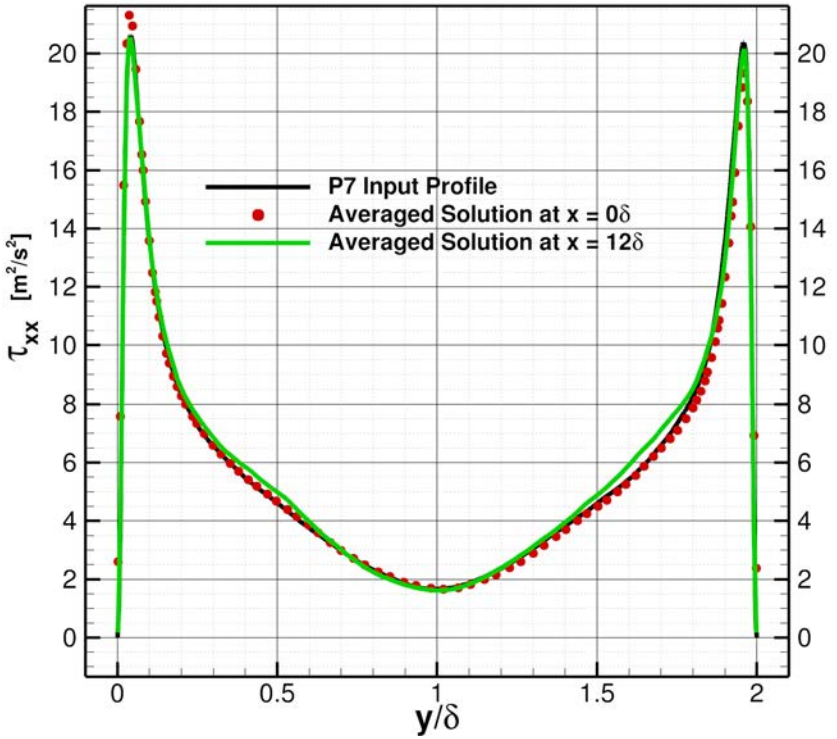


SEM P4 (5th order) solution (20 M DoF)



Q-criterion isosurfaces colored by Mach number

Axial stress profiles for inflow plane and 12 channel-half-heights downstream



The periodic P7 solution was used as the input profile for the SEM. The flow recovers the input stress profile at both the SEM inflow plane (0δ) and at 12 channel-half-heights downstream (12δ).

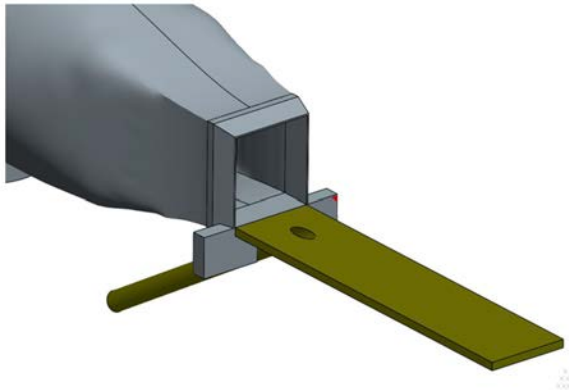
Numerical Results

Focus on THX Phase 3 at Set Point 23 with BR=1.0

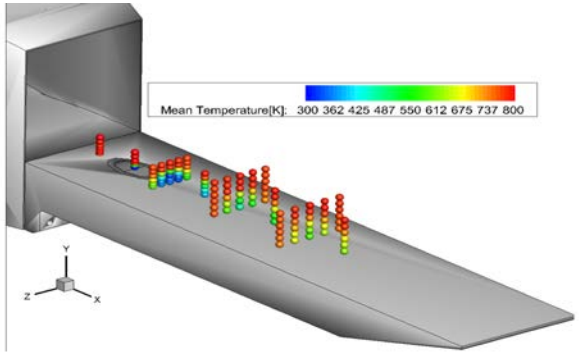
- Compare to experiment PIV and Raman Data
- FUN3D with RSM turbulence model on fine grid ("best of" RANS) – 33 million DoF
- FDL3DI using base grid – 356 million DoF
- GFR 4th order (P3) – 839 million DoF
- GFR 5th order (P4) – 1.64 billion DoF

THX 3 Hardware:

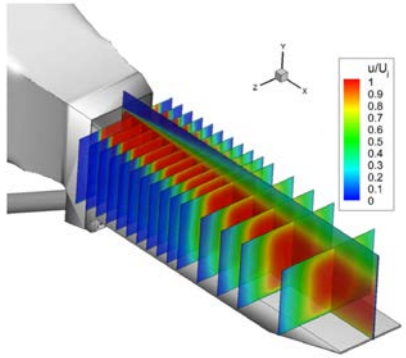
Single Cooling Hole – fundamental aerodynamic & thermodynamic study



Sample THX3 experimental measurements



Raman spectroscopy temperature measurements

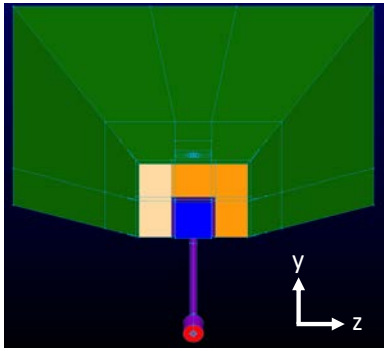


Particle Image Velocimetry (PIV) velocity measurements

GFR Grid Details

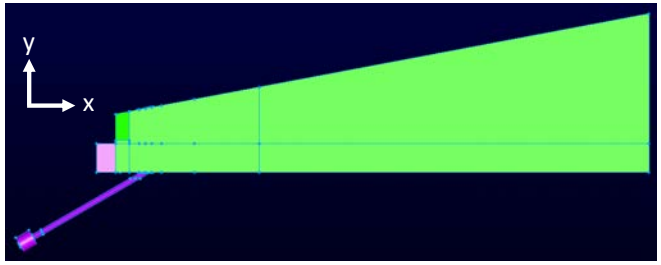
- All cases used same grid with 13,111,040 high-order grid cells
  - P3 case contains 839 million DoF
  - P4 case contains 1.64 billion DoF
- Same P3 grid used for BR=2.0

Computational Domain and Boundary Conditions



View looking downstream of square jet inflow (blue)

Purple: Adiabatic wall
Blue: Square jet SEM inflow
Red: Injector subsonic inflow
Orange: Exterior subsonic inflow
Green: Farfield
Not visible: Plate isothermal Wall
Not visible: Subsonic outflow



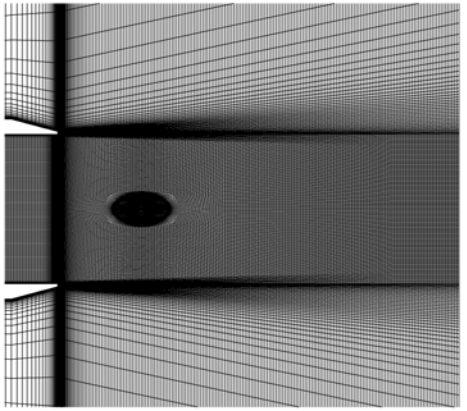
Side view of computational domain

Grid Spacings

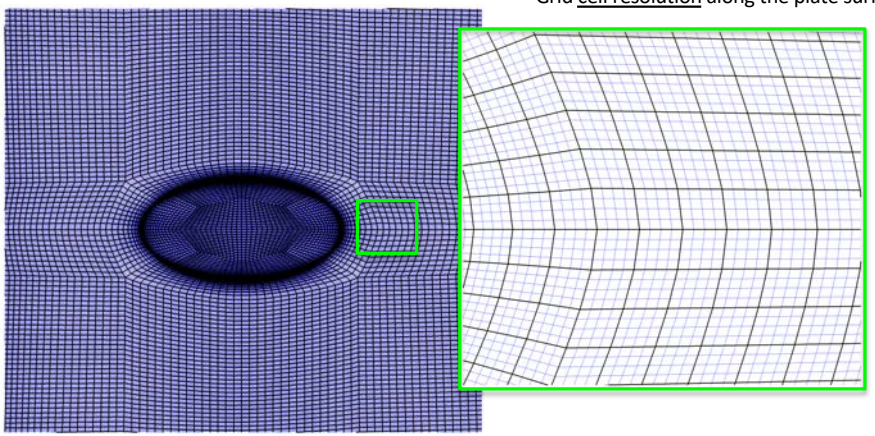
	Average Δx^+	y^+_{wall}	Average Δz^+
Grid Cell	100	2.5	62.5
P3	25	0.174*	15.625
P4	20	0.117*	12.5

*y^+ of first DoF off wall

Sponge region from end of the plate (x/D = 24) to outflow
where D is the cross-section diameter of the injector tube (0.5 in.)



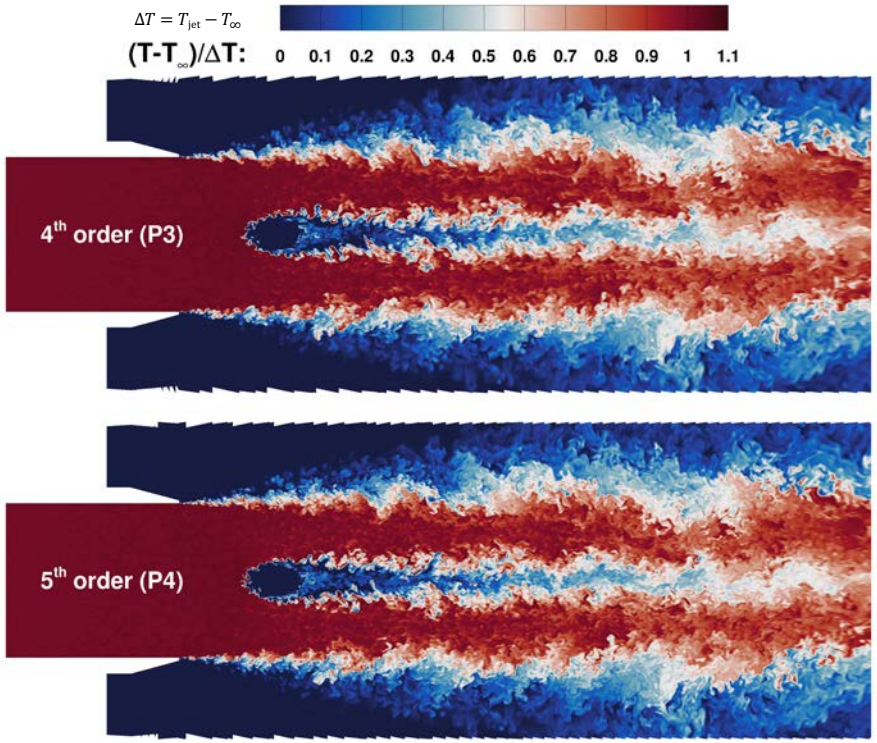
Grid cell resolution along the plate surface.

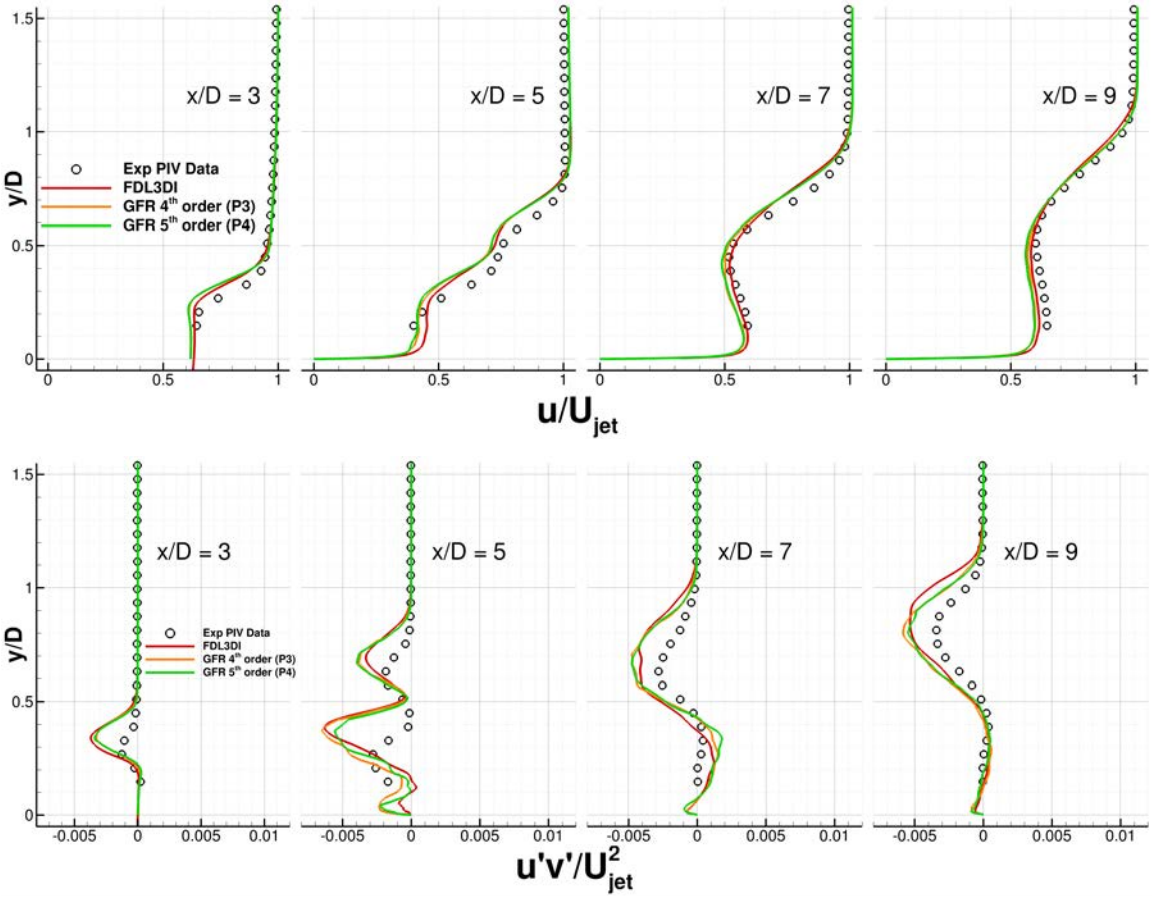


DoF resolution near the injector hole with zoomed in view on right.
Each black square is a grid cell, and the center of each blue square is a DoF.

GFR P3 vs P4

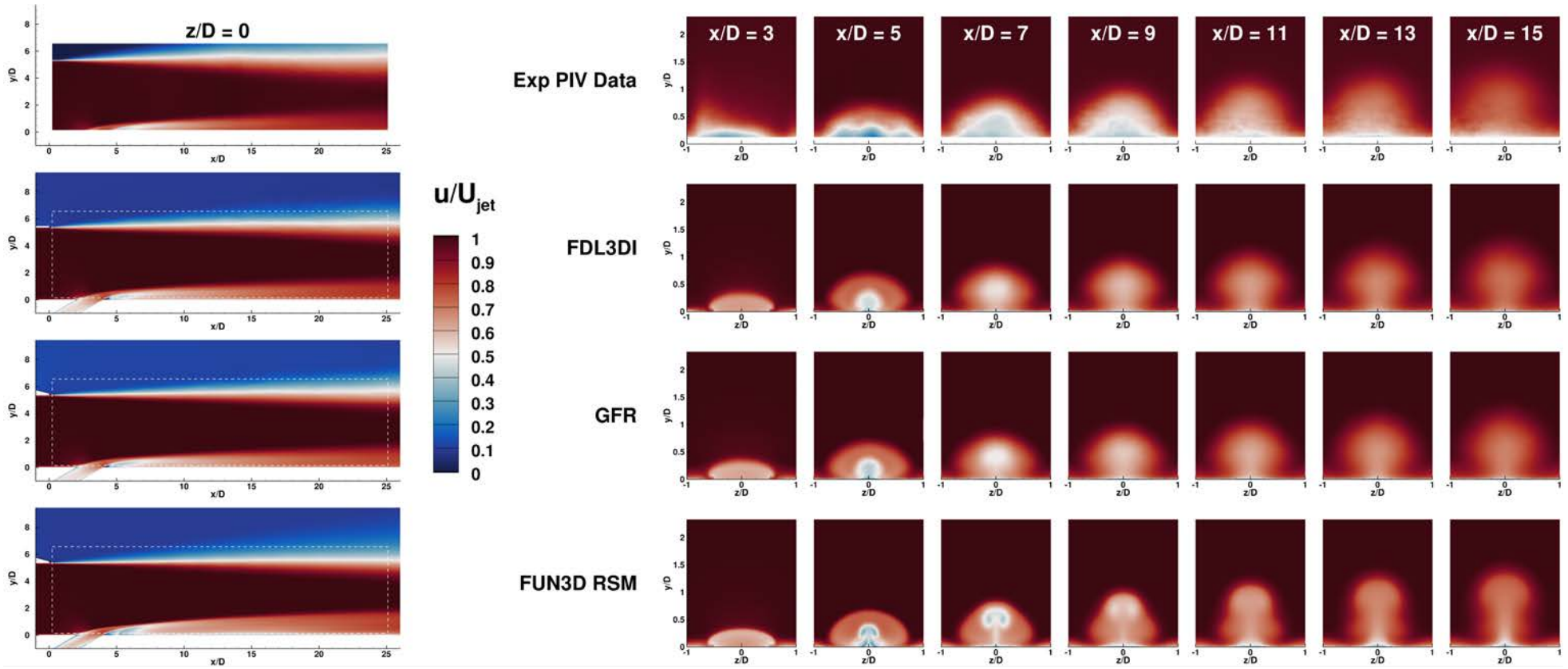
- P3 has 839 million DoF
- P4 has 1.64 million DoF
- P4 resolves more structures
- Very little difference between P3 and P4 time-averaged solutions
- Will only show P4 solutions from here on





Instantaneous temperature contours at y/D=0.1 (about 2 mm above the plate)

Mean Streamwise Velocity Contours



- The PIV cross-stream data seems to have a lot of flare from the plate.

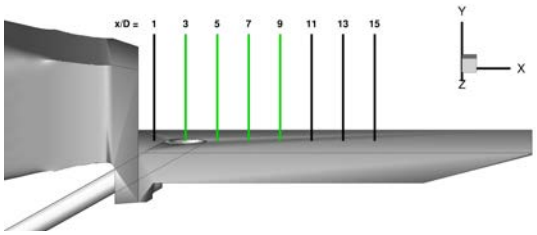
- FDL3DI and GFR look nearly identical.
- RANS predicts the cooling jet lifting off more from the plate.

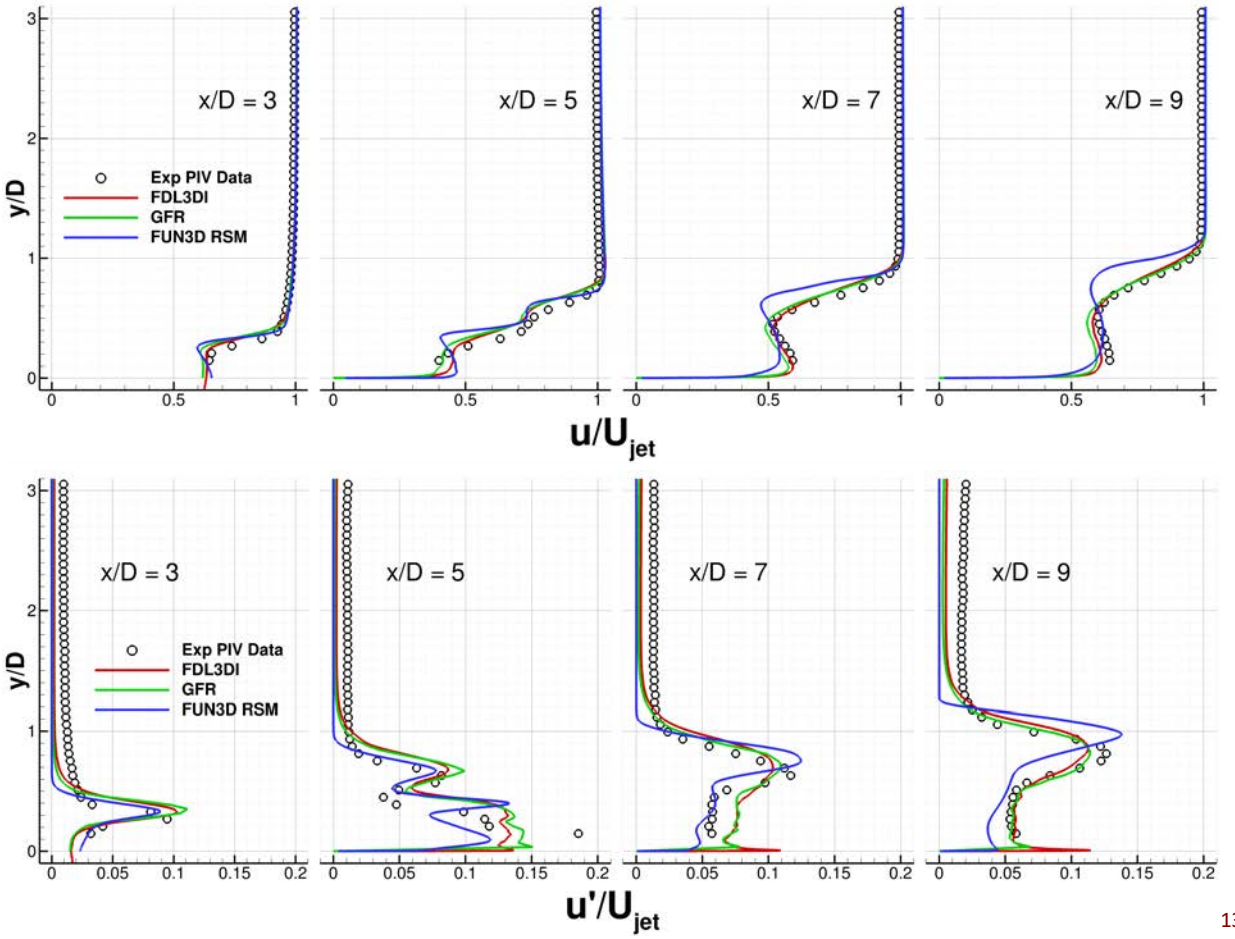
CFD Comparison with PIV Data

Set Point 23, Blowing Ratio = 1.0

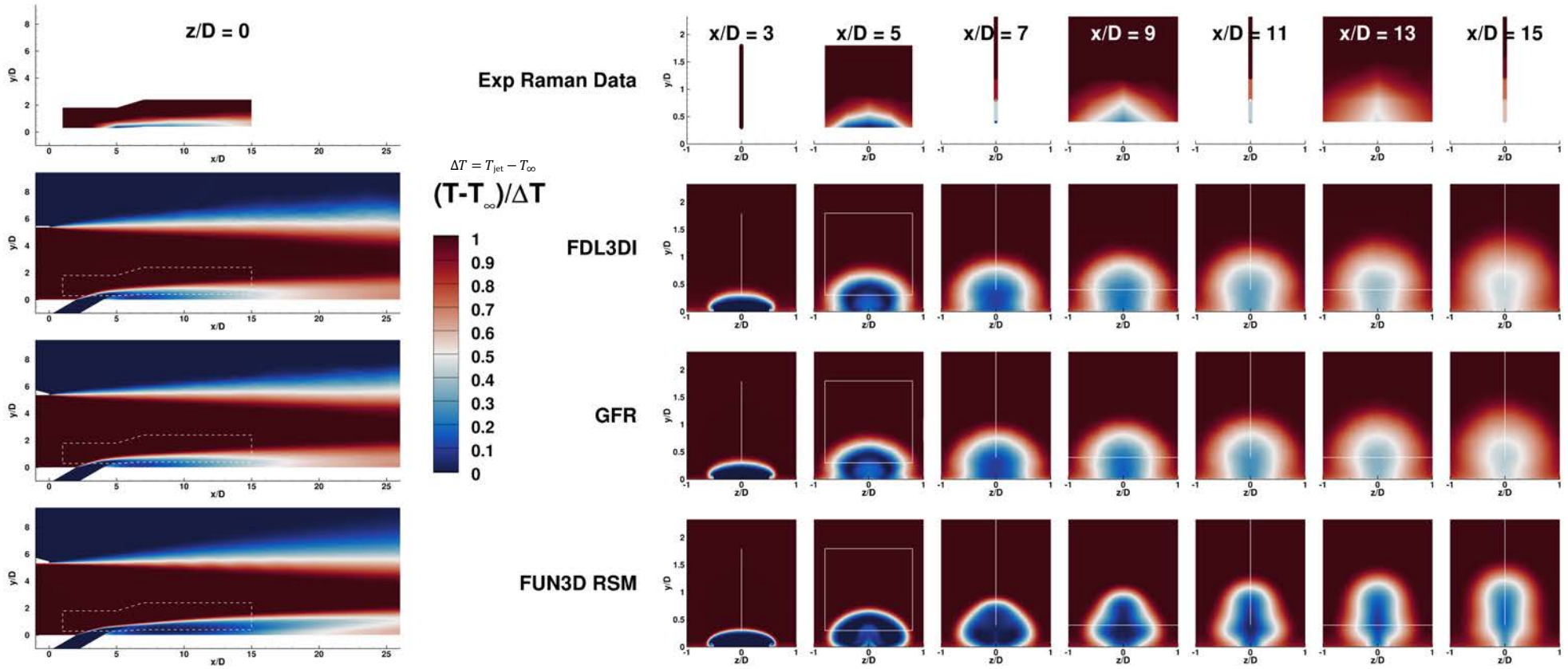
Streamwise Mean and RMS (turbulent) Velocities

- Both LES agree very well with each other and experiment for u.
- RSM enables good prediction of u' near the wall (better than eddy-viscosity-based RANS).
- LES agrees very well with near wall u' further down stream.





Mean Temperature Contours



The Raman data is very coarse (compared to PIV)

- The streamwise data has 8x6 data points at z/D = 0
- The cross-stream data has 5x6 data points at x/D = 5,9,13
- The cross-stream data has 6 vertical data points at x/D = 3,7,11,15

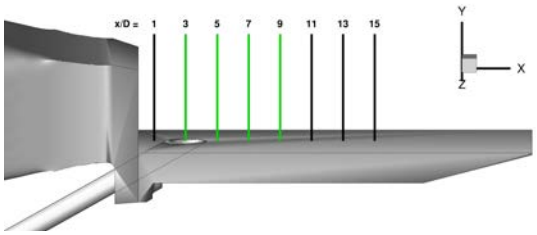
- FDL3DI and GFR look nearly identical.
- RANS predicts the cooling jet lifting off more from the plate.
- Both LES appear to correlate well to the Raman data.

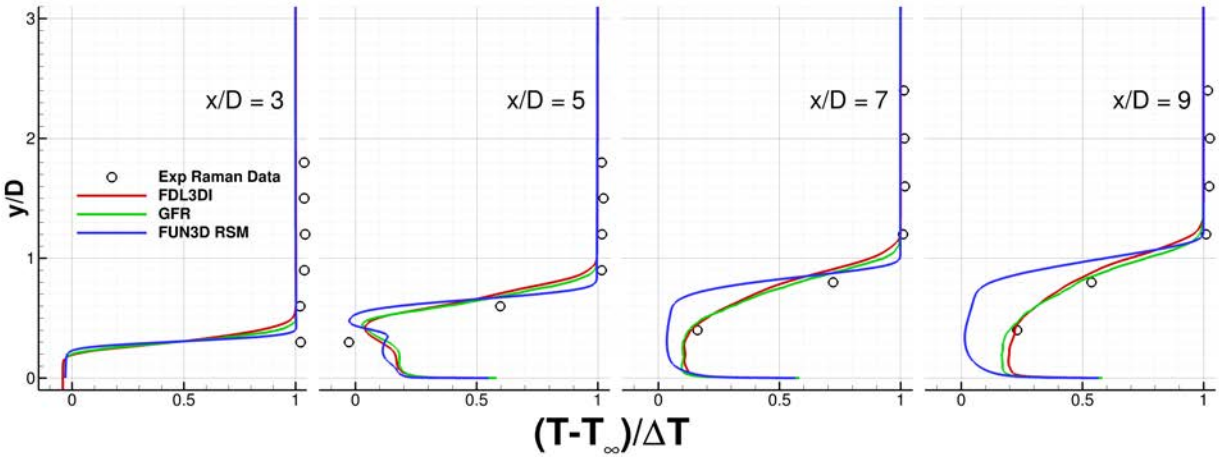
CFD Comparison with Raman Data

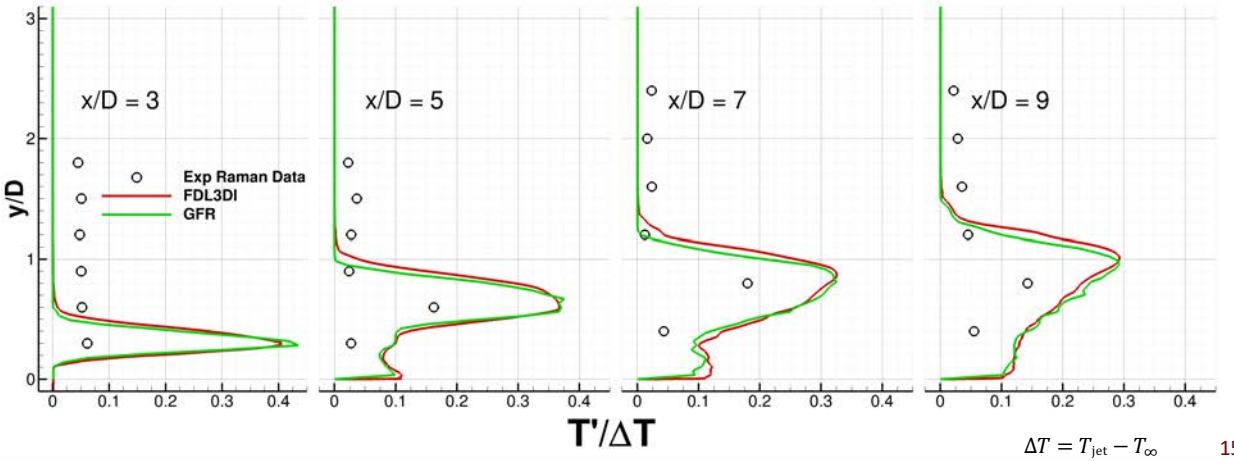
Set Point 23, Blowing Ratio = 1.0

Mean and RMS (turbulent) Temperatures

- Standard RANS methods do not provide T'
- Both LES agree very well with each other for T and T'
- LES agrees very well with experiment for T
- LES predicts higher T', but similar trends
  - This has also been seen in previous results comparing LES of heated jets to Raman T'







$\Delta T = T_{jet} - T_{\infty}$

CFD Turbulent Heat Flux

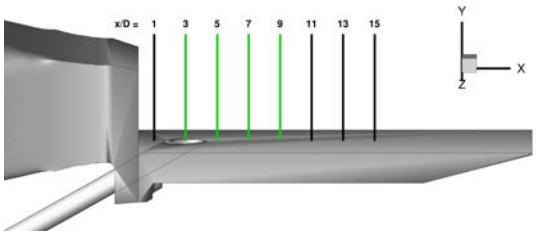
Set Point 23, Blowing Ratio = 1.0

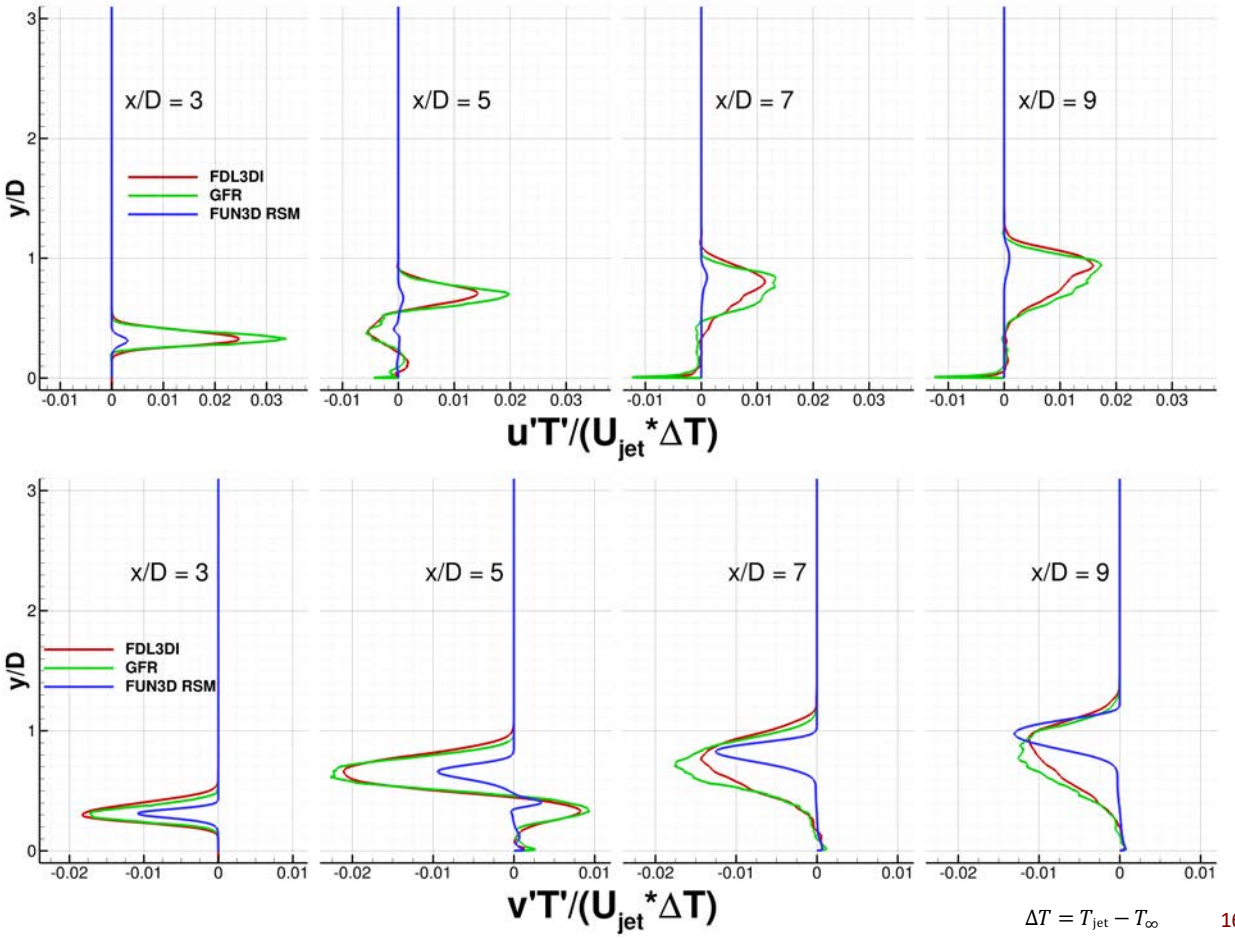
Turbulent heat fluxes

- RANS closure approximation for the turbulent heat-flux vector is dependent only on the temperature gradient.

$$q_{T_j} = \overline{\rho u_j'' h''} = -\frac{\mu_T c_p}{Pr_T}\frac{\partial \tilde{T}}{\partial x_j}$$

- Both LES agree very well with each other.
- Axial turbulent heat flux is nearly zero for RANS.





$\Delta T = T_{\text{jet}} - T_{\infty}$



Conclusions



- GFR LES agrees very closely with FDL3DI LES
  - Codes use very different numerical methods
  - Used different grid geometries and domains
  - Used different unsteady turbulence inflow boundary conditions
- LES agrees very well with experiment mean quantities
- LES agrees reasonably well with experiment turbulence quantities
- There is a significant need for unstructured grid capability
  - Structured grid requires extending grid resolution to the farfield boundaries.
  - Transitioning to unstructured cells in the exterior flowfield and sponge layer regions could save 10-100 million+ DoF.
- P4 doesn't seem to offer much improvement over P3 for BR=1.0 on this grid



Future Work



Future THX3 Computational Analysis

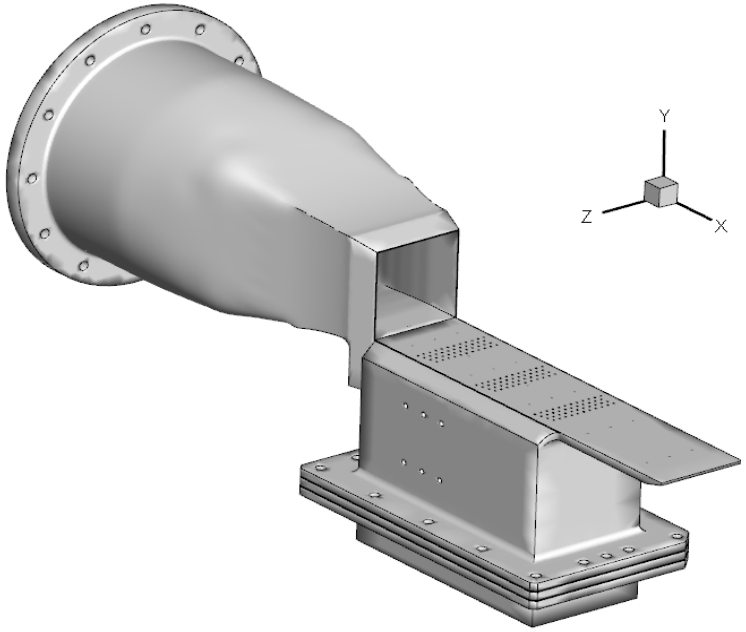
- Run case using new grid with increased cell resolution in areas of interest to test grid independence
- Look at other flow conditions
  - Set point 23, BR=0.5
  - Blowing Ratios of 0.5 and 1.0 for Set Points 27, 42, 46, 49
- Conference papers / Journal articles

Future GFR Development Work

- Unstructured grid capability
- Further stability improvements
  - Entropy variable formulation, shock-capturing
- Non-uniform P solution
  - Solution order can vary from cell to cell, but stays constant for duration of simulation
- *p*-adaptation
  - Dynamically change cell solution order as needed
- Reduce the time step restriction required for explicit methods
  - Explore implicit, implicit-explicit, and space-time methods

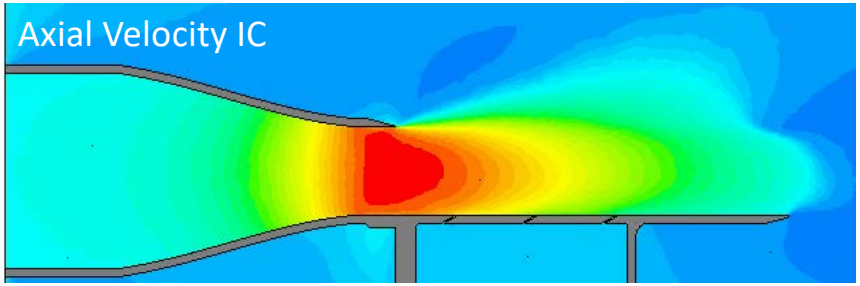
THX 4 (Porous Plate)

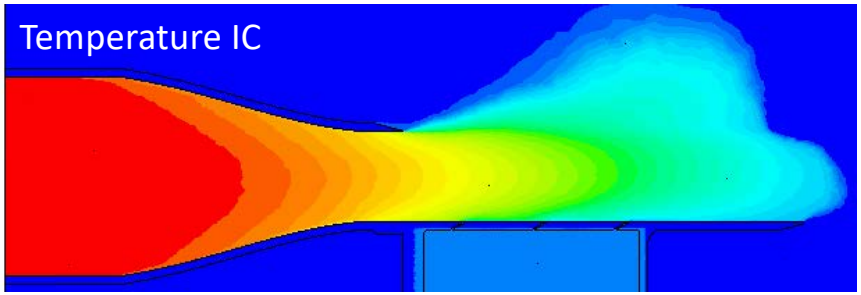
Justin Pesich
Code LTF (Fluid and Cryogenic Systems Branch)



Siemens Simcenter STAR-CCM+ Code Overview

- Finite Volume, cell-centroid based code
- 2nd order upwind scheme
- Coupled Implicit Solver uses pseudo-time-marching approach
  - Automatic CFL control
  - Specify Initial, Min, Max CFL
  - CFL adjusts automatically to promote fast convergence while maintaining stability
- Expert Initialization via Grid Sequencing
  - Solves inviscid solution on series of coarsened grids to enhance initial guess and promote convergence
  - Specify Max grid levels, Max iterations per level, convergence tol, CFL#





Sample grid sequencing output:

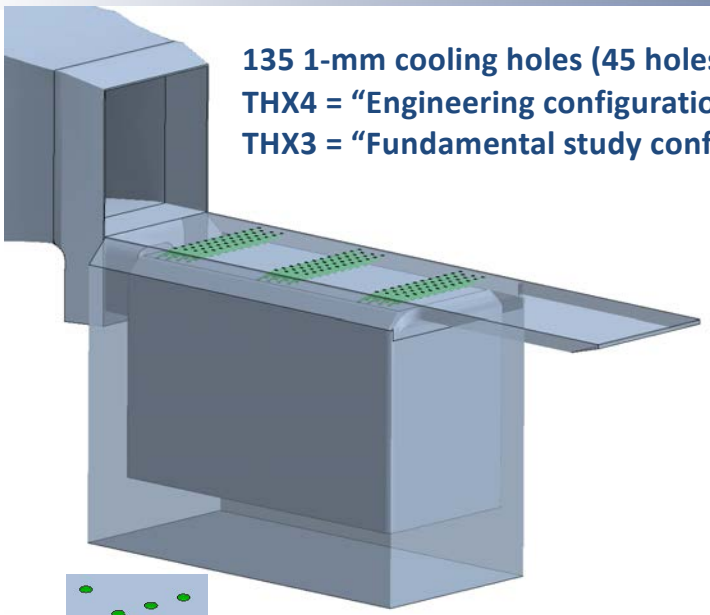
```
 Created 8 coarse grid levels ...

[ ] Fine  grid level (0) : 97114695 cells
[*] Coarse grid level (1) : 23862448 cells
[*] Coarse grid level (2) : 5703139 cells
[*] Coarse grid level (3) : 1323871 cells
[*] Coarse grid level (4) : 309684 cells
[*] Coarse grid level (5) : 71223 cells
[*] Coarse grid level (6) : 15861 cells
[*] Coarse grid level (7) : 3288 cells
[*] Coarse grid level (8) : 1199 cells

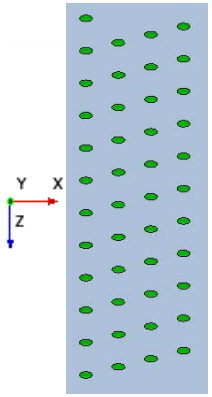
 NOTE: 8 coarse grid levels, marked [*], will be used for grid-sequencing.

Creating coarse finite-volume representations. Please wait ...
```

Model Geometry and Boundary Conditions

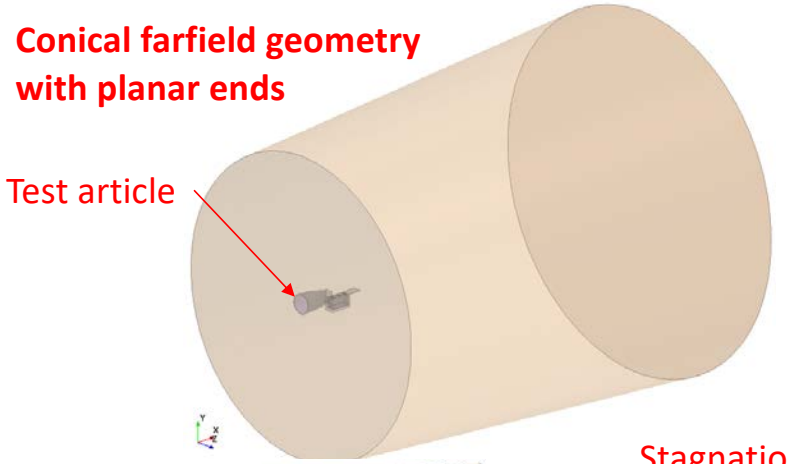


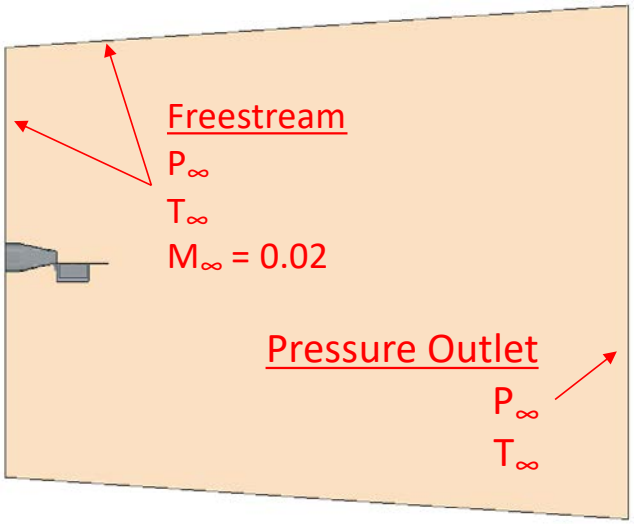
135 1-mm cooling holes (45 holes/patch)
THX4 = "Engineering configuration"
THX3 = "Fundamental study configuration"



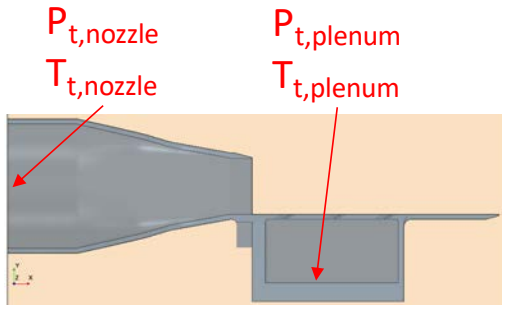
Cooling hole patch layout is not symmetric about the xy-plane; necessary to model entire domain

Conical farfield geometry with planar ends





Stagnation Inlets



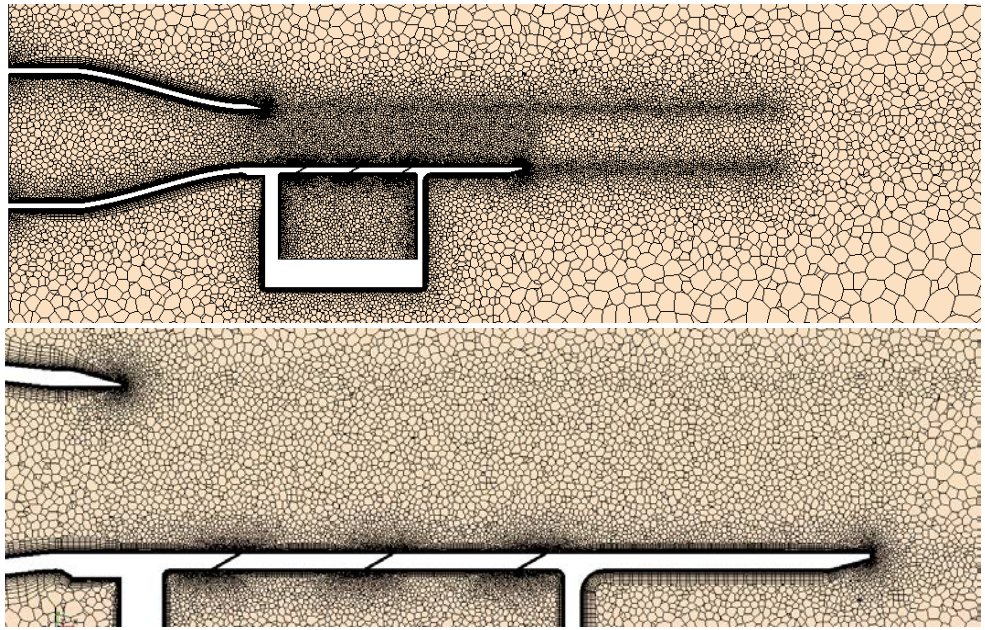
Note: TVR = 10 on all inflow boundaries

Computational Grids

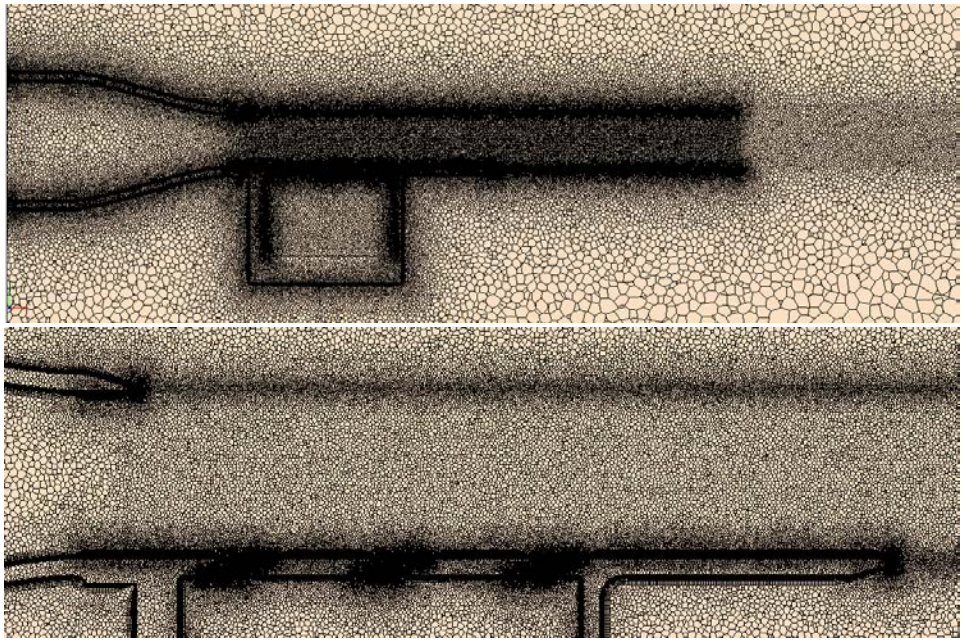
- Two Modeling Approaches:
  - **Fluid-Only polyhedral grid** used with *adiabatic* wall boundary condition
  - **Fluid-Solid conformal polyhedral grid** to solve the *conjugate heat transfer* (CHT) problem.

Grid	Fluid-Only # cells	Fluid-Solid # cells	Blowing Ratio
Coarse	26.3 million	29.9 million	0.0, 1.0, 2.0
Medium	70.3 million	78.9 million	1.0
Fine	143.3 million	143.3 million	1.0
XFine	N/A	321.4 million	1.0

Fluid-Only Coarse on z=0



Fluid-Solid Fine on z=0



Physics and Solver Settings

- Physics
  - K-Omega Menter SST Turbulence Model (both RANS and DDES)
  - Turbulent Prandtl #, $Pr_t = 0.9$
  - Ratio of specific heats, $\gamma = 1.4$
  - Dynamic Viscosity and Thermal Conductivity specified by Sutherland's Law
  - Gravity neglected (no natural convection)
  - 316 stainless material properties set via ASMH

- Solver Settings
  - CFL# ≈ 10 (min = 1, max = 20)
  - Discretization
    - RANS: 2nd order upwind
    - DDES: Hybrid Bounded Central Difference
  - Convergence Criteria
    - Temperature field slowest to converge
    - |Max – Min| < 0.005K over 100 samples

316 Stainless Thermal Conductivity

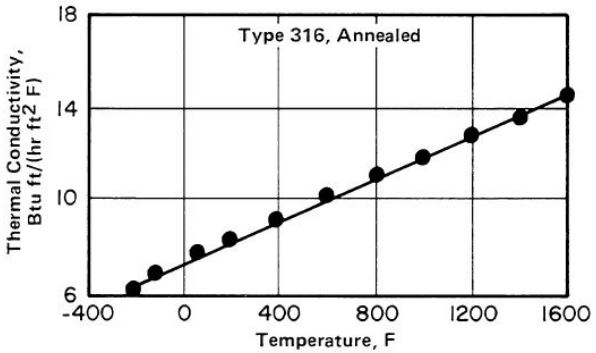
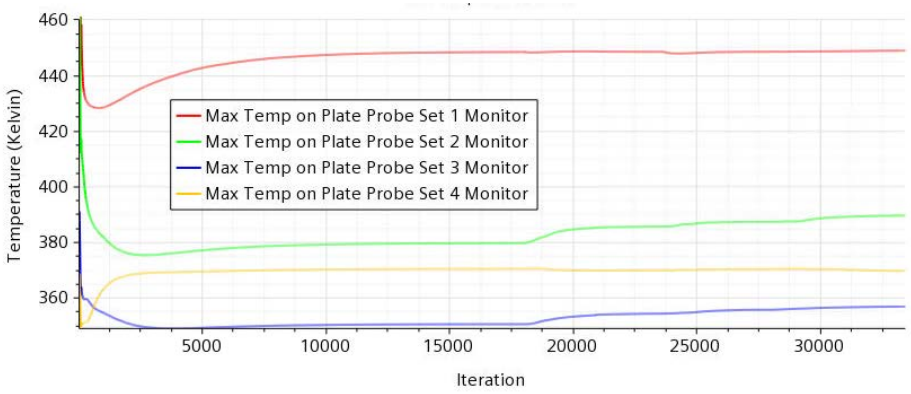


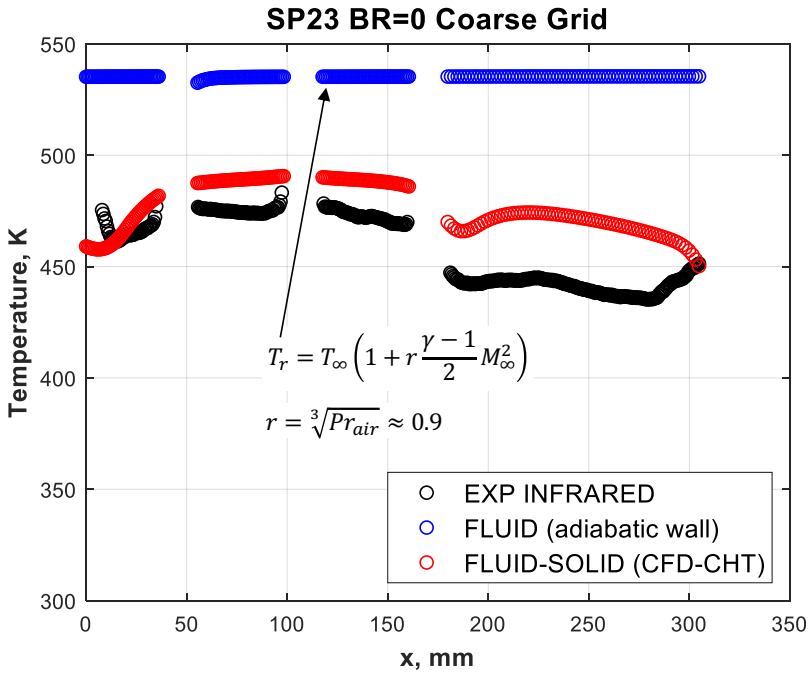
FIGURE 2.013 THERMAL CONDUCTIVITY (35)

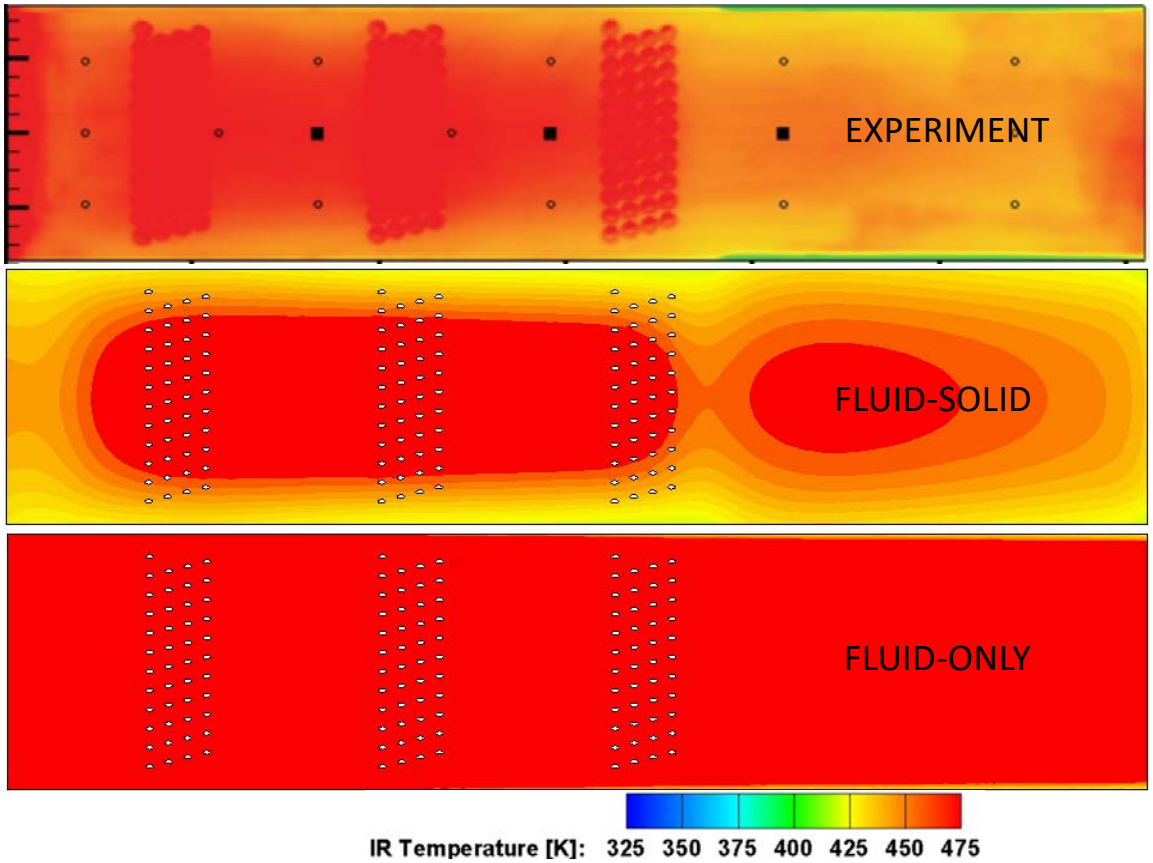
Source: Aerospace Structural Metals Handbook (ASMH) 1988 code 1307

Temperature Convergence History



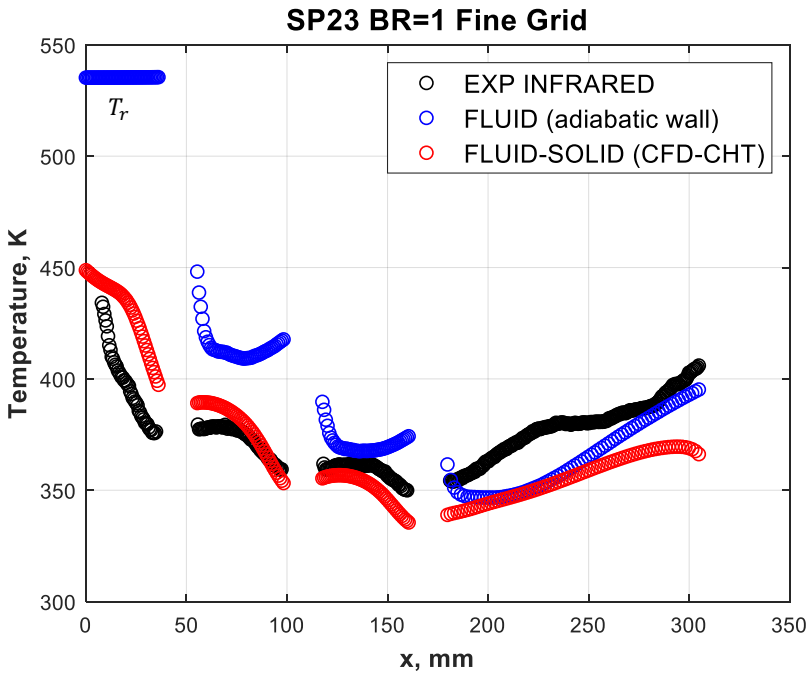
RANS Centerline Surface Temperature BR=0

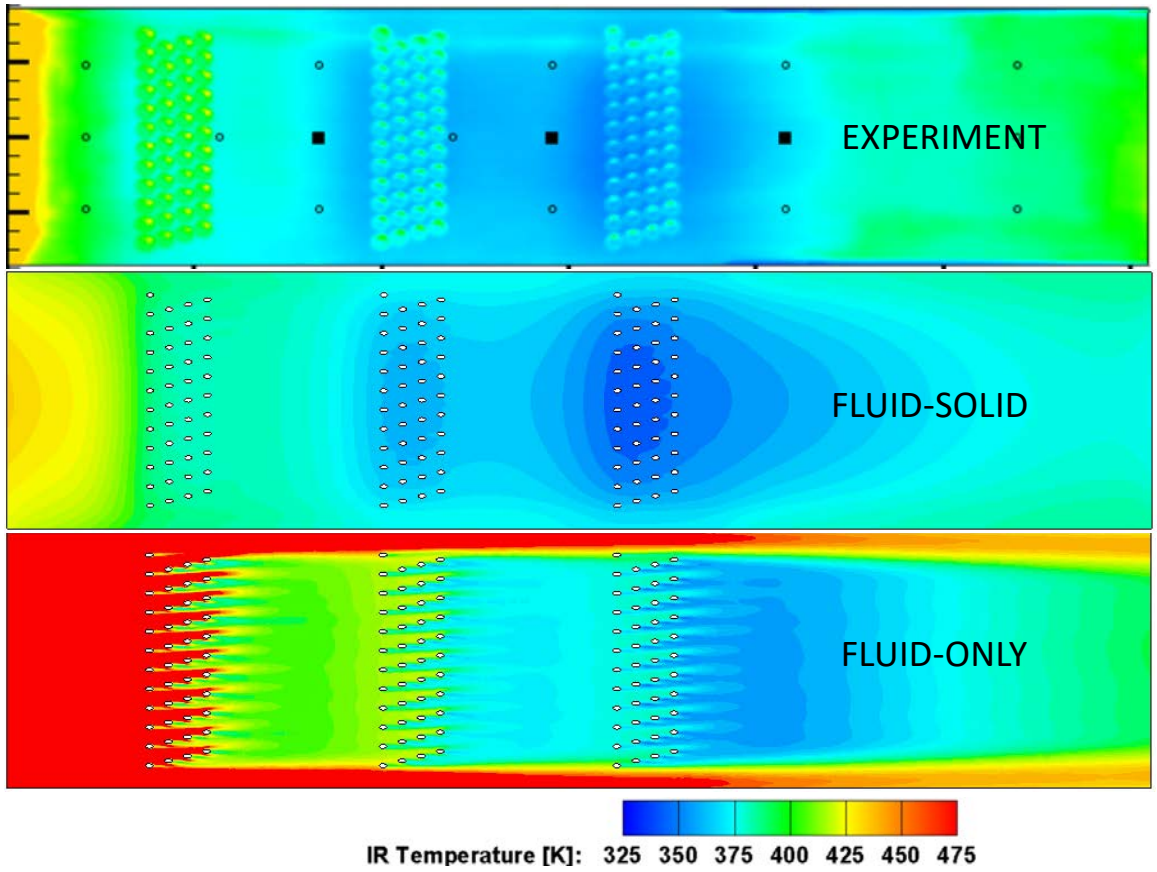




- **Thermally coupled CFD-CHT significantly improves surface temperature prediction.**
- **CFD-CHT results captures trends seen in experiment except at the very aft section of the plate.**

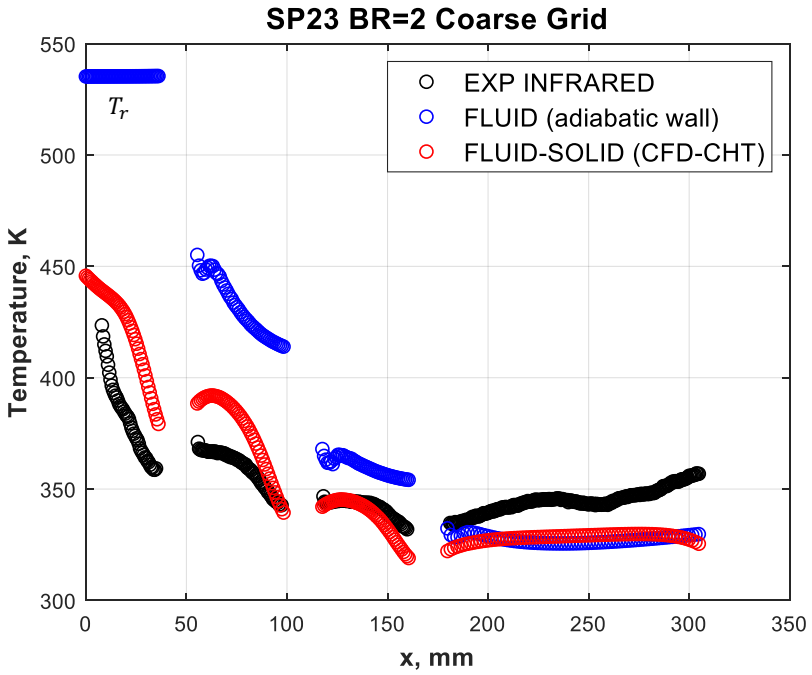
RANS Centerline Surface Temperature BR=1

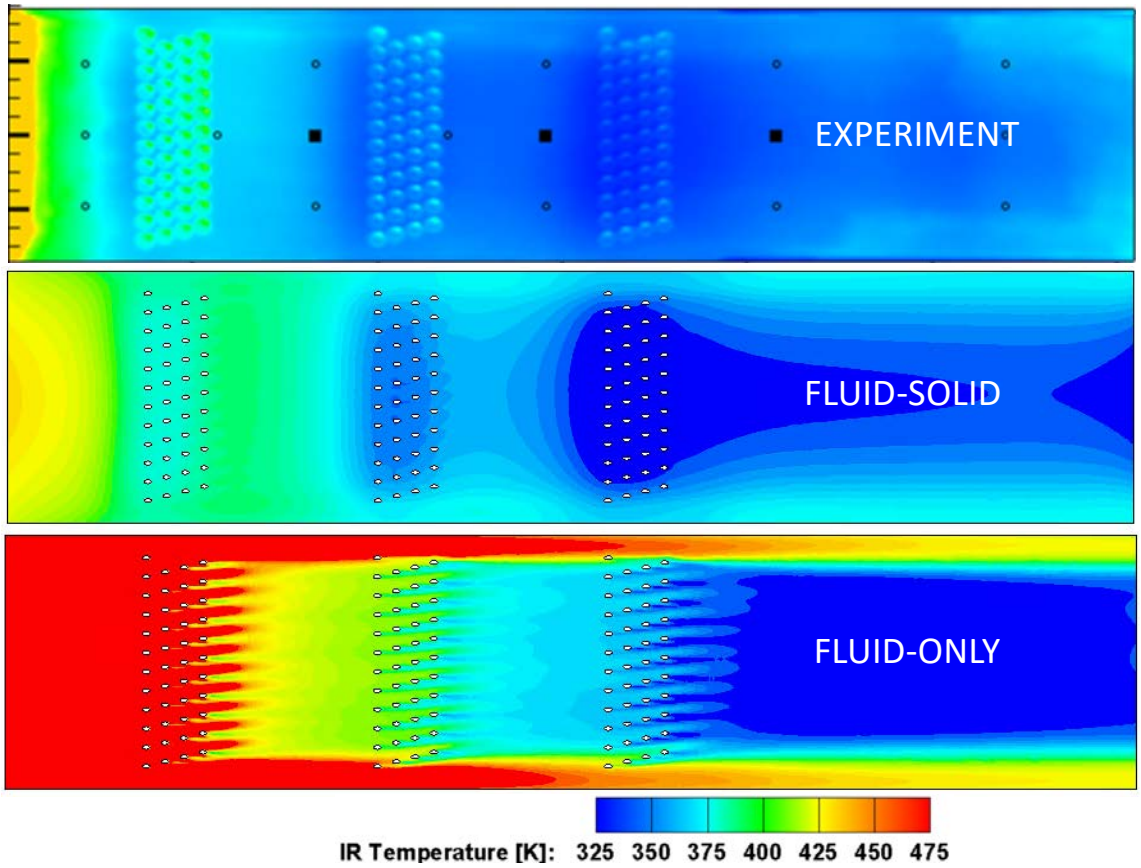




- Thermally coupled CFD-CHT significantly improves surface temperature prediction.
- CFD-CHT results captures trends seen in experiment except at the very aft section of the plate.

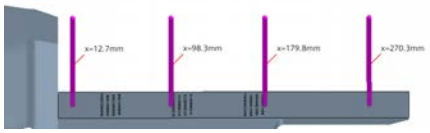
RANS Centerline Surface Temperature BR=2

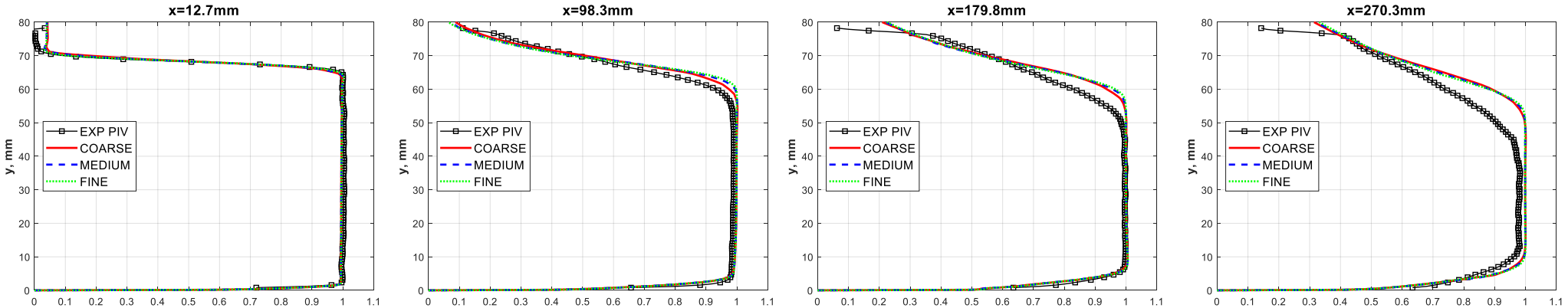




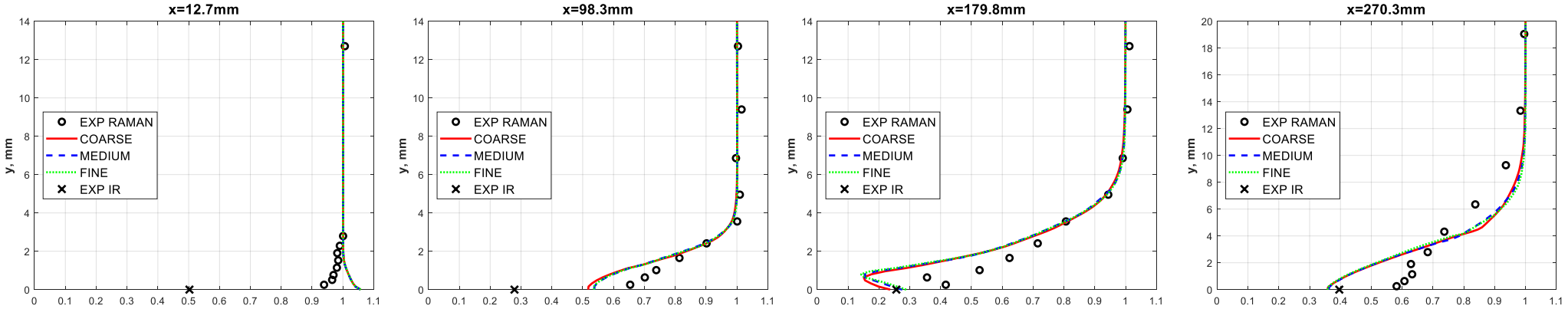
- Thermally coupled CFD-CHT significantly improves surface temperature prediction.
- CFD-CHT results captures trends seen in experiment except at the very aft section of the plate.

Fluid-Only Centerline Streamwise Profiles BR=1



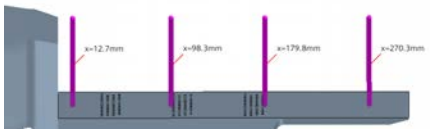


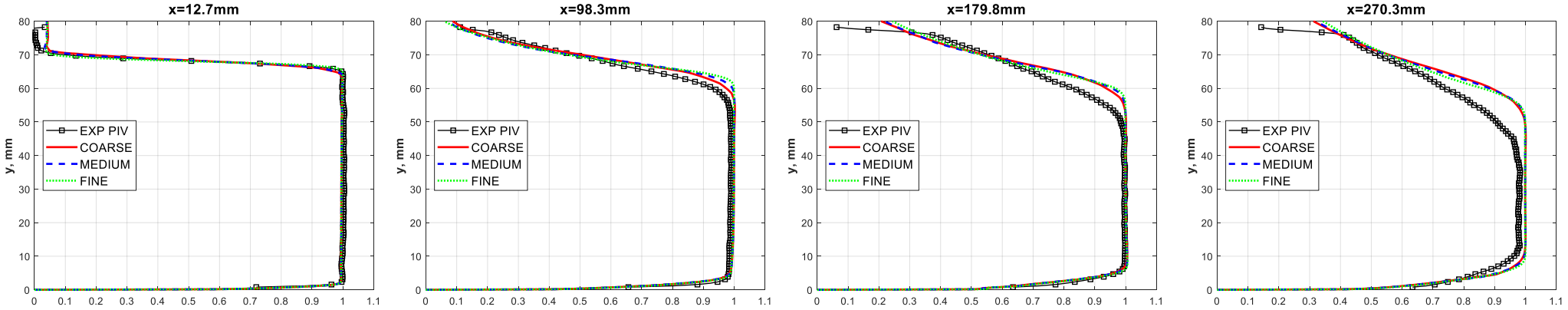
u/U_{jet}



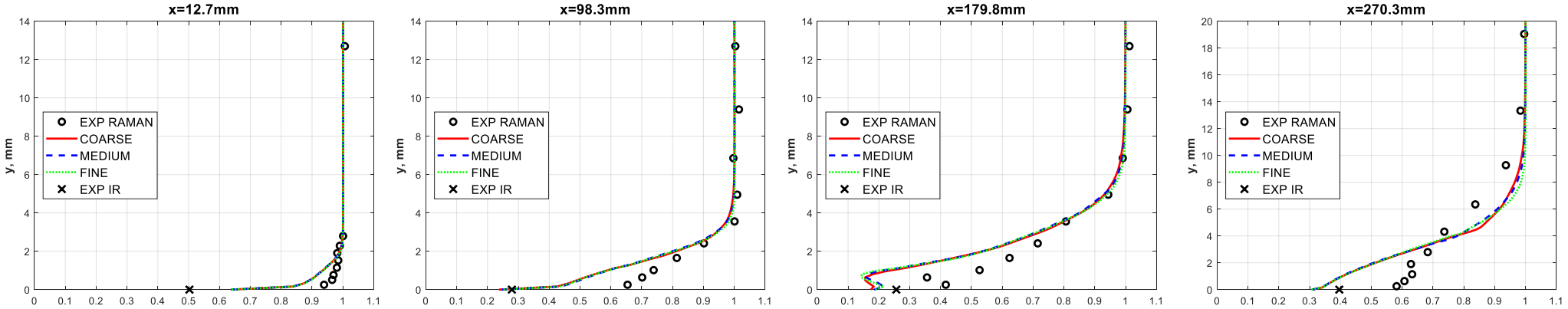
$(T-T_\infty)/\Delta T$

Fluid-Solid Centerline Streamwise Profiles BR=1





u/U_{jet}

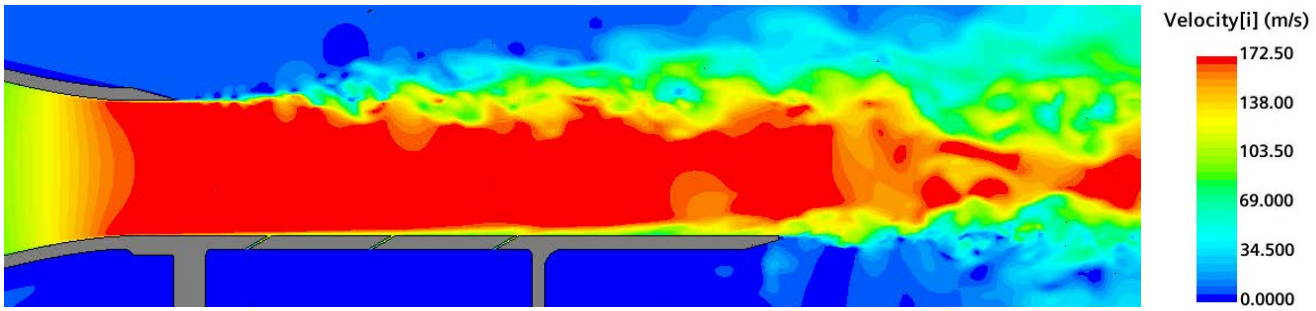


$(T-T_\infty)/\Delta T$

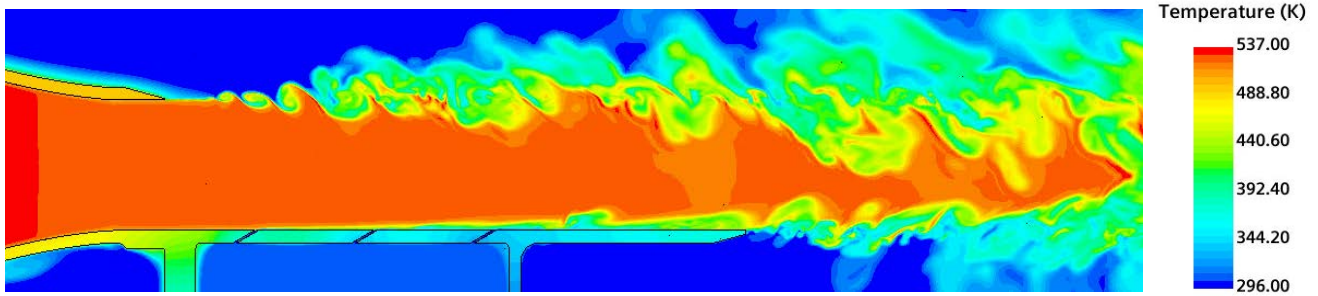
SRS (hybrid RANS-LES) Cases

- Per THX3 simulations (**20B-100B points required for wall resolved LES)** –not tractable for this case.
- Scale-Resolved Simulation (SRS) completed using hybrid RANS-LES
- Delayed Detached Eddy Simulation (DDES) technique successfully used within CFD-CHT model framework

Instantaneous axial velocity contours for Blowing Ratio = 1.0 of Fluid-Solid simulation



Instantaneous temperature contours for Blowing Ratio = 1.0 of Fluid-Solid simulation

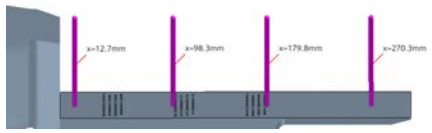


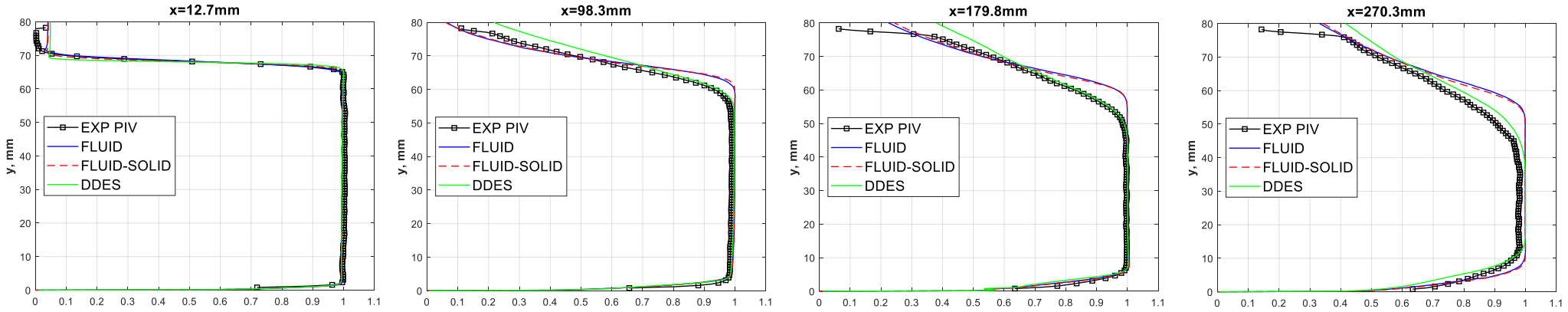
Grid	Fluid-Solid # cells	Blowing Ratio	# Cores	dt	Total Tau Averaged*	Numerical Scheme
Fine	143.3 million	1.0	5,600	1E-6 s	41	Hybrid BCD
XFine	321.4 million	1.0	5,600	1E-6 s	42	Hybrid BCD

$$*\tau = \frac{U_{jet}}{L_{plate}} t$$

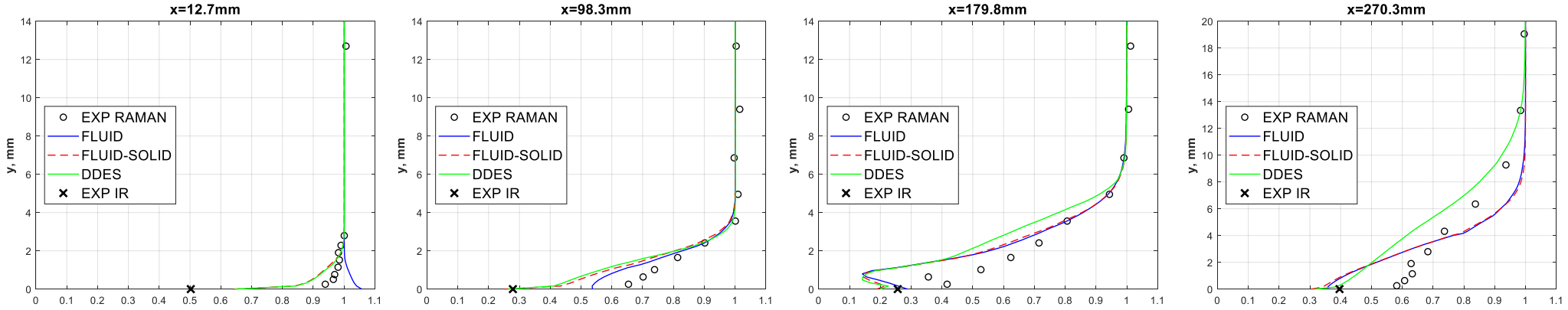
→ **2 orders of magnitude higher than FDL3DI LES**

Experiment vs RANS vs DDES BR=1



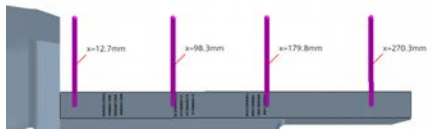


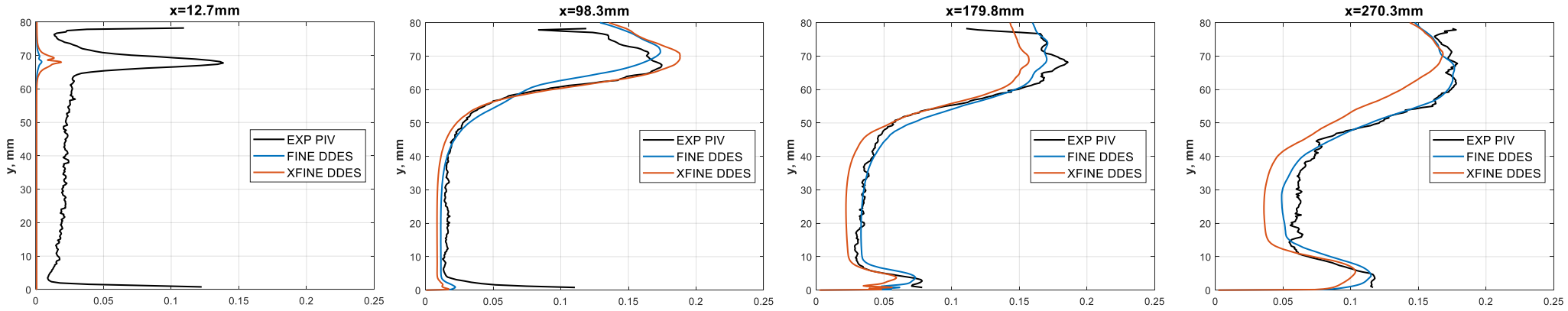
u/U_{jet}



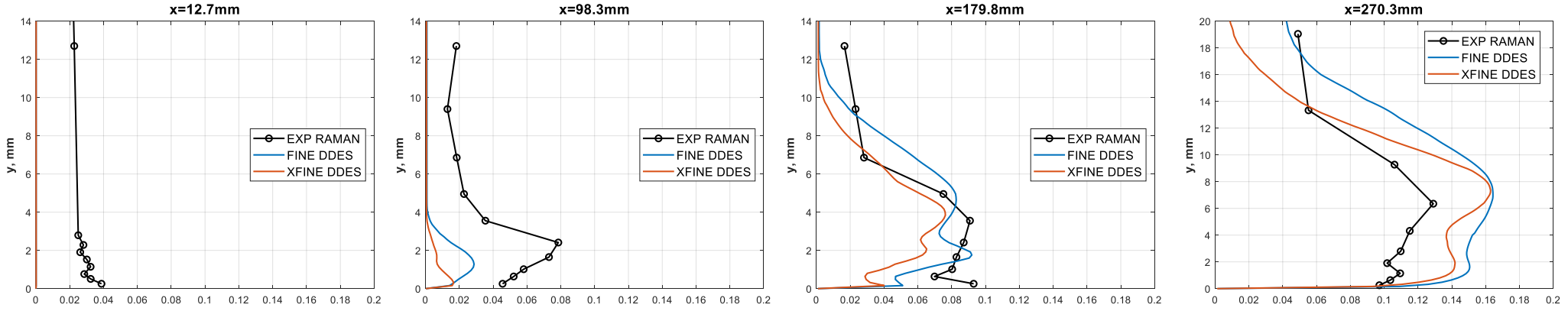
$(T-T_\infty)/\Delta T$

Turbulent Centerline Streamwise Profiles BR=1



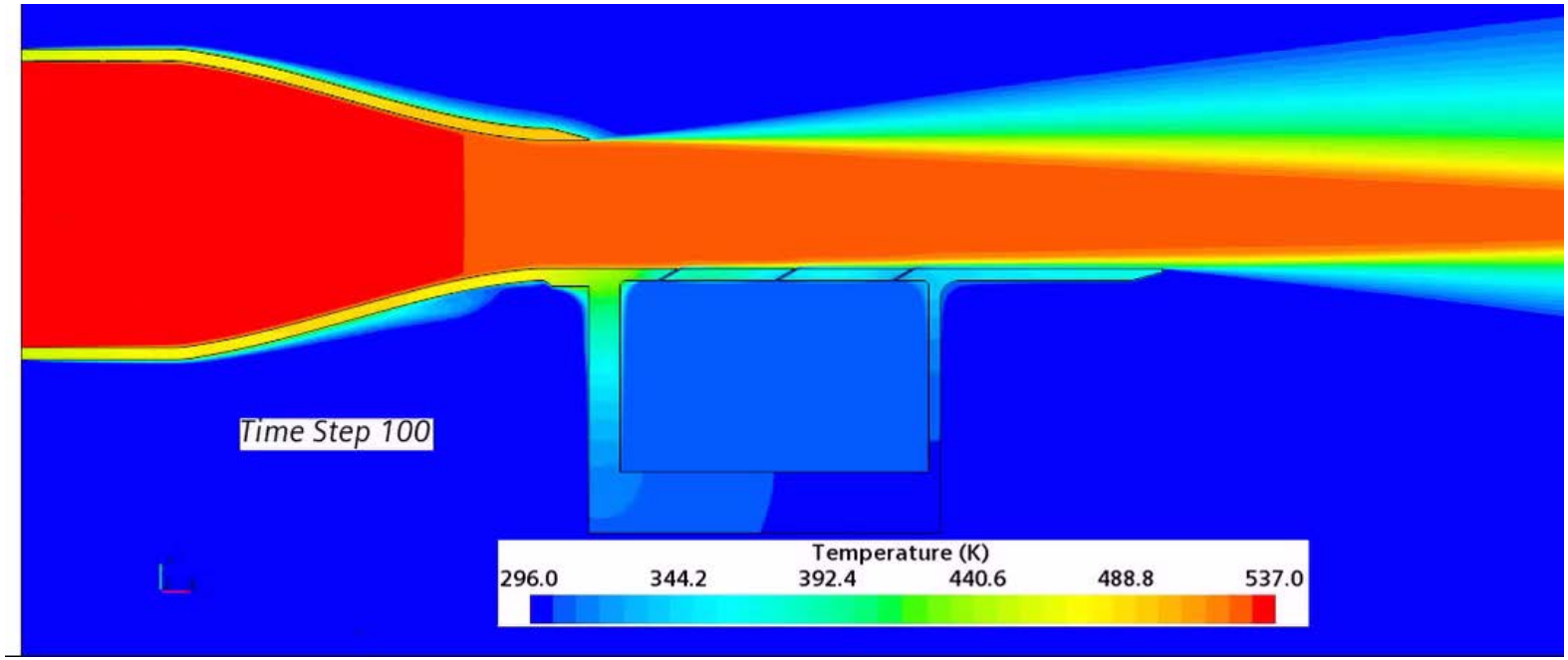


u_{rms}/U_{jet}



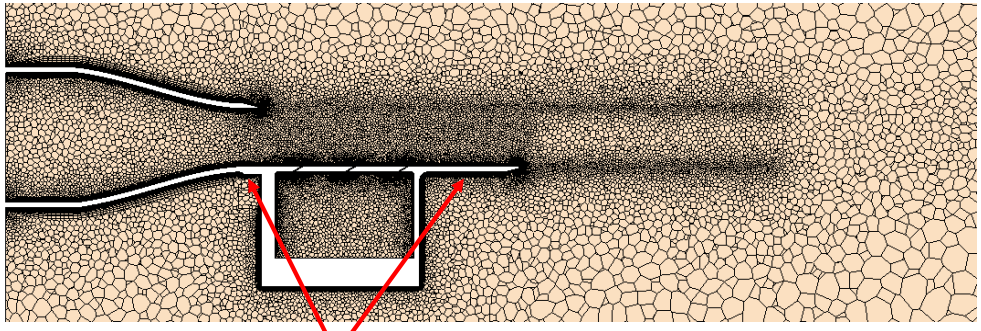
$T_{rms}/\Delta T$

DDES Temperature Animation

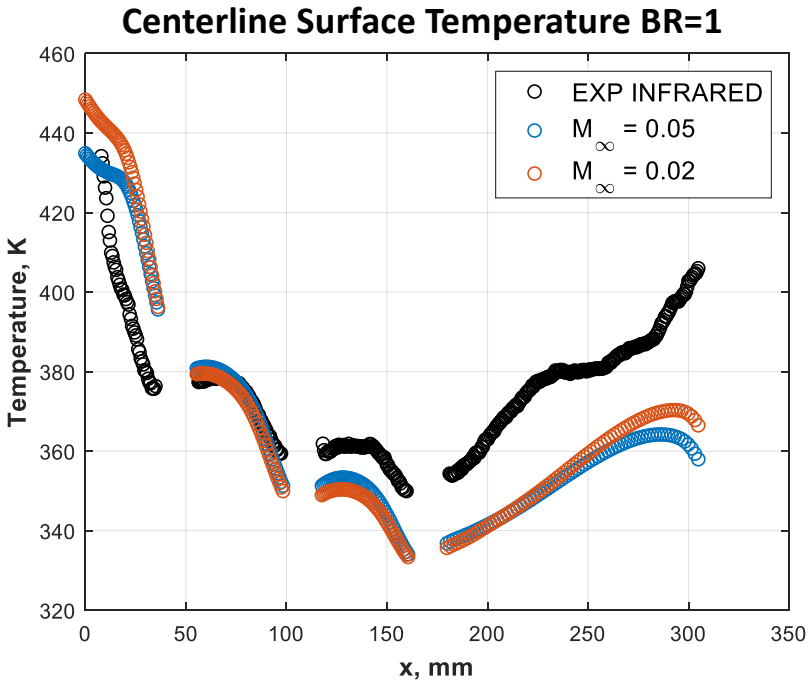


Effect of Freestream Mach Number

- Larger freestream Mach yields more efficient convective cooling of the test article near fwd and aft ends of the plate.
- These locations are exposed to the freestream whereas the middle of the plate is above the plenum



Exposed regions





Summary of THX4 Results



- **Conclusions**
  - Thermally coupled CFD-CHT framework significantly improves surface temperature prediction over CFD-alone; however CFD-CHT fails to predict temperature increase on aft section of plate.
  - RANS is still a reasonable (and still only cost-effective) approach for configurations like THX4 (relative to THX3) because focus is the aggregate effect of many holes.
  - SRS / Hybrid RANS-LES can be used within CHT framework; improved jet mixing layer and outer boundary layer predictions; similar predictions of near-wall boundary layers and wall temperatures to RANS.
  - Full LES may yield further improvement in the predictions, but would require computing capabilities not currently available.
  - Effects of freestream Mach# did not have big impacts on surface temperature prediction for this problem.



Summary of THX4 Results



- **Future Work**
  - "Multiphysics Computational Analysis of a Perforated Plate Cooling Flow", Pesich, J., Georgiadis, N., Wernet, M. submission accepted to AIAA SciTech 2021.
  - Participating in 5th AIAA Propulsion Aerodynamics Workshop Nozzle Test Case (Set Point 42 on **THX4** configuration) weekend prior to SciTech 2021.
  - Plan to investigate discrepancy in surface temperature prediction on aft end of the plate.